Effect of Roughness on Pullout Strength during Ultrasonic Bone Drilling: An in Vitro Study

A Thesis submitted in Fulfilment of the Requirement for the Award of the degree of

Master of Engineering

In

Production Engineering

By

Raj Agarwal

Registration No.: 801785007

Under the Supervision of

Dr. Vivek Jain

(Associate Prof., MED)

Dr. Vishal Gupta

(Assistant Prof., MED)

THAPAR INSTITUTE
OF ENGINEERING & TECHNOLOGY
(Deemed to be University)

MECHANICAL ENGINEERING DEPARTMENT

THAPAR INSTITUTE OF ENGINEERING & TECHNOLOGY

PATIALA

AUGUST-2019

CERTIFICATE

I, Raj Agarwal, hereby declare that the work done in this thesis entitled "**Effect of Roughness on Pullout Strength during Ultrasonic Bone Drilling: An in Vitro Study"** is an authentic record of my work carried out as requirements for the award of the degree of **Master of Engineering** in **Production Engineering** at **TIET, Patiala** under the supervision of **Dr. Vivek Jain** (Associate Professor, Mechanical Engineering Department, TIET) and **Dr. Vishal Gupta** (Assistant Professor, Mechanical Engineering Department, TIET). No part of the matter embodied in this report has been submitted to any other university or institute for the award of any degree.

Date: 22-Aug-2019

Place: TIET, Patiala.

Raj Agarwal

801785007

TIET, Patiala

This is to certify that the above declaration made by the student concerned is correct to the best of our knowledge and belief.

Dr. Vivek Jain
Associate Professor, MED
TIET, Patiala

Dr. Vishal Gupta
Assistant Professor, MED
TIET, Patiala

ACKNOWLEDGEMENT

It is my great fortune to get an opportunity to work on this challenging yet inspiring project. The learning and experience I have received here is of inexplicable value. It gives me immense pleasure to express my paramount gratitude to each one of those who made this possible.

It has been my immense pleasure to complete this project under the guidance of two renowned expertises. I would start by expressing my profound exaltation and gratitude to **Dr. Vivek Jain**, Associate Professor and **Dr. Vishal Gupta**, Assistant Professor, Department of Mechanical Engineering, Thapar Institute of Engineering and Technology for sharing his priceless experience, constructive suggestions and full support, which help me in the accomplishment in the field of biomedical. I will owe them a life time not only helping me learn new technique and to develop skills to understand things better. I am highly indebted to them for their painstaking efforts and invaluable suggestions during the period of work.

I would like to thank all members and employees of Mechanical Engineering Department, Thapar Institute of Engineering and Technology, Patiala for their everlasting support.

In the end, I wish to express my deep sense of gratitude to my parents and my siblings for supporting and encouraging me at every step of my work. It is the power of their blessings, which has given me the courage and confidence for hard work.

RAJ AGARWAL

ABSTRACT

Bone drilling is one of the most common operations used in direct approach to repair fractured parts of bones and to produce hole for screw insertion to fix the fractured parts for immobilization and alignment of parts for proper healing. The failure of screw is due to strength between the bone and screw, which majorly depends upon the Pullout strength of cortical screw. Pullout Strength is the force required to pull a screw out of its foundation in the bone. As after fixation, major forces acts on the fixation screw of the implanted device in the bone. Therefore, it need to make sure that screw must fit into the place or grasp the bone with in the drilled hole.

The intended focus of this research is to see the effect of roughness induced during the bone drilling operation on Pullout strength. This may be expected that a drilled hole in a bone exhibit more Pullout strength with more surface roughness. The probable reason is that more anchoring is provided by the roughened surface. Also, how the apatite formation will enhance further with this roughness during various time span is also to be explored during the research. An ultrasonic drilling process is employed for the purpose and it is expected that varying the grit size of a drilling burr result in different outcomes. Hence, a process optimization with an objective to enhance the surface roughness and effect of this enhanced roughness on Pullout strength would be the key findings of the research.

TABLE OF CONTENTS

LIST OF TABLES

LIST OF FIGURES

Dedicated to my loving mom and dad

(Mrs. Madhu Agrawal and Mr. Yashpal Agrawal)

1.1 INTRODUCTION

Bone are active and living tissues being remoulded constantly. It is a composite tissue having hard outer layer made of crystalline calcium phosphate (hydroxyapatite) with small amounts of other mineral substances, covering a soft spongy structure made of the protein collagen. Outer layer gives strength and inner honeycomb-like structure containing matrix gives flexibility to the body. With structurally supporting the body, it also protects vital organs. These layers provides an environment for bone marrow to create blood cells. They also act as storage bank of many minerals such as calcium. The bone are stiffer and stronger at higher stain rates, which is a way to compensate for the higher loads and stresses imposed by strenuous activity or super physiological loading.

1.1.1. HUMAN BONE

Bone is the infrastructure of human body, it provide a rigid framework that offers protection and support, as well as attachment sites for muscle that are essential for local motion like running, walking, climbing, swimming and all forms of locomotory movements **[1].** Bones are living, metabolically active and growing tissue that are dense connective tissue. There are total 206 distinct bones present in the human body and these bones are of four different shapes, which are long bone, short bone, flat bone and irregular bone.

Bone tissue is made of distinct types of bone cells. The properties of bone are hard, brittle and having poor thermal conductivity. The bone structure is composed of two tissues, which are cortical and cancellous bone as mentioned in figure 1.1. Cortical bone is exterior surface region, which is made up of hard dense tissues.

Whereas cancellous bone are the inner surface regions. The cortical bone takes charge of the main compressive loads, also known as compact bones. The cancellous bones are spongy and porous in nature, they are found at the ends of long bone. Both kind of tissues, cortical and cancellous contains living cells, which helps makes repair when bone is broken or injured. Cortical bones contributes 80% of weight in a human skeleton because they are very denser and are the first layer to be cut in every surgical operation. Whereas cancellous bones frequently contains red bone marrow where the blood cells production occurs **[1]-[2].**

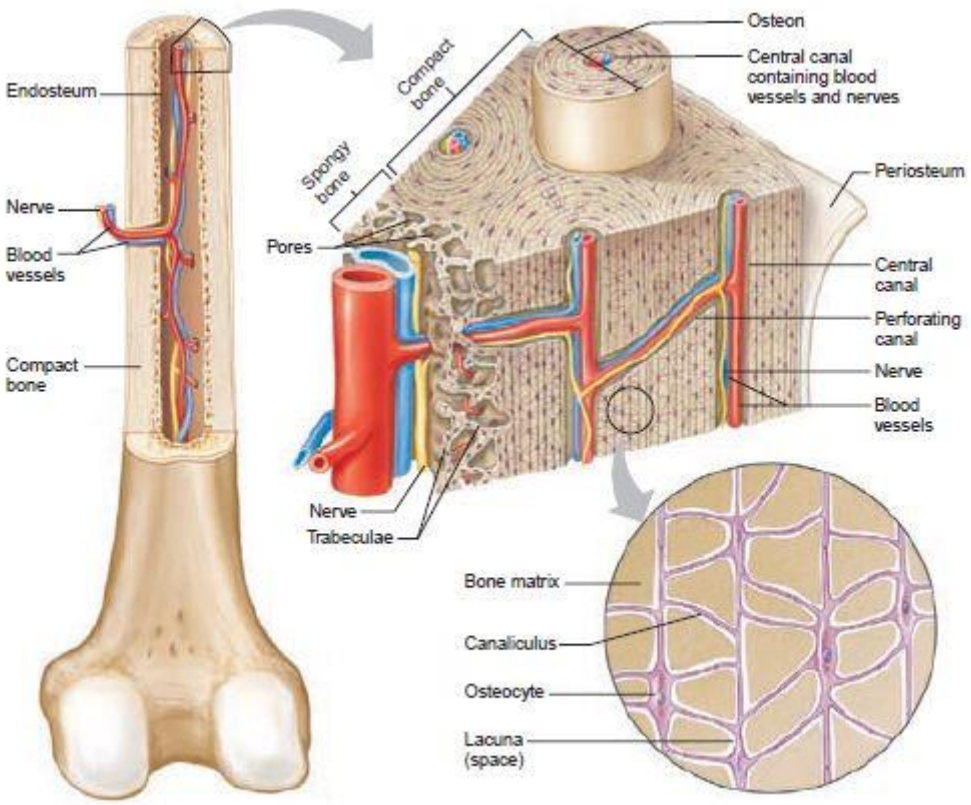

Figure 1.1 Human cortical and cancellous bone **[3]**

The mechanical properties of bone is crucial for the survival of human. The bone is based on its bone composition and bone structure are majorly important for mechanical properties. As the bone helps to strengthen the body, so mechanical behaviour of bone is exceedingly important for estimating the fracture risk. Some part of body are constantly under the compressive loads, which may increase the risk of fracture**.**

1.1.2. PORCINE BONE

Porcine bone has very similar type of mechanical and thermal properties as human bone structure as mentioned in Table 1.1. Humans bone and porcine bone, both are highly dependent on dietary quality since symbiotic microorganisms.

Medical researchers used porcine collagen for bone regeneration and showed good physicochemical properties. In addition, porcine bone is biocompatible in nature and are one of the perfect xenograft for replacing human bone structure **[4].** The new generated bone formation through osteoconductivity, proving to be a reliable bonegraft biomaterial alternative for GBR (guided bone regeneration) treatments **[5]**.

Table 1.1: Differentiation of properties of porcine cortical bone and human cortical bone **[6]**, **[7]**

Mechanical Properties	Porcine cortical bone	Human cortical bone
Young's modulus (GPa)	16.7	15
Poisson's ratio	0.3	0.35
Yield strength (MPa)	105	180
Specific heat(J/KgK)	1640	1330
Thermal conductivity (W/mK)	0.452	0.43
Tensile strength (MPa)	106	130
Density (Kg/m^3)	1640	1800

1.2. FRACTURE OF BONE

Bone fracture is a medical condition where the continuity of the bone is broken partially or completely and are very common problem due to sports injuries, age factors, transport and industrial accidents, etc. During fracture, bone breaks or do not align with each other. Bone fracture occurs at the point where the physical force exerted on bone is much stronger than the bone itself. Bone fracture can majorly be classified into two types; diaphysis fracture, proximal and distal segment fractures which can be sub divided into three types of fracture as mentioned in Figure 1.2 **[8]**.

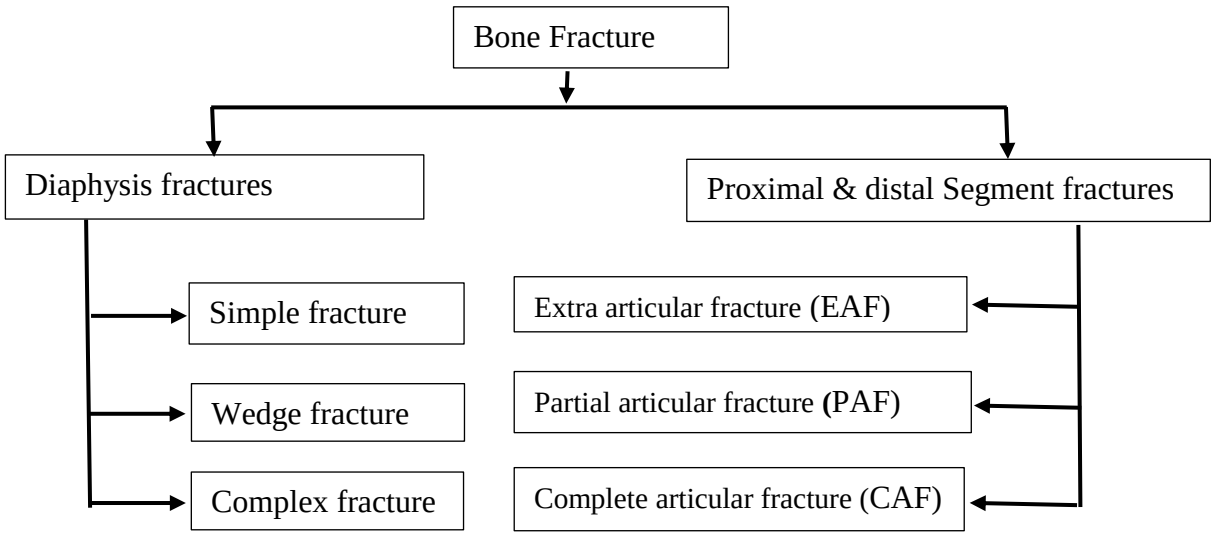

Figure 1.2 Types of human bone fracture **[8]**

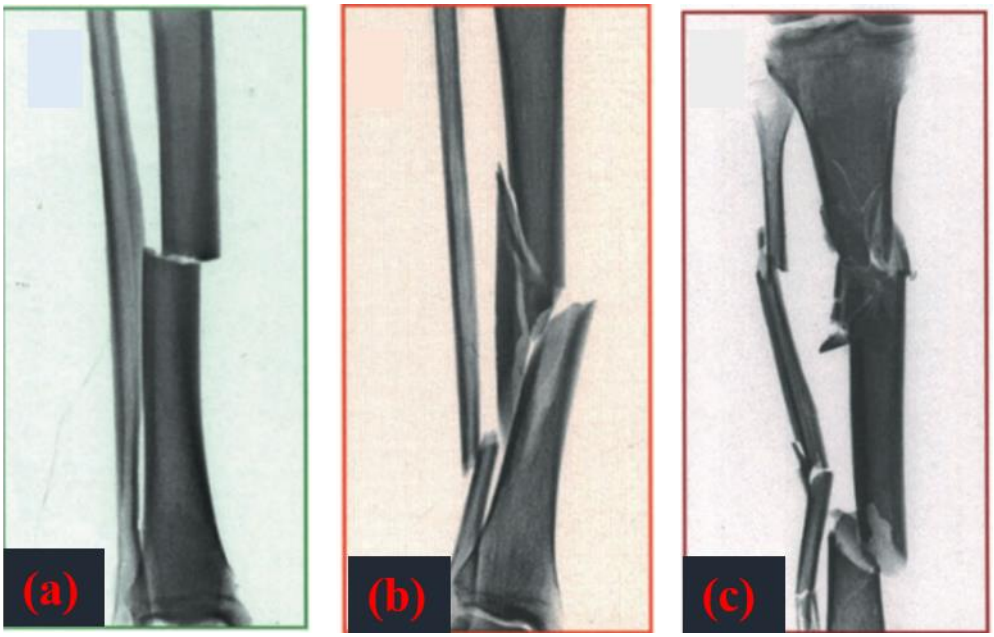

Figure 1.3 (a) simple, (b) wedge, and (c) complex bone fracture **[8]**

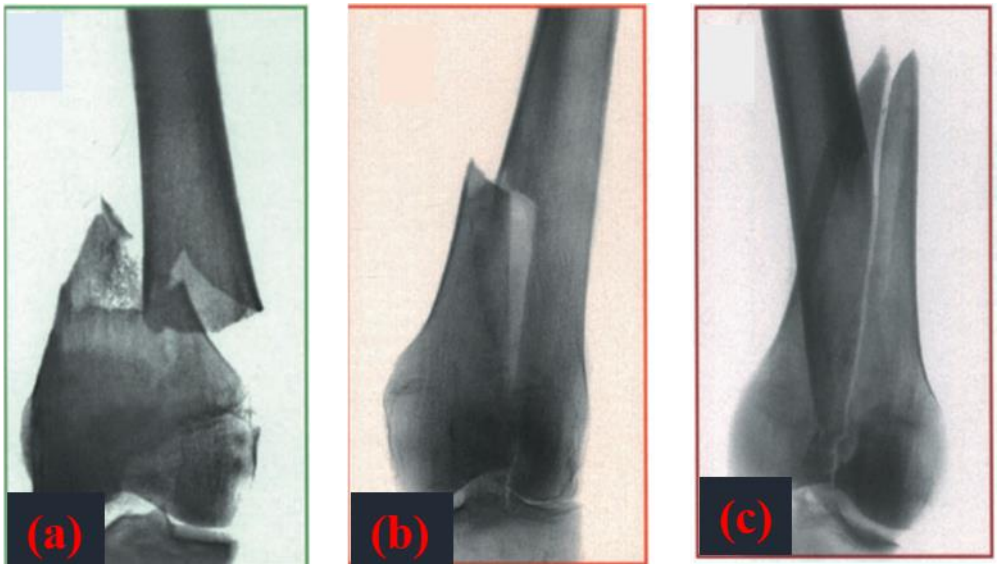

Figure 1.4 (a) EAF, (b) PAF and (c) CAF **[8]**

1.3. METHOD TO TREAT BONE FRACTURE

Treatment of bone fracture usually involves restoring of fractured bone to their initial position and immobilizing them until restoring and reconstruction of bone takes place. There are two ways which are mainly used for treatment of bone fracture i.e., direct and indirect method as mentioned in figure 1.5. The indirect method is a time taken process, in this method the body part is fixed from outside and restrict to move relatively. For outer fixing of bone plaster cast, body cast, orthopaedic cast are used. There are some limitation with indirect method like wrong alignment of bone and long healing process, this method is also known as conventional method.

To overcome these limitations direct method is introduced by orthopaedic and trauma related surgeons. In this method, fractured part of bone is treated internally and directly to reposition and secure the bones. Immobilization is done by fixation of bone with the help of implants, and to be place implants at right position drilling of bone is done. Direct approach includes bone drilling, bone grinding and bone grafting. It eliminates the misalignment problem of bone but introduces a new problem i.e. thermal narcosis, which means completely or partially damage of neighbouring part (soft tissues) of bone which cannot be regenerated again once burned. During drilling of bone, heat is generated due to which thermal burning of soft tissues occur which may result in the failure of bone generation and screw implant failure **[12]**.

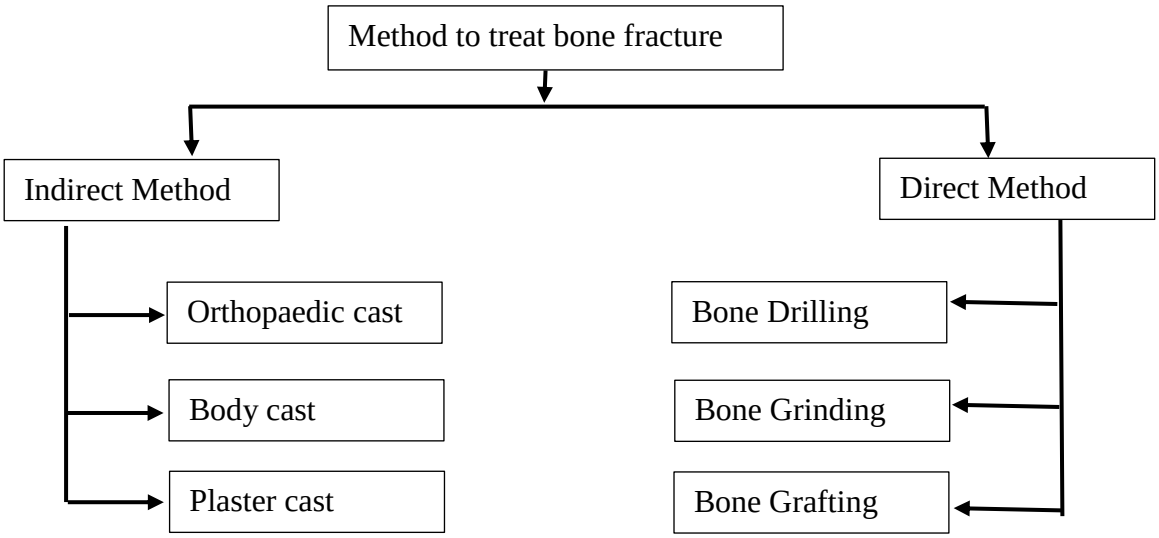

Figure 1.5 Method to treat a fractured bone

1.4. BONE DRILLING

One of the principle method to repair and reconstruct the fractured parts of bone is based on drilling of bone and fixing its separate parts together with the help of screws. Morphology of the drilled hole surface and fixative components such as screws, wires, pins and hooks influences strength of bonds between them. Purpose of bone drilling is to provide support to the fractured part at the direct level and helps for healing of the bone fracture faster **[10]**.

This orthopaedic drilling of bone is very much similar to mechanical drilling process, which results the reactive forces and increase temperature of surrounding bone material, which can cause the osteonecrosis in some of cases and affect the reliability of surgery. The heat is generated due to friction between drill bit and bone surface, which is the cause of cell death, and change in natural properties of bone. When the temperature is elevated above the threshold

value, bone resorption may occur due to thermal exposure, which results thermal necrosis. The temperature rise in bone drilling above the thermal threshold (around 47°C for 1 minute or 50°C for 30 seconds) **[11]** is a prime concern. The twisted drill bit used for drilling with the heat generation zone is shown in figure 1.6. When bone is overheated, the risk of implant failure is significantly increases. Rather than temperature, failure of implant can occur due to many other factor as mentioned below **[12]**:

1. Occlusal overload and peri-implantitis together are two main cause factors for failure of implant.
2. A low insertion torque of implants that are planned to be immediately loaded.
3. Lack of initial implant stability.
4. Implant insertion in places with small bone volume.
5. Implant insertion in the maxilla or in the posterior region of the jaws.
6. Greater number of implants placed per patient.
7. Use of shorter length implants.
8. Inexperienced surgeons inserting the implants.

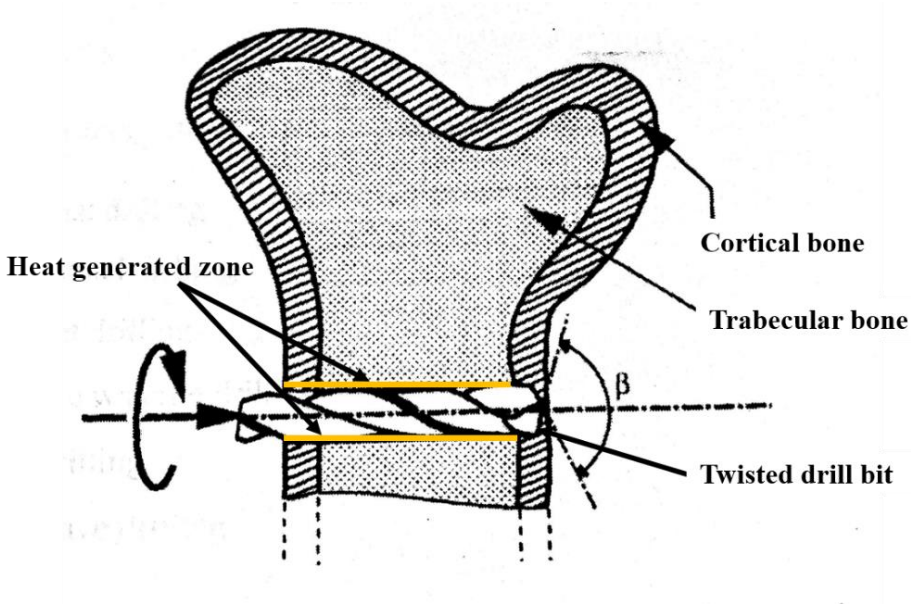

Figure 1.6 Drilling through bone with heat affected zone **[11]**

After drilling the bone, implant is placed and bone screws are inserted into the drilled hole. Bone screws are specifically designed to function effectively in the bone into which they are installed. Bone health and density, wound location, and fracture type are considered to

determine the appropriate design of the screw used. Bone screw type can be classified into two types: cortical screws and cancellous screws as shown in figure 1.7.

Cortical and cancellous screws are classified by the layers of bone that they interact with. The cortex of a bone is the hard outer shell covering the entire bone. The human sternum is very shallow and both cortices of the bone can easily interact with a screw. A bicortical design is desired by surgeons due to the mechanical stability it provides the system; however, a bicortical screw puts the organs under the sternum at risk of being punctured by the screw tip.

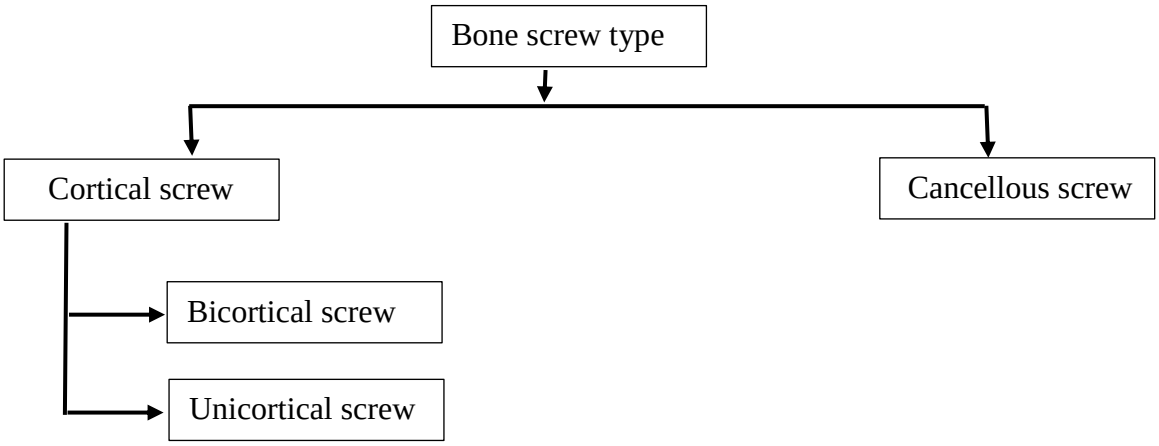

Figure 1.7 Types of bone screw **[12]**

Cortical screws have a high thread count, and low thread depth and pitch. Since the cortical section of the bone is harder and denser than the cancellous portion; thus, less thread penetration into bone tissue is needed for stability. Cancellous bone screws have a lower thread count and pitch, but higher thread depth (Figure 1.8). Due to the soft, less dense, and more porous nature of cancellous bone, cancellous screws require more surface area to be in contact with tissue for mechanical stability.

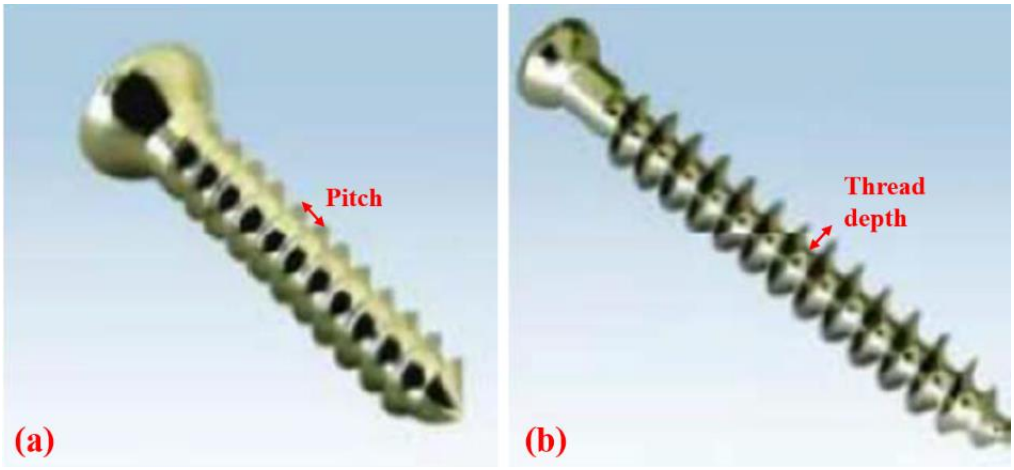

Figure 1.8 (a) Cortical Screw (b) Cancellous Screw **[12]**

There are two variations of cortical screws: bicortical and unicortical. These differ by the number of bone cortices they puncture during insertion. Bicortical screws are commonly used in bone and yield more mechanical stability by obtaining purchase through both cortices as shown in figure 1.9. Unicortical screws only puncture one cortical layer (figure 1.9), the surface of their insertion point. Unicortical screws also affect the median layer between cortices. Although less mechanically stable, unicortical purchase prevents accidental puncture of tissues or organs near the impacted bone. Medical researchers found that bicortical fixation within the sacrum can provide a greater resistance to pullout in the early stages of osteoporosis when being compared to a unicortical screw augmented with bone cement **[13]**.

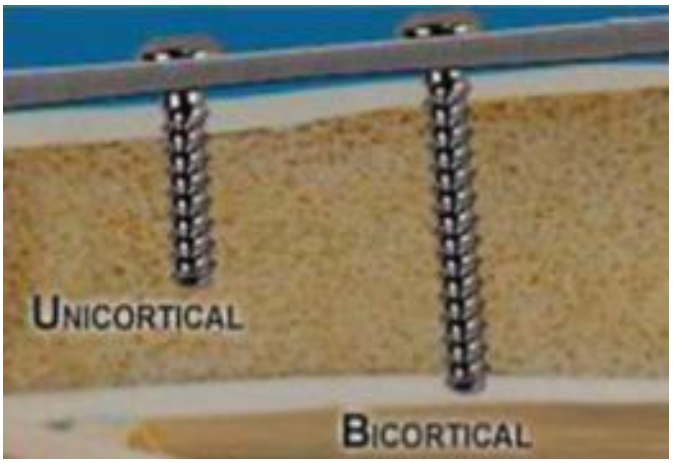

Figure 1.9 Unicortical and bicortical screw systems **[13]**

The body portion can have various configurations for facilitating bone in-growth, such as indentations, a roughened surface, such as by acid etching, specialized coatings, such as hydroxyapatite, sintered beads etc. Because the body portion of the screw facilitates bone growth, the screw will be more firmly mounted to the bone. It has been observed by the researchers that the screw is more rigidly mounted to the bone, wherein the body portion includes a roughened surface for facilitating bone in-growth **[14]**.

As after fixation of screws, the major forces acts on the fixation screw of the implanted device in the bone. Therefore, it need to make sure that screw must fit into the place or grasp the bone with in the drilled hole. Screw loosening is a clinical problem in lumbosacral fusions, especially in osteoporotic patients. The failure of these bone screws are due to less sustainability between the bone and the screw, this may be due to less force and anchoring strength between them. This anchoring strength is also known as pullout strength. In simple term, the pullout strength may be defined as the force required pulling a screw out of its foundation in the bone.

1.5 MOTIVATION

The bone fracture are very common, and hence it needs better care while drilling of bone so the problems associated with bone drilling like less surface roughness, high microcracks. Hence, present work is focused on the concept of bone drilling to control the surface roughness of bone. In order to increase the pulllout strength of joint, there must have a deep relation between the surface texture of the bone, design of drilling tool and cortical screw.

The motivation behind this dissertation is to reduce the implant failure and increase the stability of cortical screw in the bone. It had been reported that, the implant failure rate for lower leg osteosynthesis is around 2.1-7.1% **[15]**. Hence better anchoring strength between the screw and the bone. Using rotary ultrasonic bone drilling, increasing the stability of cortical screws by varying the past researchers various parameters. With the aim for measuring increasing the surface texture of bone less failure due to screw loosening failure. The focus of this study is to find an optimal condition where the increase in surface texture of bone leads to maximize the pullout strength of cortical screw for bone screw joint. The main reward of present work is to decrease the rate of failure due to bone screw joint and increase the sustainability of bone screw joint. It can only be possible by using distinct types of tools with introduction of difference in abrasive grit sizes, which can lead to optimized surface texture with improved pullout strength.

CHAPER: 2 LITERATURE REVIEW

Most of orthopaedic surgeries are based on the bone drilling for fixing plates and implants with the cortical screws. Healing of bone and sustainability of joint is directly depends upon the drilling parameters i.e. rotational speed, drill diameter, feedrate, drilling force, temperature generated, microcracks in bone etc. The present work is focused on to enhance the pullout strength, which leads to bone screw fixation stability. The pullout strength may affect due to following reasons:

1. Drilling procedure.
2. Thermal necrosis during bone drilling.
3. Microcracks generated during drilling of bone.
4. Insufficient bone growth during healing of bone.
5. Less anchoring strength and improper screw design.

Therefore, the present literature is divided into following areas.

- Bone drilling procedures: conventional and ultrasonic method.
- Thermal necrosis observed.
- Microcracks and surface morphology of bone after drilling of bone.
- Apatite formation.
- Screw design.

2.1 STATUS BASED ON BONE DRILLING

Matthews and Hirsch investigated the elevated temperatures while drilling in cortical structure of human femur at several rates of rotation and at several level of drill pressure for elevated temperature durations at the drill hole wall. They recorded greater cortical temperatures, succeeding 100 degrees centigrade, when drilling without a proper coolant system. In case of both magnitude and duration of elevated cortical temperatures, the applied drill force was found to be more dominant factor than drilling speed. It was observed that as we go in depth during drilling, the drill force was increased, which guides to increase in temperature. It was found that any form of irrigation is effective only when fluid stream is allowed to be directed at the penetration point of cortex. Figure 2.1 shows the fractured bone undergoes healing with direct approach of bone drilling. In this figure, screw is inserted in implants of cortical bone at the left side and cannulated screw is inserted in the cancellous bone at the top **[16]**.

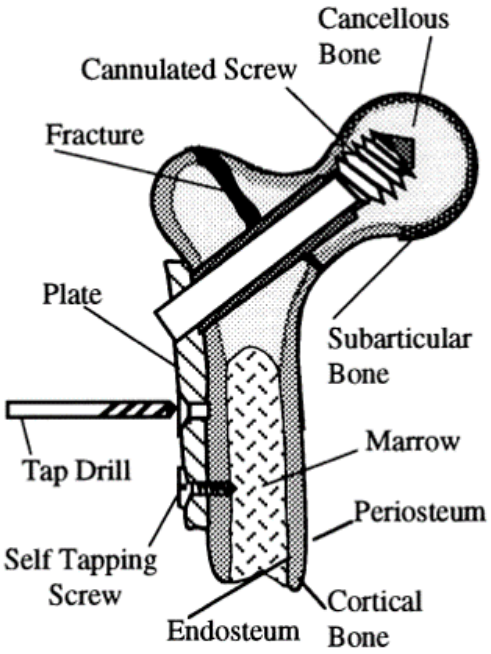

Figure 2.1 Bone drilling for surgery **[16]**

Pandey et al. had conducted experiments on bovine bone for optimizing the drilling parameters i.e. spindle speed and feedrate in view of minimizing the force and temperature generated during drilling. It was noted that feedrate has the highest contribution (81.94%) to the composite desirability. The investigation with feedrate of 40mm/min and rotational speed of 500rpm had highest performance index and are the recommended process parameters setting for minimum temperature **[17]**.

Li et al. investigated the heat generation during drilling of bone by establishing a finite element method (FEM) based three-dimensional model focusing on feedrate, spindle speed and drill diameter. They revealed that if any of three parameters rises, it would increase the drilling temperature. Then empirical formula was given by them to predict temperature rise and to optimize the parameters. They also introduced the idea of intermittent feed drilling, to be more effective in reducing thermal necrosis to bone tissue **[18]**.

Udiljak et al. had studied effect of drill bit geometry on temperature rise and axial drilling force. This study shows that cutting speed statistically has no significant effect on axial drilling force, but affects the temperature rise. Authors had conducted some experiments with standard surgical drill and 2-phase drill, and they found that using 2-phase drills there is minimum increase in bone temperature **[19]**.

2.1.1 Status based on conventional bone drilling (CBD)

Conventional bone drilling (CBD) uses a twisted surgical drill bit and normal drilling of bone is performed. It is the current drilling procedure and extensively used for orthopaedics surgeries and dentistry. The conventional twisted surgical drill bit that is used in surgeries is shown in Figure 2.2. CBD introduces a new problem of osteonecrosis. It is a disease resulting in the form of temporary or permanent loss of blood supply to the bones. Without blood, the bone tissue dies, and ultimately the bone may collapse.

Figure 2.2 Surgical drill bit used for conventional bone drilling **[20]**

The resultant cutting force ***R*** on one of the lips is resolved into three orthogonal components: P_x (thrust force), P_y (radial force) and P_z (principal cutting force) as shown in Figure 2.3. Section AA shows clearance and rake angle at any position of the cutting edge, the bone chip and the plane of shearing of the chip **[21]**.

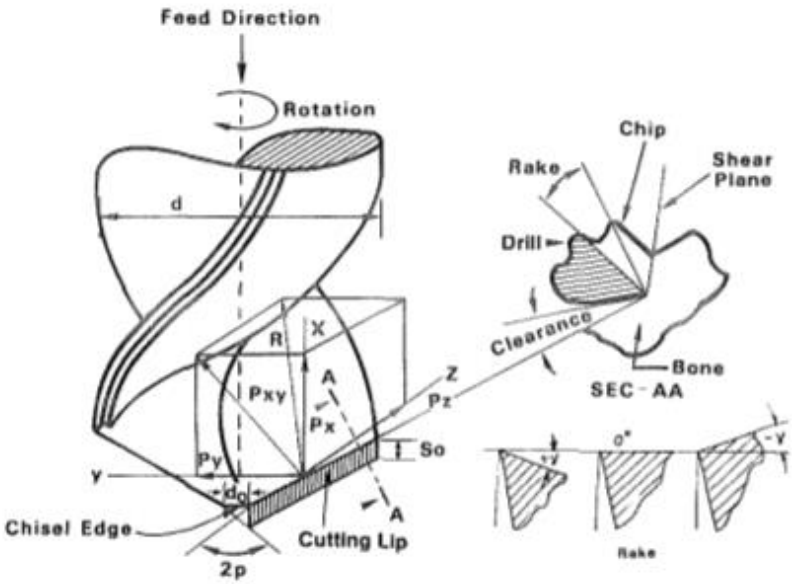

Figure 2.3 Section of tool with bone **[21]**

Alam et al. compared two drilling methods, conventional drilling (CD) and ultrasonic-assisted drilling (UAD). According to his results using UAD, forces were reduced. Experiments were performed with a constant drill diameter of 4 mm while varying the feed rate and spindle speed.

They concluded that force and torque could be reduced with increase in the rotational speed and decrease in the feed rate **[22]**. ***Shakouri et al***. reported similar findings but in their study, the feed rate was kept too high. Because of very high feed rate cracks were produced in the bone and delamination was observed in the bones **[23]**.

Gupta et al. used conventional bone drilling of porcine bone and varied various drilling parameter for observing the temperature variation during drilling. The diamond coated hollow tools with grit size 80-100 (very coarse) were used and compared with conventional twisted drill bit. Various parameters which were varied are rotational speed, feedrate and outer diameter. According to conclusions diamond coated hollow tool with very coarse abrasive grit size generates lower temperature as compared to conventional twisted drill tool. There was a major difference between the temperature of twisted drill bit (70.8°C) and diamond coated hollow drill bit (48.2°C) because lower spindle speed and lower feedrate generates a lower temperature. As the temperature of bone during drilling process continuously increased with respect to the spindle speed and drill diameter for both the types of drill tools **[20]**.

Singh et al. investigated thermal necrosis study on bovine bone. They tried to demonstrate that temperature could be reduced far below the critical values if an optimized set of drill parameters are implanted. Thermocouple actuator was used for measuring the change in temperature of bone. They concluded that lower will be the rise in bone temperature, if higher, are the drill speed and feedrate and with the increase in depth of hole leads to maximum drilling temperature. Based on this study, they suggested high drill speed, high feedrate and reduction in contact area between bone and drill. In addition, the temperature rise was minimum, when the feedrate was high **[24]**.

Wang et al. performed conventional drilling on bovine bone by varying process parameters like rotational speed, feedrate and drill bit diameter. According to the results, feedrate is very important parameter that had to control to avoid breaking of the bone. In addition, feedrate is directly proportional to forces generated. Also, chip formation process changes with higher speed, which might be affecting the bone as friction coefficient decreases. As tool diameter is responsible for force and torque increases. due to increment in the diameter of tool, the cross section area between the tool and bone changes **[25]**.

During CBD, the bone is under compression state and the temperature could increase more than 47°C and cause irreversible osteonecrosis. The result is weakened contact of implants with bone and possible loss of rigid fixation **[9], [15]**. It had been reported that temperature increases when specimen is under compression state and drop when under tensile state **[15], [26]**.

2.1.2 Status based on ultrasonic bone drilling (UBD)

Ultrasonically assisted drilling for cutting bones and fixing implant are becoming popular in orthopaedic, neuro and dental surgeries. It is one of the advanced technologies that has been developed to overcome most of limitations of conventional drilling. The tool is inserted in an innovative piezoelectric transducer, which was designed and manufactured to provide rotation ability as well as longitudinal ultrasonic vibration for the drill. In this, vibrational frequency and amplitude is given to abrasive coated tool with the help of a transducer. The ultrasonic power is supplied from the ultrasonic generator to the piezoelectric actuators–the element which generates ultrasonic vibration. Because tool performs rotary as well as longitudinal motion, there is no continuous contact between the tool and bone which produces less force generation and less temperature, also better surface texture **[23], [26], [27], [28]**.

Singh et al. (2015) had published, that using ultrasonic drilling of bone, there is absence of mechanical forces, which led to better surface finish of bone and finer surface throughout the bone without any burr formation as compared to conventional bone drilling as mentioned in figure 2.4 **[10]**.

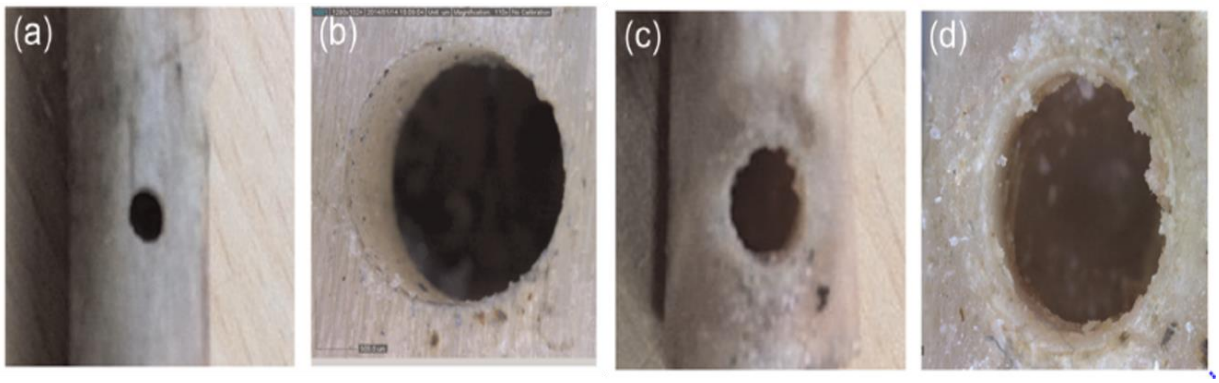

Figure 2.4 (a) Ultrasonically drilled bone (UDB), (b) magnified image of UDB, (c) conventional drilled bone (CDB), (d) magnified image of CDB **[10]**

Gupta and pandey used rotary ultrasonic drilling (RUD) of pig bone for controlling the temperature rise. He used diamond coated hollow tools for drilling bones. Thermocouples was

used for measuring the temperature changes of bone. The effect of parameters (rotational speed, feedrate, amplitude, drill diameter) on change in temperature at different location during drilling of bone was observed. The conclusion shows that conventional drilling method generates higher temperature as compared to rotary ultrasonic drilling of bone. This is because temperature increases with increase in rotational speed, feedrate and drill diameter, but decreases with increase in vibrational amplitude **[26]**.

Singh et al. introduces a new surgical vibrational bone drilling technique. While performing vibrational bone drilling, the twisted drilling tool vibrates in longitudinal direction at a specific frequency and rotates on its axis with a fixed feedrate. Bovine bone was used for this investigation. For heat generation the major process parameter was rotational speed. Its contribution on the result was 80.53%. At low rotational speed (600 r/min), osteonecrosis was very low, and at high rotational speed (3000 r/min), there is high damage in terms of osteonecrosis. Hence, according to results, vibrational drilling technique showed less damage as compared to conventional drilling specimens **[27]**.

Alam and Mitrofanova focused on forces generated during conventional and ultrasonically assisted tool. Fresh bovine bones were used for studying the influence of feedrate and drilling speed. Two drilling techniques were used for this investigation i.e. ultrasonically assisted drilling (UAD) and conventional drilling (CD). UAD was found to reduce a drilling thrust force compared to CD. It was observed that UAD produces hole with minimal effort and avoid unnecessary fracture to bone surface. Higher cutting speed induces greater material removal rate, which increases the production rate. With distinct set of parameters drilling speed (600-3000 rpm), drill diameter (4mm), drill cutting edge angle (65 degree), federate (10-50 mm/min) for both conventional drill and ultrasonic assisted. Vibration amplitude (5-25) and vibration frequency (10-30) in ultrasonic assisted. UAD was more advantageous as compared to CD in case of improved chip removal rate from drilling site and decrease in force generation, which helps surgeons to penetrate tool with lower effort **[22]**.

Wang Yu et al. conducted the study on bovine cortical bone for comparing the micro-crack level formed in vibrational drilling (VD) and conventional drilling (CD) process. Their experimental results explored using VD gives fewer and shorter microcracks as compared to the CD as shown in figure 2.5. Shorter the microcracks means that less fatigue damage and less stress fracture. It was also concluded that temperature decreased, with the increase the level of vibration frequency and amplitude **[29].**

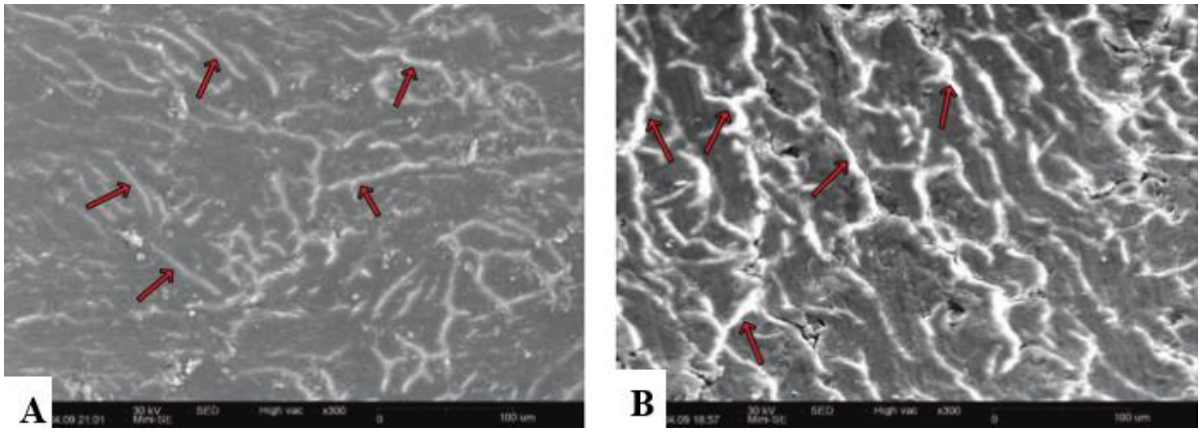

Figure 2.5 SEM images of drilled bone (a) Vibrational drilling, (b) Conventional drilling **[29]**

Gupta et al. investigated effect of rotational speed and feedrate on chip formation in (UBD) ultrasonic bone drilling and conventional drilling (CD). In addition, concluded that at high speed, forces are reduced and large sized chips are formed. The reason is at low rotational speed, there is high mean friction coefficient between tool and bone interface. At higher feedrate, more material is removed in a given time as compared to lower feedrate. Chip produced in UBD are small sized as compared to CD. As amount of the material cutting is less, the deformation energy is also less, which is converted into heat generated, thus leads to less temperature rise in case of UBD. Figure 2.6 shows the chip formation during drilling of bone. At figure 2.6 (a) speed is 500 r/min and CD is done which shows heavy size chip whereas figure 2.6 (b) express rotational speed of 1500 r/min. As figure 2.6 (c) shows the smallest sized chip during UBD at rotational speed of 2500 r/min. Hence, high amplitude vibration is preferred for minimal thrust forces. Stress on the bone can be calculated by dividing trust force by cross section area of tool **[30].**

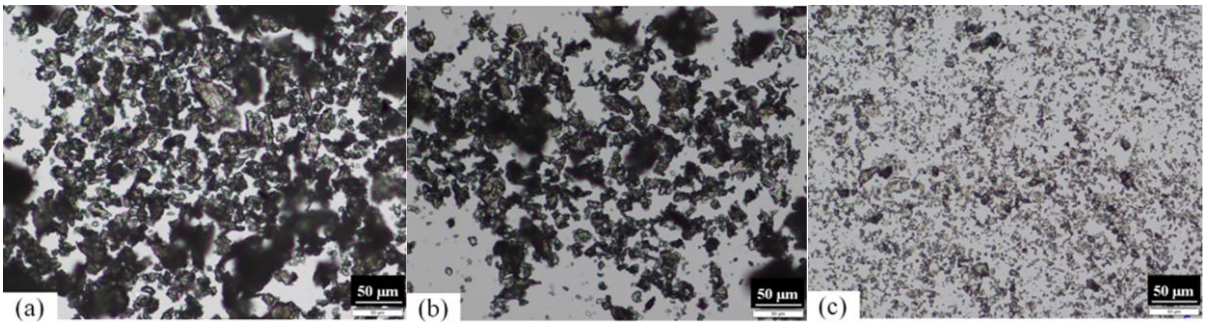

Figure 2.6 Images of produced chips of bone obtained at (a) 500 rpm, (b) 1500 rpm and (c) 2500 rpm **[30]**

The main aim of using ultrasonic bone drilling (UBD) is to reduce the forces, which lead to less heat generation and less microcracks.

2.2 STATUS BASED ON SURFACE ROUGHNESS

The healing of fractured bone is inversely proportional to microcracks generated in bone surface and heat generation during drilling of bone is directly proportional to drilling speed **[16]**. In addition, the major problems that occurs during drilling are due to bad surface topology of bone surrounding and the surface topology of bone depends upon the surface roughness of bone. Many of the researchers, studied about the surface topology and texture of bone surface.

Alam et al. observed the surface roughening as a means of enhancing bone ingrowth on bovine bone drilled specimen. He compared two drilling techniques i.e. conventional and vibrational drilling of bone for optimizing the surface roughness of drilled bone specimen. According to the results, it was concluded ultrasonic assisted drilling produces smoother and fine surface texture of hole surface as compared with conventional drilling **[31].**

Singh et al. studied surface topology of bovine bone and concluded that better finish and better quality holes are observed with ultrasonic machining due to less mechanical forces gives finer surface of bone specimen as compared to conventional drilling. According to results, on increasing rotational speed and feedrate, the surface roughness of bone was also increased. The lowest surface roughness was observed at his experiments with the drilling parameters of rotational speed 600 rpm, feedrate of 10mm/min and using twisted drill bit **[10]**.

Singh et al. optimized process parameters for better quality characteristics for drilled hole during bone drilling. He uses three types of drill bit, which are twisted drill, hollow drill without abrasive and solid abrasive coated drill bit on bovine cortical bone. According to him for better surrounding surface, the twisted drill bit should be used as compared to hollow and abrasive drill bits **[32] .**

Singh et al. focused on optimizing the major drilling process parameters i.e. rotational speed and feedrate for surface roughness and material removal rate. The experiments were performed on cortical bovine bone as it has similar properties (Tensile strength, Compressive strength, Density, Thermal conductivity) as the human bone. According to the results, on increasing the rotational speed, the measured surface roughness was decreasing. By SEM images, it was evidenced that using twisted drill bit produces fine and uniform circular hole. Whereas using diamond abrasive coated tool, the surface texture of bone was rough and non-uniformly distributed as shown in figure 2.7. According to his results, the fine surface texture of bone using twisted drill bit gives better surface finish of bone **[33].**

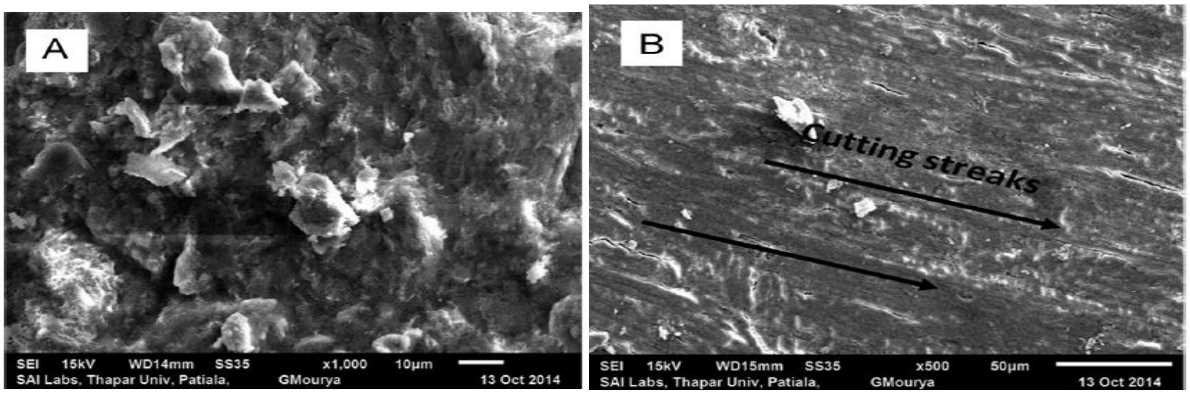

Figure 2.7 Bone drilled using (a) abrasive coated tool, (b) twist drill tool [33]

The poor surface finish of bone enhances the increase in microcracks level that is the main reason for decrease in elastic modulus and stiffness of bone. In addition, if the length of cracks in bone is equal to, or greater than, 300 µm then these microcracks cause bone failure, but below 300 µm length, the bone can be repaired **[28]**.

2.3 STATUS BASED ON PULLOUT STRENGTH

Chao et al. focused on the pullout strength and failure pullout energy of distinct pedicle screw in osteoporotic cadaveric model. This study helps to determine the axial pullout strength of cortical screw through the mechanical testing. Cement- augmented, cannulated-fenestrated pedicle screws in an osteoporotic cadaveric thoracolumbar was studied. From the results it was found that better initial fixation strength and better revision characteristics in cannulated-fenestrated screws than the Cement-augmented screws **[34]**.

Kim et al. in 2012 compared cylindrical pedicle screw with the conical core and cylindrical threaded screws. From the pullout results, it was concluded that the conical core and cylindrical thread screw performed, 23–37% better in Pullout testing than true cylindrical screws **[35]**.

Abshire et al. compared conical pedicle screws with cylindrical pedicle screws of the same thread surface area and thread pitch to optimize initial stiffness and fixation strength. The pedicle screw pullout failure is due to bone mineral density, screw thread area and pedicle morphology. The screws were instrumented on porcine lumbar vertebrae and axial pullout testing is performed on both the screws. According to results, the conical screw offers improved axial strength as compared to cylindrical screw. The bone core surrounding of conical screw is more as compared to cylindrical screw as shown in figure 2.8. The conical screws provide 17%

increase in the pullout strength and 50% increase in initial stiffness as compared to cylindrical screw **[36]**.

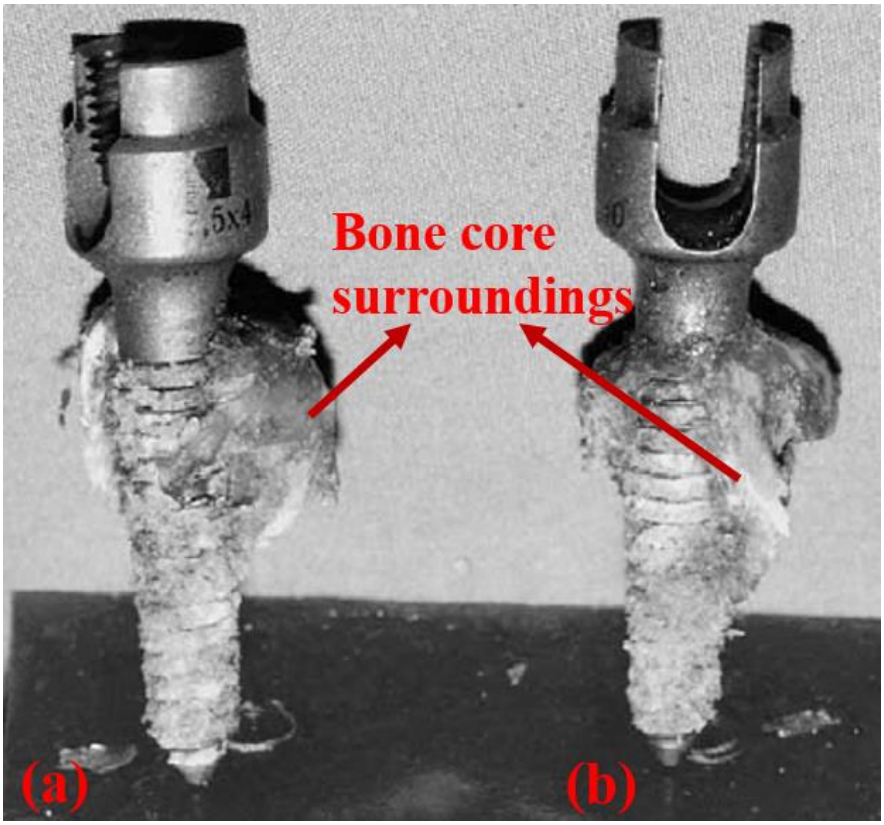

Figure 2.8 Screw threads after pullout (a) conical screw (b) cylindrical screw **[36]**.

Zdero et al. compared 3.5 mm and 4.5 mm standard bicortical screws inserted into synthetic third generation composite femurs used to measure pullout strength and compared to existing adult human cadaveric. For 3.5 mm screws, the measured extraction shear stress in synthetic femurs (23.70–33.99 MPa) was in the range of adult human tibias (24.4–38.8 MPa). For 4.5 mm screws, the measured values in synthetic femurs (26.04–34.76 MPa) were also similar to adult human specimens (15.9–38.9 MPa). According to results, the 4.5 mm screws showed statistically higher stress required for extraction than 3.5 mm screws **[37]**.

Zhang et al. investigated the interaction of bone material and purchase length on screw pullout strength, the experiments was carried out on human spine. The results showed that failure of the connection between bone and screw was due to bone shearing. The cortical shell resists around 50% of the pullout strength for a screw of 4mm in major diameter and 22mm in length. The stability of the inserted surgical screw is dependent on bone material. The significance of the purchase length on the pullout strength of cortical screw will be much lower than that in cancellous bone screw **[38]**.

Gracco et al. determined the effects of variations in thread shape on the axial pullout strength of orthodontic miniscrews. Self-tapping and self-drilling miniscrews of diameter of 2 mm and a thread shaft length of 12 mm used on synthetic bone. Thread design is most influenced parameter to pullout of the orthodontic miniscrews. According to results, the buttress reverse thread shape provided the greatest pullout strength **[39]**.

Hui Wu et al. performed in vitro study for pullout strength of orthodontic palatal. Thirty palatal mini-implants (2 mm in diameter) of three brands (Absoanchor, Bio-Ray, and Lomas) were manually driven into artificial bone (Sawbones) to a depth of 5 mm. The pullout strengths of all the brands were significantly greater than routine orthodontic forces. The vertical pullout strength of the absoanchor mini-implants was the lowest among the tested brands, and the horizontal pullout strengths of the Lomas and Absoanchor mini-implants were significantly higher than that of the Bio-Ray mini-implant **[40]**.

Gupta et al. in 2017 had performed experiments on rotary ultrasonic bone drilling (RUBD) and focuses on investigation of microcracks and pullout strength of cortical screws of porcine bone drilled holes as shown in figure 2.9..

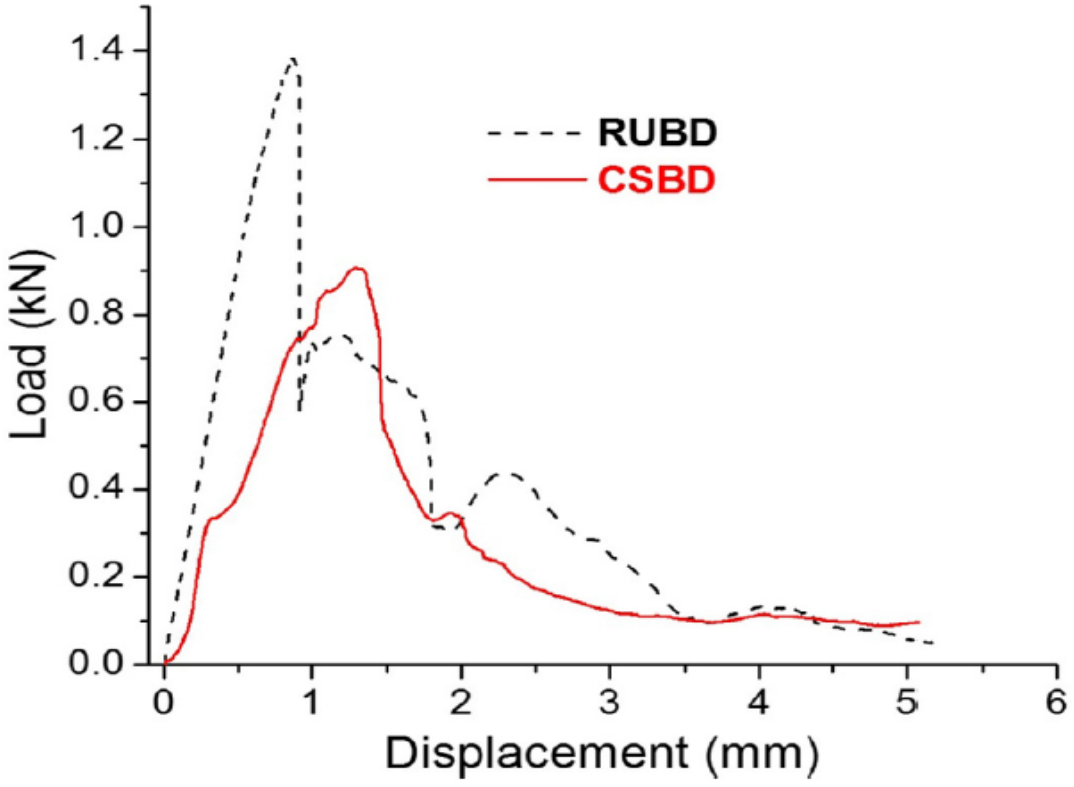

Figure 2.9 Axial pullout strength results for cortical screw **[28]**

According to conclusions, higher the rotational speed of drilling leads to decrease in the width of microcracks. Comparing both the drilling techniques, it was clear that axial pullout strength of cortical screw increases with higher rotational speed and the strength of screw decreases with the increase in feedrate. However, the pullout strength of cortical screws inserted in the RUBD drilled holes are consistently higher as compared to CBD as shown in figure 2.9. Hence, RUBD is a better alternative to CBD techniques. RUBD generated less damage to bone and providing higher stability for implants, as increase in length of microcracks of bone led to decrease in the strength of bone screw joint. As the hole drilled by rotary-ultrasonic are free from micro cracks and give better anchorage to the screw **[28]**

According to the literature review, the damaged bones are not capable of holding the implants and screws for a very long time. The anchorage strength of screw and microcracks in bone are the main reason for the stability of screw.

2.4 REVIEW ON SBF

Tadashi Kokubo et al. described that a material is able to grow the apatite on its surface in simulated body fluid (SBF). The apatite produced on surface in the living body, and bonds to living bone through this apatite layer. Hence, examination of apatite formation on surface of a material in simulated body fluid is useful for predicting in vivo bone bioactivity of the material**.** According to him, SBF can be used for screening bone bioactive materials before animal testing and the number of animals used **[41]**.

Singh et al. prepared simulated body fluid for preservation of PLA scaffolds porduced by additive manufacturing technique. He used SBF solution to analyze the apatite growth in fabricated scaffolds. Due to apatite growth, weight of specimens firstly increased but then decreased. During his experiments, pH value was measured and noticed that it is decreasing with increasing time period. The major outcomes of this investigation exposed that scaffold having maximum porosity with 60% of infill percentage. The apatite growth represents the maximum bone cell growth in porous structure of PLA. Hence, for implant material PLA scaffolds can be used instead of titanium implants for healing little fractures and for big fractures, a titanium implants can be preferred **[42].**

FAN Xin et al. analysed the bone-like apatite formation on the surface of biocomposite material of stainless steel (316L SS) in simulated body fluid. The results showed that calcium

deficient apatite is bone-like apatite with excellent bioactivity. In addition, stainless steel biocomposites are excellent bioactive materials and possess promising applications as biomedical materials. Figure 2.10 is shown to explain the effect of immersion time of HA60/316L on pH value of SBF on serval days. Before immersing in SBF the pH value was 7.33 but from 0 day to day 14, the influence of pH value increases during early days. At day 7 the maximum pH reached was noted 7.55 approx. mentioned in Figure 2.10 **[43]**.

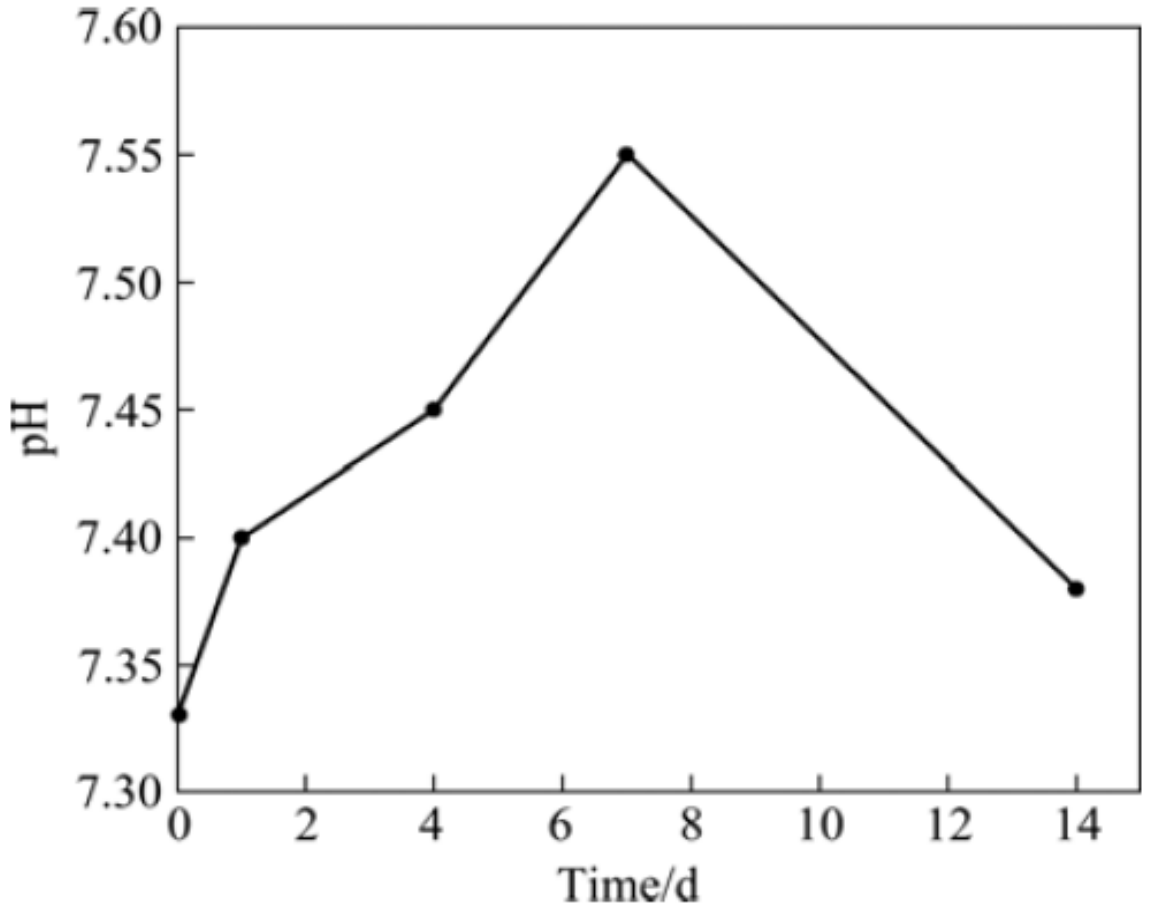

Figure 2.10 Effects of biocomposites immersion time in SBF on pH value **[43]**

Giavaresi et al. investigated on biological assessment of bone healing around uncoated and hydroxyapatite (HA)-coated pedicle screws in osteopenic bone. According to results, the uncoated stainless steel showed significantly lower bone-to-implant contact in osteopenic bone compared with HA-coated stainless steel because HA significantly improved bone ingrowth in healthy bone and enhances bone-to-implant contact. As well as at the inner thread area of pedicle screw, bone microhardness significantly increased in HA-coated surface **[44]**.

2.5. RESEARCH GAP & ANALYSIS

- After analyzing the literature gap, it can be seen that maximum work is done on the conventional bone drilling as compared to ultrasonic bone drilling.
- As per the author's knowledge, no study is focused on variation in grit sizes of diamond drill bits, during conventionally and ultrasonically bone drilling.
- Conventionally, in most of the studies, the objective is to reduce the surface roughness in metallic components machined with ultrasonic process. Enhancement of surface roughness and its benefit is scantly reported.
- In medical community no study focused on relating the surface roughness with the pullout strength of bone-screw joint during ultrasonic bone drilling.
- No articles were focused on effect of using SBF solution for checking the pullout strength of bone screw joint.

2.6. PROBLEM FORMULATION

According to literature survey, incidence of screw loosening of cortical screw ranges from 0.6% to 11% and it might be even more higher in osteoporotic spines **[45]**. It had been reported that the implant failure rate for lower leg is around 2.1-7.1% **[15]** and it is even higher than failure rate for upper limbs because of the physiologic stress during locomotion.

Keeping in mind the literature gap and analysis, also due to failure rate of cortical screw, the present dissertation is focused on **Effect of Roughness on Pullout Strength during Ultrasonic Bone Drilling: An in Vitro Study.**

2.7. OBJECTIVES OF THE PROPOSED WORK

- To optimize the machining parameters during rotary ultrasonic drilling of bone in view of maximizing the surface roughness.
- To investigate the screw embedded samples for apatite formation in SBF solution for distinct intervals of time.
- To examine the pullout strength of the bone - screw joint after distinct intervals of time.

2.8. METHODOLOGY

The complete methodology to be followed is expressed in figure 2.11.

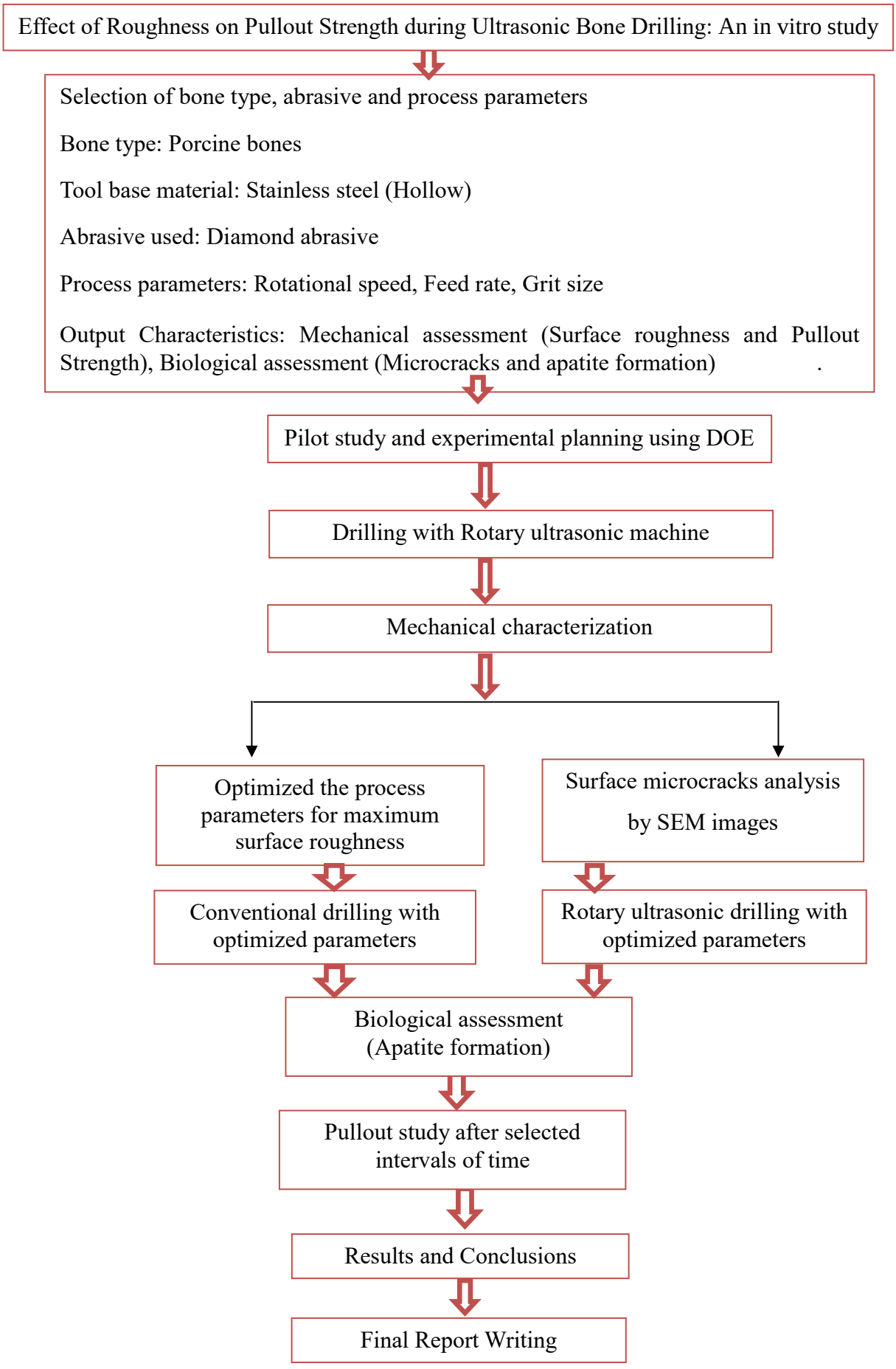

Figure 2.11 Flow chart for methodology

CHAPER: 3 MATERIALS AND METHODOLOGY

For performing bone drilling, specifications of drill bit, workpiece details, fixtures arrangements, drilling procedure and selection of major parameters are presented and expressed as follows:

3.1. WORKPIECE NOMENCLATURE

In vitro study is done on fresh porcine femur bone that is to be used as workpiece for drilling holes; bone was acquired from a local animal slaughterhouse as shown in Figure 3.1 (a). No animal was killed or euthanized for this investigation. Fresh pig bone was chosen because they have similar thermal and mechanical properties as of human bones **[4], [6], [7], [46]**. The porcine was approx. 11 months old and 89 kg of weight. Firstly distal and proximal ends of porcine bone was removed, then bone samples were cleaned and suitable samples of uniform area (flat surface of mid diaphysis), which can be used for investigation, were taken out from the mid-diaphysis section of the bone Figure 3.1 (b).

Figure 3.1 (a) porcine bone specimen for experimentation, (b) clean bone specimen from mid-diaphysis section

3.2. TOOLING DETAILS

From literature, it can be seen that a hollow tool possess more material removal rate (MRR) as compare to a solid tool in case of ultrasonic machining **[20]**. Moreover, it is expected that an abrasive coated tool reduce the force, temperature, thermal necrosis and microcracks, which

may be useful for pullout strength. Diamonds grits are used in the tool as they as biocompatible in nature and do not harm human body. Keeping, this in mind a hollow drilling tools is designed and fabricated by electroplating method of diamond abrasive particles with distinct grit sizes on the hollow shank of material stainless steel (Figure 3.2). These tools were fabricated from Ajex & Turner Wire Dies Company, India.

As per the availability constraints in size of the diamond grits, they are taken as coarse type (grit size of 230-270); Medium type (grit size of 140-170) and Fine type (grit size of 60-80). Hollow drill tool was designed therefore they act as an ultrasonic horn. They were designed with distinct inner and outer diameters.

The outer diameter (D_o) of tool was 3.5 mm, which is similar to mostly used conventional surgical bit whereas inner diameter (D_i) was 2.5 mm with constant wall thickness of 1mm. For confirmation about the grit sizes of diamond abrasives microscopy is performed on tools and images are shown in Figure 3.3.

Figure 3.2 three distinct diamond abrasive grit size hollow drill tools

3.3. DESIGN OF FIXTURE

Fixing of bone must be proper, otherwise the bone will disturbe from drill point as large rotational speed and forces may disturb the location of bone during drilling. Therefore, the porcine bone was fixed in a fixture very carefully. Hence, for the purpose, fixture has been designed with suitable dimensions and proper material of acrylic sheet. Cushioning is also provided in the fixture for subsequent sides of bone for stability. Figure 3.4 (a) and (b) shows the 2D view of fabricated fixture with the suitable dimensions chosen and the fabricated fixture.

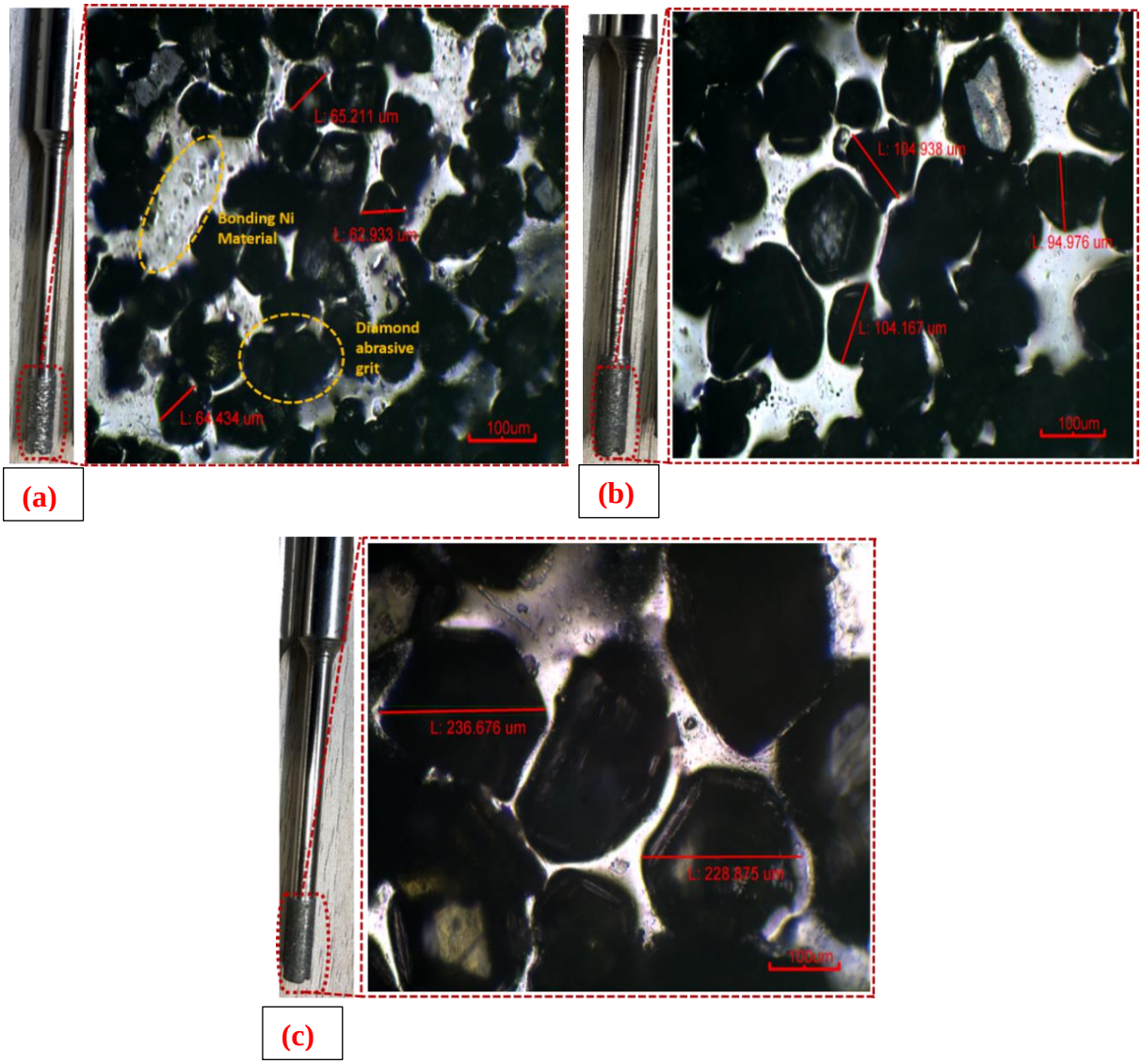

Figure 3.3 distinct microscopic images of (a) Fine type (b) Medium type and (c) Coarse type; of diamond abrasive hollow tools

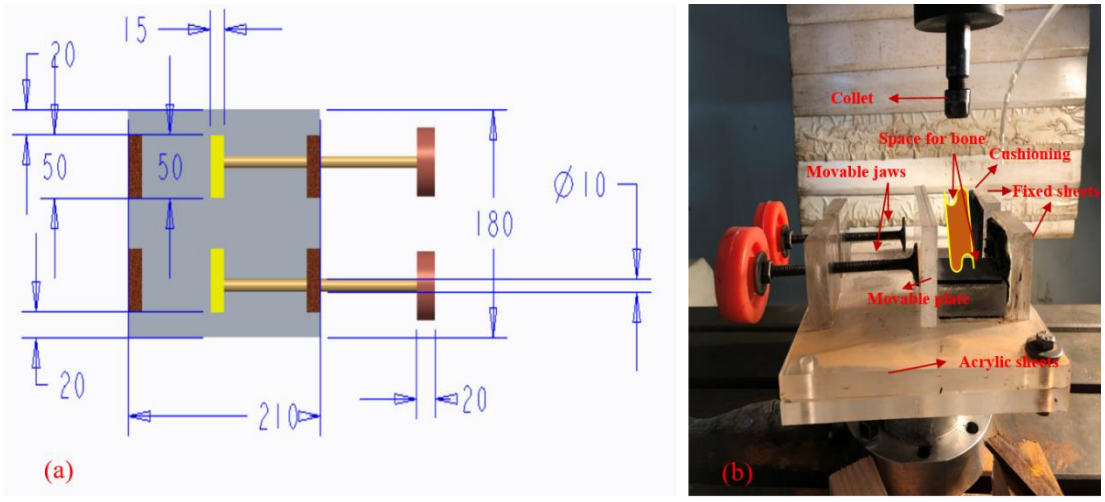

Figure 3.4 (a) 2D schematics of fixture, (b) fabricated fixture with cushioning to hold bone specimen

3.4. EXPERIMENTAL SETUP

The ultrasonic vibration tool setup is fixed at the chuck of CNC machine; also, designed diamond hollow tools were attached to horn of piezoelectric transducer which provides the linear acoustic vibration from transducer. The feed is provided by the stepped motor connected to a lead screw assembly. A base housing design has been made which provides the space for ultrasonic generator. A generator (frequency 20 kHz and power 800 W) to the ultrasonic device with carbon brushes and copper slip rings supplied electric signals. The CNC machine operated at tool feedrate ranging from 10 – 1000 mm/min and the spindle speed of drilling is 500 to 5000 rpm. The bone specimen was held in a special designed and fabricated bone-holding fixture. The complete experimental setup easily explained by Figure 3.5.

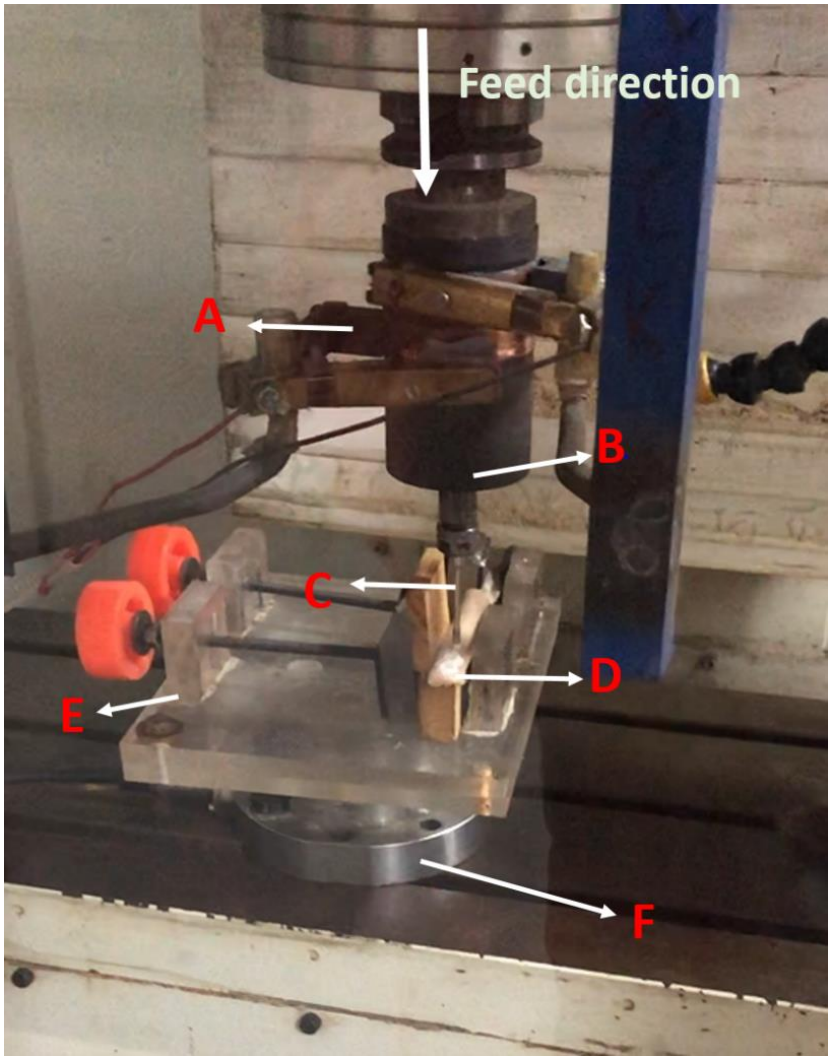

Figure 3.5 Experimental setups of UBD: (a) carbon bushes; (b) transducer; (c) hollow drill bit; (D) bone sample; (E) fixture; (F) dynamometer

3.5. SELECTION OF MAJOR PARAMETERS

The process parameters that are to follow in the experiments are taken from the literature review, machine constraints and commercial availability in the market. The selected major process parameters are rotational speed (in rpm), feedrate (in mm/min) and grit size. The screw diameter and drill diameter all kept constant parameters for throughout the complete experimentations. For ultrasonic bone drilling (UBD), the amplitude and vibrational frequency selected remains constant, which is 20 μm and 20 kHz respectively. Whereas, both the factors amplitude and vibrational frequency are not applicable for conventional bone drilling (CBD).

3.6. DESIGN OF EXPERIMENT

As discussed above in literature review, a number of variables are involved in bone drilling process and virtually all these variables affect the surface roughness. Thus, only the major dynamic variables were considered in this study. Three process parameters are selected as the control factors with each of 3 levels. These parameters and their level had been selected based on literature review as well as preliminary study. The rotational speed, feedrate and gritsize may varied according to their selected range of parameter. The parameters are mentioned in table 3.1 with their levels and values.

Table 3.1: Levels of parameters used in drilling

S. No.	Factors	Level	Value
1	Feed rate (mm/min)	A1	10
		A2	30
		A3	50
2	Abrasive Type	B1	Fine (60-80)
		B2	Medium (140-170)
		B3	Coarse (230-270)
3	Rotational Speed (RPM)	C1	500
		C2	1500
		C3	2500

Version of DOE was standardized by Dr. Taguchi, also known as Taguchi method. This technique is very user-friendly (easy to apply) and applied for improving the quality of product **[47]–[49]**. Various strategies are used to ensure an appropriate choice of runs. One of them is

Taguchi's orthogonal scheme. This orthogonal scheme is used in the present investigation as it is one of the most cost-effective, powerful, robust, and systematic statistical approach, which can reduce number of trials efficiently, also used when required to get the most favourable solution of any practical issues **[44]**. This scheme is very valuable and important to get the favourable and optimized set of parameters with minimum number of experiments. The experimental trials are decided based on the number of process parameters and the selected levels for experiment.

Orthogonal array selector can assist in determining how many trials are necessary and the factor levels for each parameter in each trial. Select the process parameters up to three levels and prepare the design of experiment in Mini Tab to check the optimum effect of individual parameter on the properties of bone. The L_9 orthogonal was selected for this investigation, which takes into account of three factors with their three levels as mentioned in table 3.1. as per L_9 approach, total number of experiments performed was nine. The degree of freedom for this set of levels is six; all the experimental control variables used in drilling of bone and their levels based on design matrix are given according to their run order in the table 3.2.

Table 3.2: Matrix for experimentation based on L_9 Orthogonal arrays for three process parameters

Run Order	Orthogonal array (L_9)	Feed Rate (mm/min)	Abrasive Grit Size	Rotational Speed (RPM)
1	L_1	50	70	500
2	L_2	50	155	1500
3	L_3	50	250	2500
4	L_4	30	70	1500
5	L_5	30	155	2500
6	L_6	30	250	500
7	L_7	10	70	2500
8	L_8	10	155	500
9	L_9	10	250	1500

3.7. DRILLING PROCEDURE

The ultrasonic drilling of porcine bone was carried out on CNC machine. Experiments are performed in three sets for all distinct types of tool. In the first set of experiments, fine type abrasive diamond tool was used, secondly the medium type and finally coarse type hollow diamond tool was used. The program for operating the CNC machine is mentioned in ANNEXURE A at the end. The drilling parameter and sequence of experiments was chosen accordingly to run order as mentioned in Table 3.2 (from L1 to L9). The drilled bone specimen are shown in figure 3.6. The produced size of drilled hole was 3.5 mm as similar to diameter the diamond hollow tools (3.5 mm). These holes were made to check and optimize the output parameter of surface roughness (Ra).

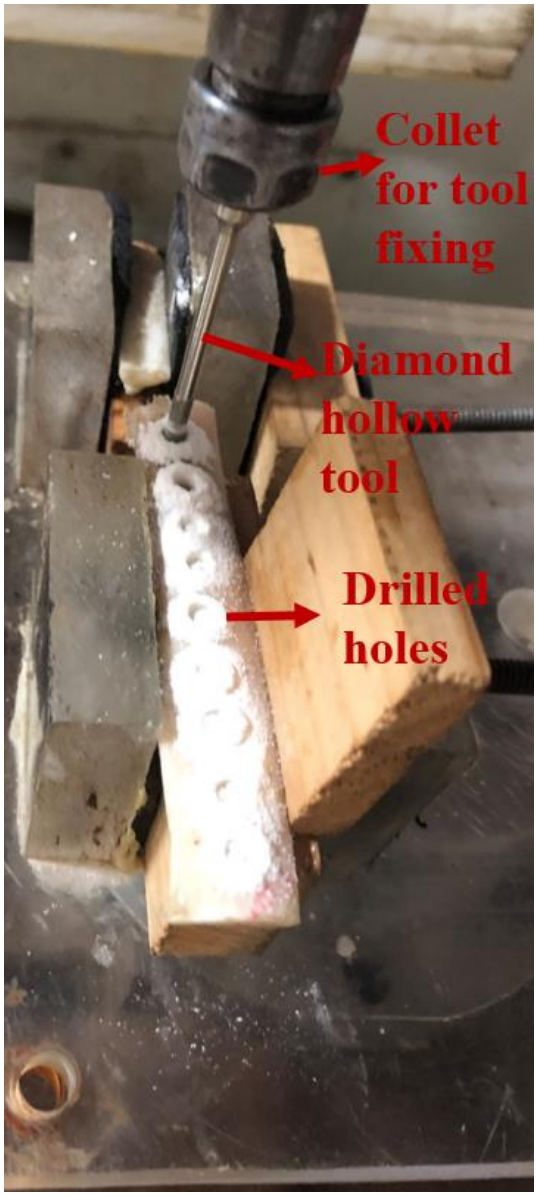

Figure 3.6 Drilled bone specimens

3.8 SAMPLE PREPARATION FOR Ra/ SEM CHARACTERIZATION

After selection of design matrix of process parameters, the bone specimen will be drilled with the parameters of orthogonal L_9 matrix. The experimentation is performed and the drilled bone sample is sliced carefully using surgical hacksaw along the axis of the bone to avoid the damage on the bone surface as described in Figure 3.7. The surface roughness is performed in the sliced bone samples.

The sliced samples was preserved in a buffered solution of 10% formalin solution and 90% of saline water.

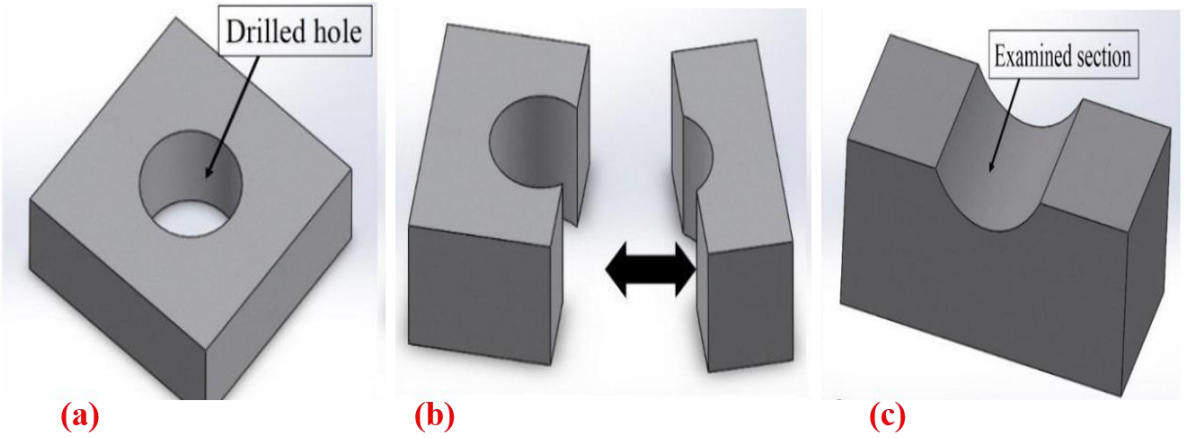

Figure 3.7 a) Specimen with drilled hole; b) Cross section view of Specimen; c) Examined section where roughness of the specimen is to be checked

After drilling the bone, the bone is carefully sliced into two pieces using surgical blades, after blading them, samples looks dirty and unclean. This affects the surface roughness (Ra) measurement and SEM characterization. Therefore, sliced bone is kept in hydrogen peroxide for 10 minutes, secondly samples are washed in enzyme detergent for 15 minutes, thirdly they are placed in a solution of 20% hydrochloric acid (HCL).

Then they are washed with distilled water, finally they are dried on incubator at temperature to 45 ^{0}C for whole night. Figure 3.8 explains complete stepwise process involved in it. Figure 3.9 depicts the samples before and after cleaning.

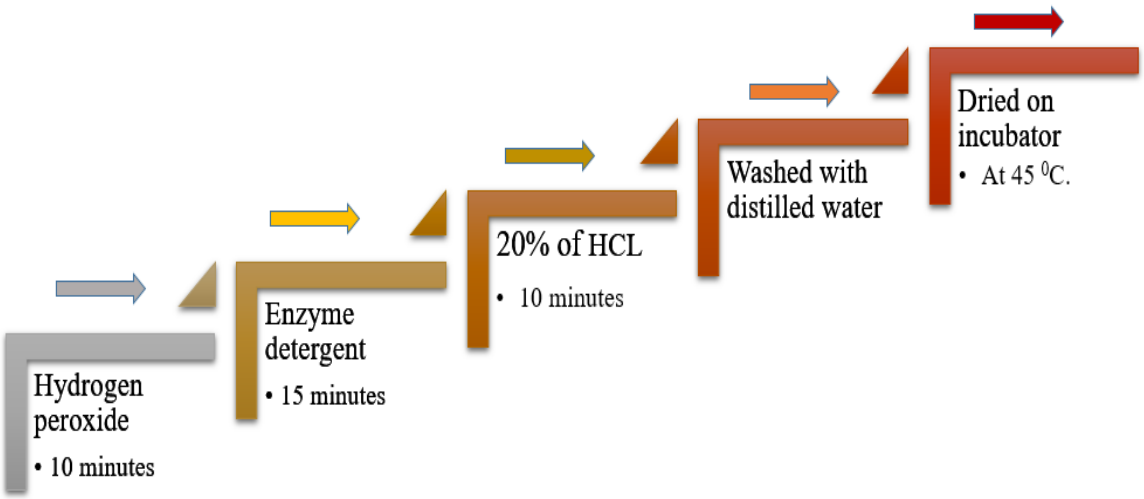

Figure 3.8 complete process of sample preparation

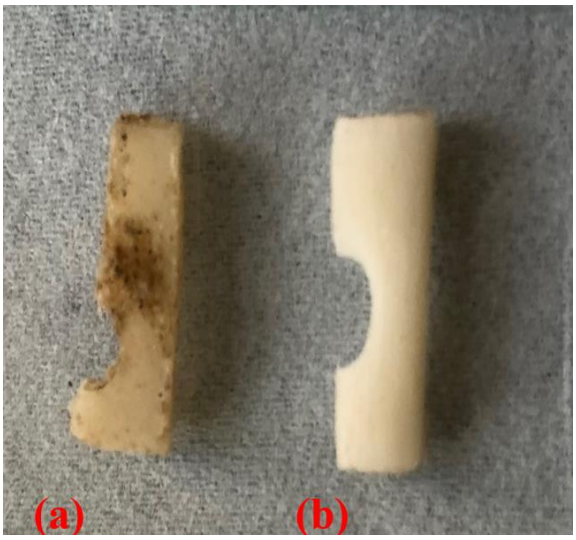

Figure 3.9 (a) Sample before preparation (b) Sample after preparation

3.9. MECHANICAL ASSESSMENT

Surface roughness (Ra) gives a general description for height variations in surface of a material. For knowing the surface texture of bone specimens all samples were tested for Ra measurement.

3.9.1 SURFACE ROUGHNESS

All the samples are characterized for surface roughness (Ra) using Mitutoyo SJ400 surface roughness tester. In addition, four reading were measured for surface roughness for each

sample (two reading at each one side of cutted sample from bottom of the cut section to the top) as shown in Figure 3.10. The cutting length of stylus was 0.08 mm and repetition (n) =1.

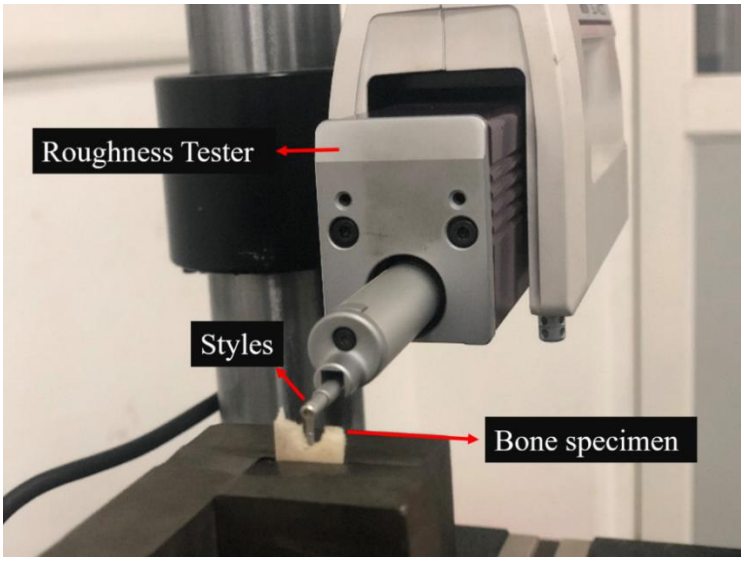

Figure 3.10 measuring Ra of drilled bone using surface roughness tester

3.10. EXPERIMENTATION (PART II) (FOR PULLOUT STUDY)

Based on result of surface roughness of bone specimen, the maximum and minimum value of surface roughness and corresponding parameters is noted and chosen as the basic parameters for pullout strength study. With same optimized parameters, conventional drilling is also attempted and corresponding roughness is noted down. In case of conventional bone drilling (CBD), the twisted surgical drill bit procured from Max orthopaedic, Patiala as shown in Figure 3.11 will be used. Whereas in ultrasonic bone drilling (UBD) the hollow diamond drill bit at optimized parameter will be used. The outer diameter of both hollow tool and twisted surgical tool are same as 3.5 mm.

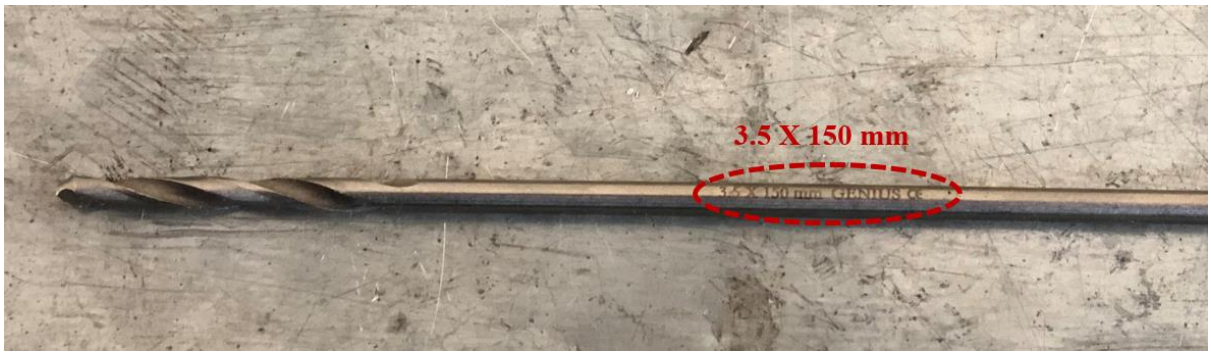

Figure 3.11 twisted surgical drill bit

3.10.1. CORTICAL SCREWS

After ultrasonic bone drilling (UBD) and conventional bone drilling (CBD), at optimized parameters, cortical screws are inserted in bone specimens using CNC machine up to same depth of cut of 40 mm. The care has been taken while inserting the cortical screw so that a constant pressure is applied throughout the insertion of screw. As extra pressure during insertion of screw may damage and harm the surrounding tissues of bone. Ideally, the cortical screw must be at 90^{o} from the bone. The inserted screw must be straight as uniformly axially inserted because during pullout study, one should get the complete vertical force (R_V), which will be the complete force exerted by the screw in the vertical direction. Whereas if a screw is inserted at an angle, the resultant force will have two components. One is in horizontal direction (R_H) and another in vertical direction (R_V) as shown in figure 3.12.

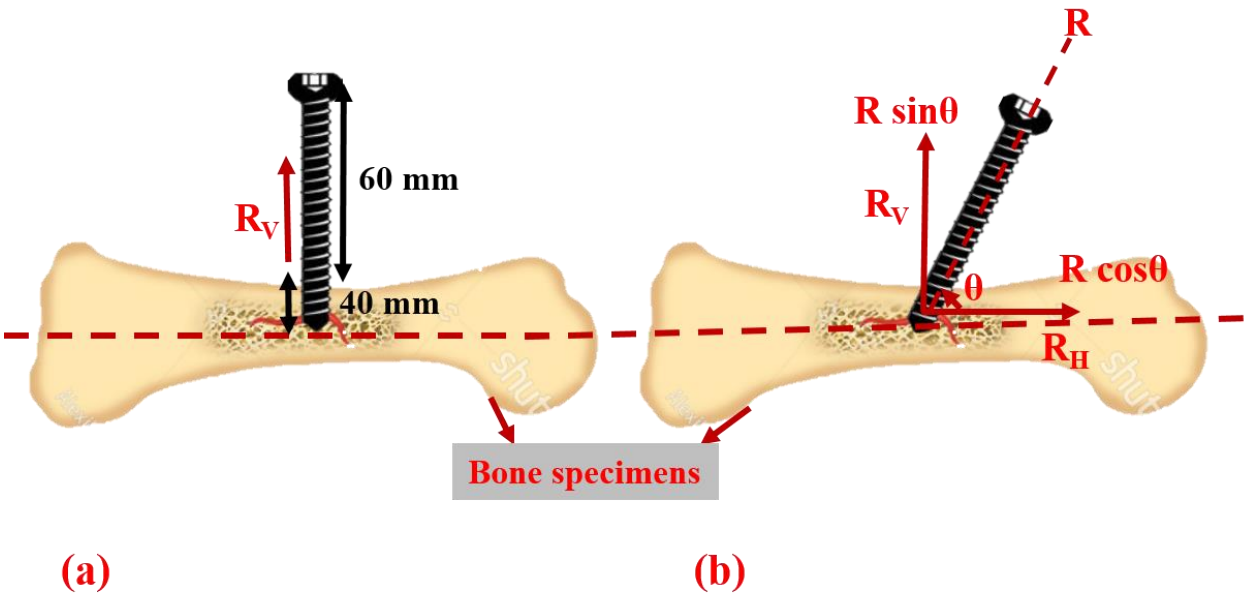

Figure 3.12 (a) bone with aligned and axially inserted screw, (b) bone with misaligned screw

The specifications of cortical screw are mentioned in table 3.3. Stainless steel cortical screws are used as per surgical standards because they are biocompatible in nature, they do not harm human body. The diameter of cortical screw is 4.5 mm as per surgical standard because orthopaedic surgeons uses drill tool diameter of 3.5 mm. Also, a length of 100 mm is used to hold the screw in pullout arrangement properly. The inserted bone-screw samples are shown in Figure 3.13 (a) and then they are cut in the same section using surgical hacksaw as shown in Figure 3.13 (b) and prepared samples for UBD and CBD are ready as shown in Figure 3.13 (c).

Table 3.3 Cortical screw specifications

Serial No.	Parameters	Specifications
1	Diameter	4.5 mm
2	Length	100 mm
3	Head diameter	8 mm
4	Pitch	1.75 mm
5	Material	Stainless steel
6	Grade	SS 316 L

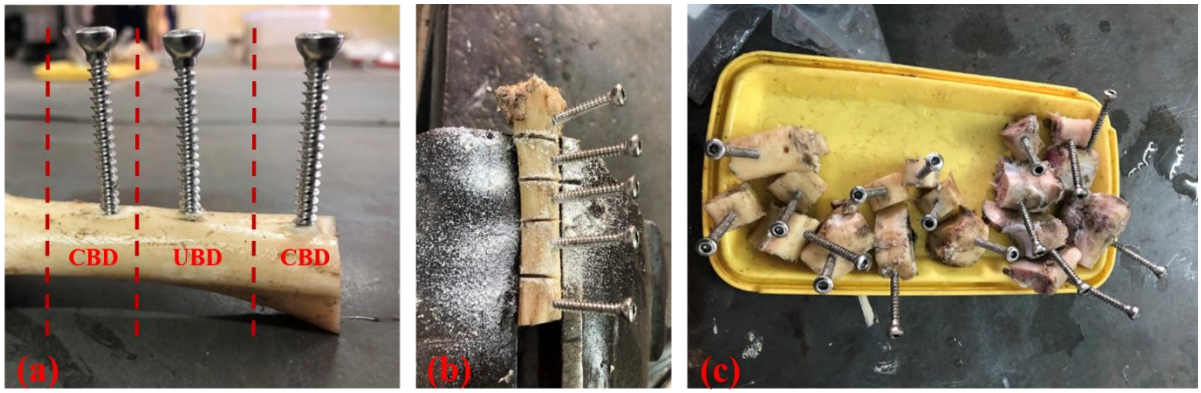

Figure 3.13 (a) screw inserted in bone samples, (b) slicing of bone sample, (c) prepared bone-screw samples

3.11. BIOLOGICAL ASSESSMENT

Biological assessment of bone is a biological survey of bone healing, apatite growth, Histomorphometry, solutions used during treatment like simulated body fluid (SBF), modified SBF(m-SBF), ionized SBF (i-SBF), improved SBF (n-SBF) etc.

3.11.1. Simulated Body Fluid (SBF)

SBF is an artificial fluid, which has almost equivalent ion concentration to human blood plasma. Various biomedical materials are used for SBF study, because of the ability to form apatite. It is widely used for in vitro study for various biomedical research. It is a combination of various reagents, which mainly helps for ion exchange and behave like human blood plasma.

In other words, we can say that it is an artificial blood plasma to assess the bioactivity of various artificial materials **[41]**. The table 3.4 shows the ion concentration of SBF with compare to human blood plasma [41], [43].

Table 3.4 Comparison of human blood plasma and SBF for ion concentration [41], [43].

Ion concentration (mMol/L)			
No.	Reagents	Simulated Body Fluid	Human blood plasma
1	Na^{+}	142.0	142.0
2	K^{+}	5.0	5.0
3	Mg^{2}	1.5	1.5
4	Ca^{2+}	2.5	2.5
5	Cl^{-}	147.8	103.0
6	HCO^{-3}	4.2	27
7	$HPO^{2-}{}_{4}$	1.0	1.0
8	$HCO^{2-}{}_{4}$	0.5	0.5
9	pH	7.4	7.2-7.4

The big advantage of SBF solution is, can save the life of animals that was used during the duration of animal experiments [41], [43]. For the preparation of SBF, distilled water and ion-exchanged is used; also, the powder reagents, which are majorly used as chemicals are as follows: NaCl, Na_2SO_4, $NaHCO_3$, KCl, $K_2HPO_4.3H_2O$, $CaCl_2$, $MgCl_2.6H_2O$, $(HOCH_2)3CNH_2$ and 1 mol of HCL.

3.11.2. PREPRATION OF SBF

The simulated body fluid is prepared in the research laboratory of Department of Biotechnology, TIET; Patiala, as per the following steps.

1. Take a 1000 ml plastic beaker, washed it with distilled water, and then dry to remove the water content and moisture. Alternative of water can use sprit to clean the beaker.
2. Take 600-800 ml distilled water in the plastic beaker and cover it with transparent glass.
3. Put the beaker on magnetic stirrer plate (figure 3.14) and dissolve the weigh reagents one by one as per given the table 3.5, Make sure that add another reagent when last one dissolved properly.
4. Adjust the temperature of the prepared solution at 37.5^0 c +- 0.5^0 c. Check the pH value of the solution using pH meter and adjust it around 7.4. To adjust the pH value can add 1N-HCL as acid. After getting required pH value, pH meter is removed from the solution and add water up to 1000 ml.
5. The total volume of water should be 1000 ml if use the quantity as per reagent table 3.5.
6. Transfer the solution from beaker to plastic bottle in which bone are kept and stored it in incubator at 37^0 c of temperature because it is the core human body temperature. Make sure the solution should be transparent as mentioned in Figure 3.14, if see some substances in solution while storage, don`t use this solution and prepared it again. The hot plate magnetic stirrer is used for proper mixing of reagents to water uniformly for preparing the SBF solution as shown in Figure 3.14.

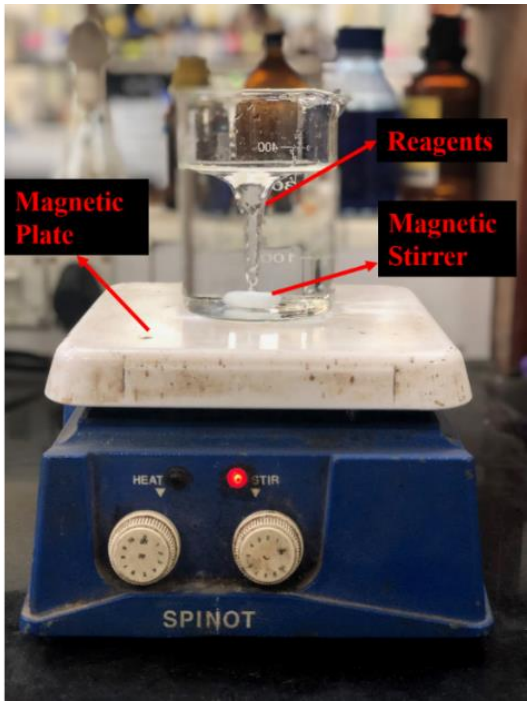

Figure. 3.14 Preparation of SBF on hot plate magnetic stirrer (Courtesy: Biotechnical Lab, TIET)

Table 3.5 Quantity of distinct reagents of SBF.

Serial No.	Reagents	Amount
1.	NaCl	7.995 g
2.	$NaHCO_2$	0.351 g
3.	KCl	0.225 g
4.	$K_2HPO_4\,3H_2O$	0.227 g
5.	$MgCl_2\,6H_2O$	0.306 g
6.	1M-HCL	41 ML
7.	$CaCl_2$	0.276 g
8.	NA_2SO_3	0.070 g
9.	$(CH_2OH)_3CNH_2$	6.056 g

3.12. PRESERVATION OF SAMPLES IN SBF

After preparing the SBF solution and inserted cortical screw, bone samples are preserve in the SBF solution for biological assessment and further mechanical characterisation. The bone-screw samples are filled with SBF solution in 150 ml plastic bottles and labelled these bottles with label strip with distinct nomenclatures as shown in Figure 3.15.

1. (CX1) Conventional maximum parameter as sample 1.
2. (UX1) Ultrasonic maximum parameter as sample 2.

The samples are characterized for apatite formation at an interval of 7 days. Example: the apatite formation is observed after 7 days (17-4-2019), then after 14 days (24-4-2019), then after 21 days (1-5-2019) and finally after 28 days (8-5-2019). The bone-screw samples persevered in SBF are shown in Figure 3.15.

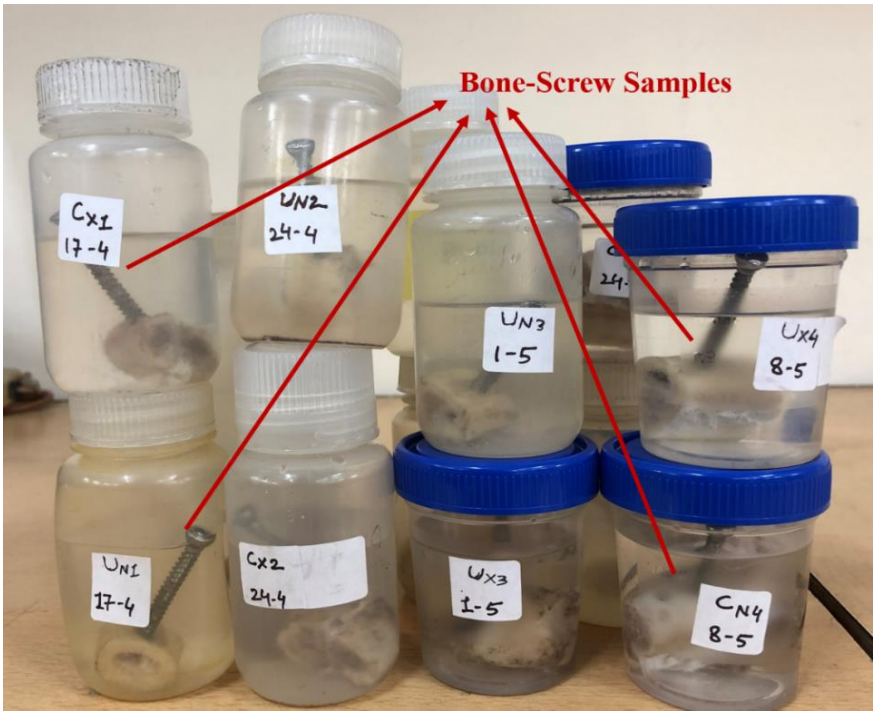

Figure 3.15 Bone-screw samples preserved in SBF solution

The temperature of the solution should maintain with the range equal to normal human body temperature. So, the temperature controller incubator is used to store the SBF bottles. The temperature of the incubator adjusts at 37^0C and revolution per minute around 130 RPM. All the bottles inside the incubator are placed properly as shown in Figure 3.16, switch ON the incubator.

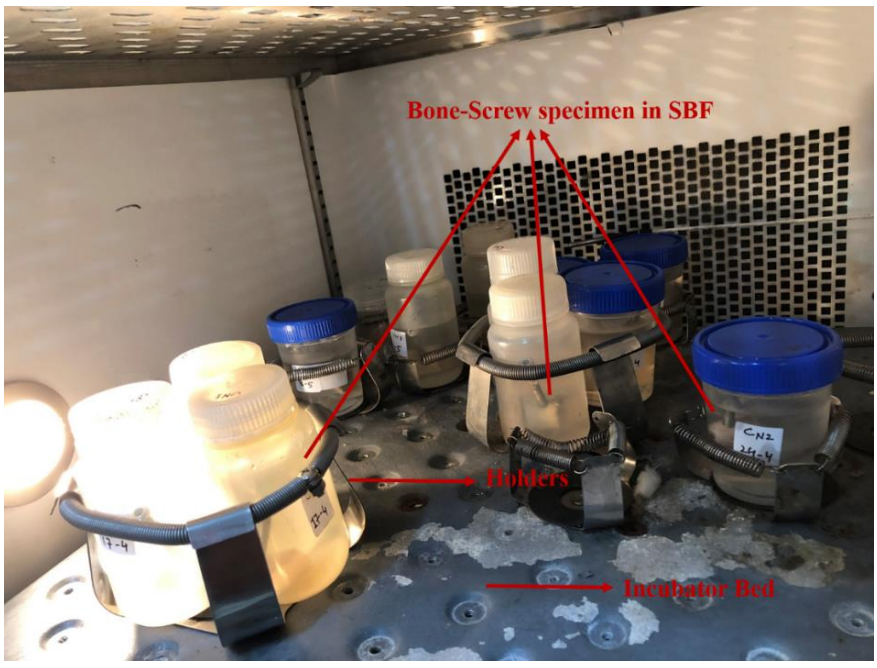

Figure 3.16 SBF Bone-Screw bottles preserved in incubator at 37^0C

3.13. pH VALUE MAINTANCE

The solution was monitored for pH value measurement two times a week using pH meter. The pH value of blood plasma of human is 7.2-7.4, so it is very important to maintain the pH value of solution as near it. The pH of SBF solution directly affect the apatite formation rate. The higher acid nature of the solution or lower pH value enhance the formation rate. The technique to check the pH value of the SBF is using a level probe dipped in the solution as shown in figure 3.17.

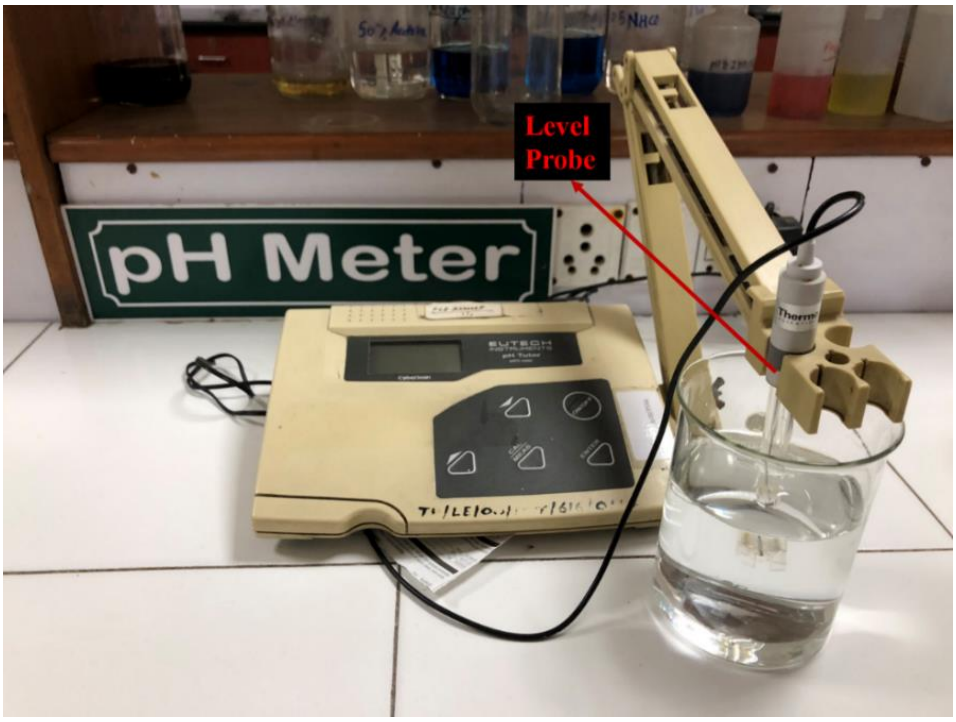

Figure 3.17 pH meter for measurement of SBF pH value. (Courtesy: Biotech Lab, Biotechnical department; TIET)

3.14. APATITE FORMATION

Measuring microscope (Figure 3.18) represent the Nikon Eclipse E100 microscope used to check the microstructure of the specimens and apatite formation or calcium phosphate growth on the surface of immersed specimens for distinct periods. The magnified lenses are varying from 10X/0.10 with high magnification to 10X/0.1 with low magnification images.

The growth on the bone is due to biocompatible nature of bone. The growth of apatite increases with increase in the time spans. The microscopy is done at the normal drilled bone and when the drilled bone is kept in SBF solution, and the difference in the growth of bone can observe

in Figure 3.19, it represents the bone image with the microscopic view to observe the apatite formation on the bone hole. As the grown bone supports more and provides higher sustainability to cortical screw.

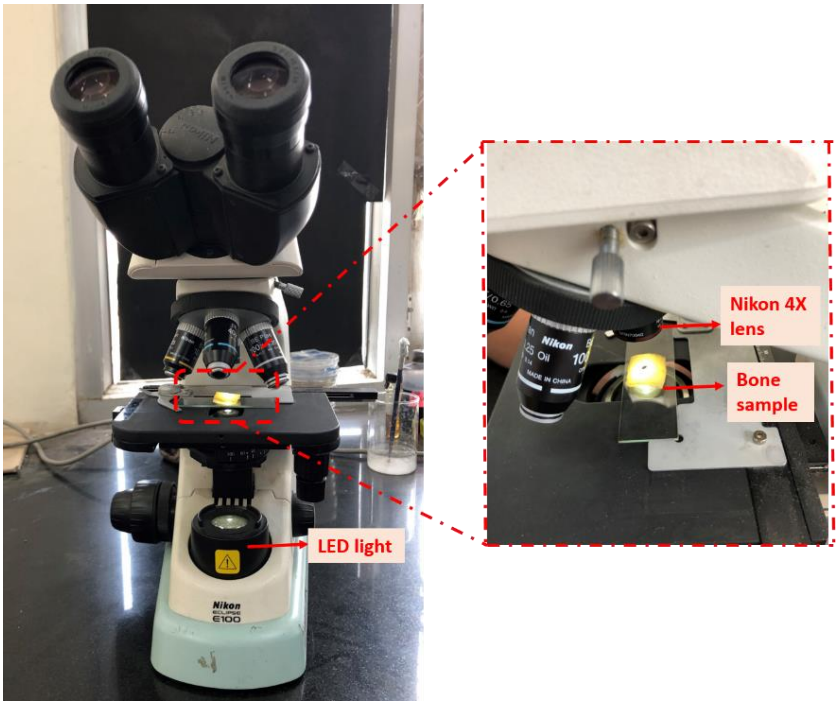

Figure 3.18 Nikon Eclipse E100 microscope for view of apatite formation on bone specimens

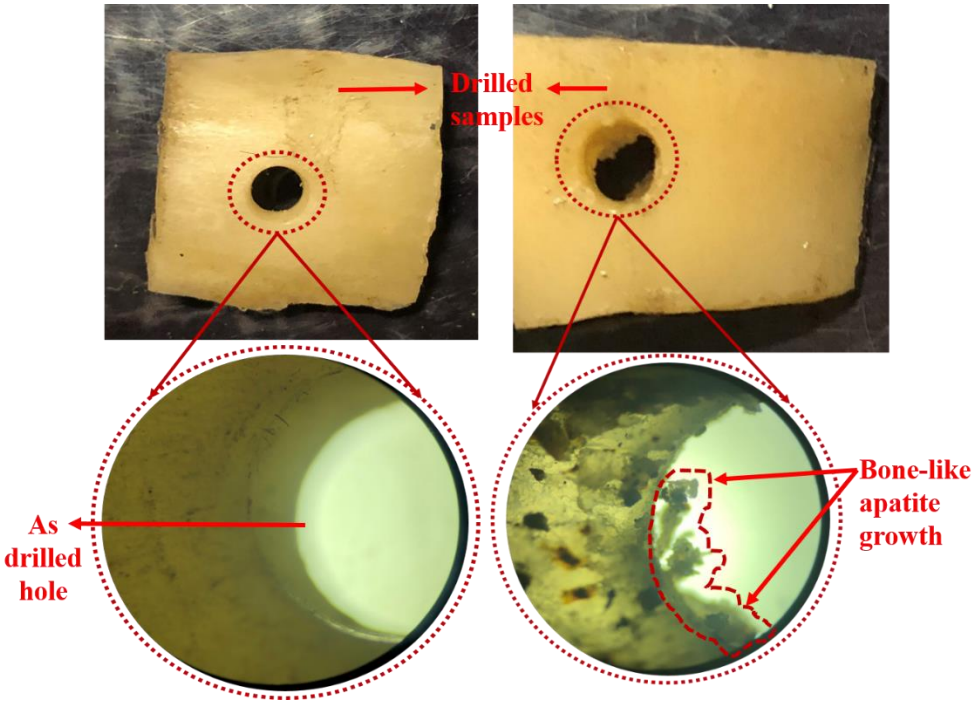

Figure 3.19 Magnified images of bone sample to observe the apatite growth

3.15. PULLOUT MEASURMENT

After getting the knowledge about the microstructure of bone growth, the parameter that produces maximum, minimum rough peak surface on the bone, and those parameters were used, and prepared bone screw samples were tested for observing the pullout strength of cortical screw. Pullout strength is one the major reason for the implant failure because the sustainability between the bone and the screw reduces, which reduces anchoring strength and leads to failure like screw loosening and implant failure.

3.15.1. FIXTURE FOR HOLDING BONE SCREW JOINT

As the screw is already inserted in the bone and kept in SBF solution, it is very difficult to fix the bone screw samples directly in the Universal Testing Machine (UTM). Therefore, a special fixture has been designed for holding the bone screw joint in the UTM machine. The bone must be fixed properly to pull the screw from bone screw samples. This fixture is produced with cast iron and consist of two parts. One has to connect at the upper movable jaw of UTM machine for fixing the cortical screw and other part is fixed at the bottom jaw of machine for holding the bone screw samples. Upper part of the fixture is cobbled together in milling machine for given dimensions and at the sides of upper fixture two holes were machined on both the sides to fix the screw head properly as shown in Figure 3.20 (a).

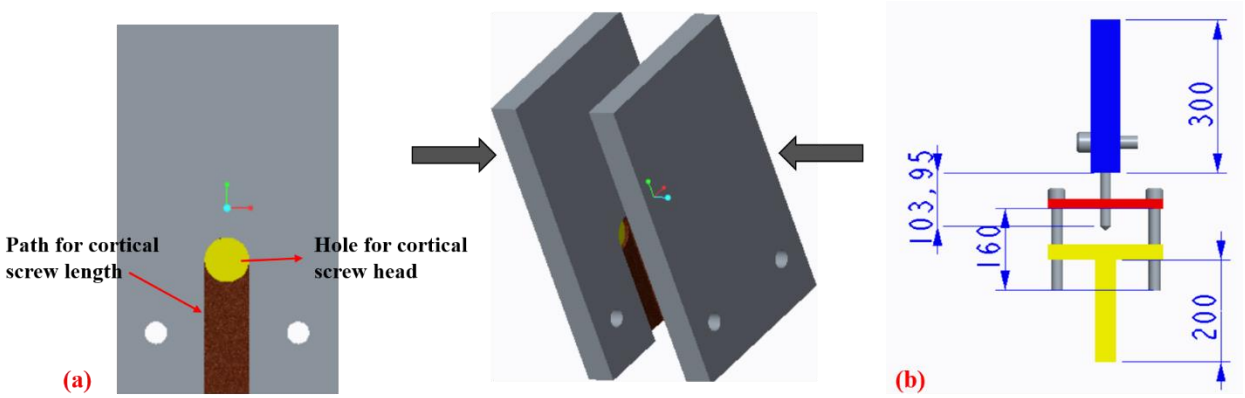

Figure 3.20 (a) CREO model for upper fixture, (b) CREO model with dimensions for bone screw holding fixture

Where as in the lower fixture for holding bone screw, welding is done at T side for giving base to bone screw joint and fix at lower jaw of UTM machine. CREO model of holding fixture is

expressed in Figure 3.20 (b). After fabricating fixture bone screw sample is kept in between lower and upper fixture and fixed with four screws because of uncertain shape of bone sides of upper fixture can be managed accordingly.

3.15.2. FIXING BONE-SCREW SAMPLES

Maximum efforts has been made to fix the bone in the fixture in perpendicular direction (axially at 90^{o}) to the bone as shown in figure 3.21 (a). The samples, which were not axially perpendicular to the bone, were removed as shown in figure 3.21 (b) because we will not get the proper value of pullout strength during fixing in universal testing machine (UTM). It will give the value of two forces, vertical force (R_V) and horizontal force (R_H) as explained in figure 3.21 (b).

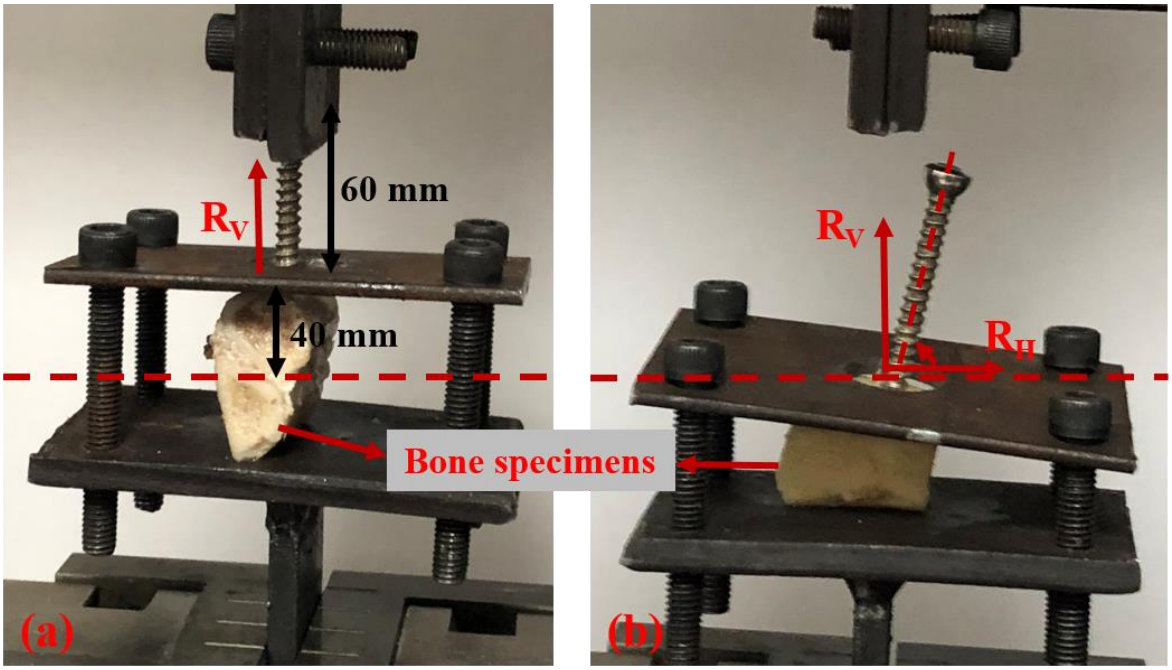

Figure 3.21 (a) axially fixed bone screw sample in fixture, (b) misaligned bone screw sample fixed in fixture

The bone screw samples were tested for pullout strength of the cortical screw in a UTM machine of Zwick/Roell Z005 as shown in Figure 3.22. This machine has maximum capacity of 10 KN. The bottom jaw of machine is fixed whereas the upper jaw is movable for testing the tensile strength.

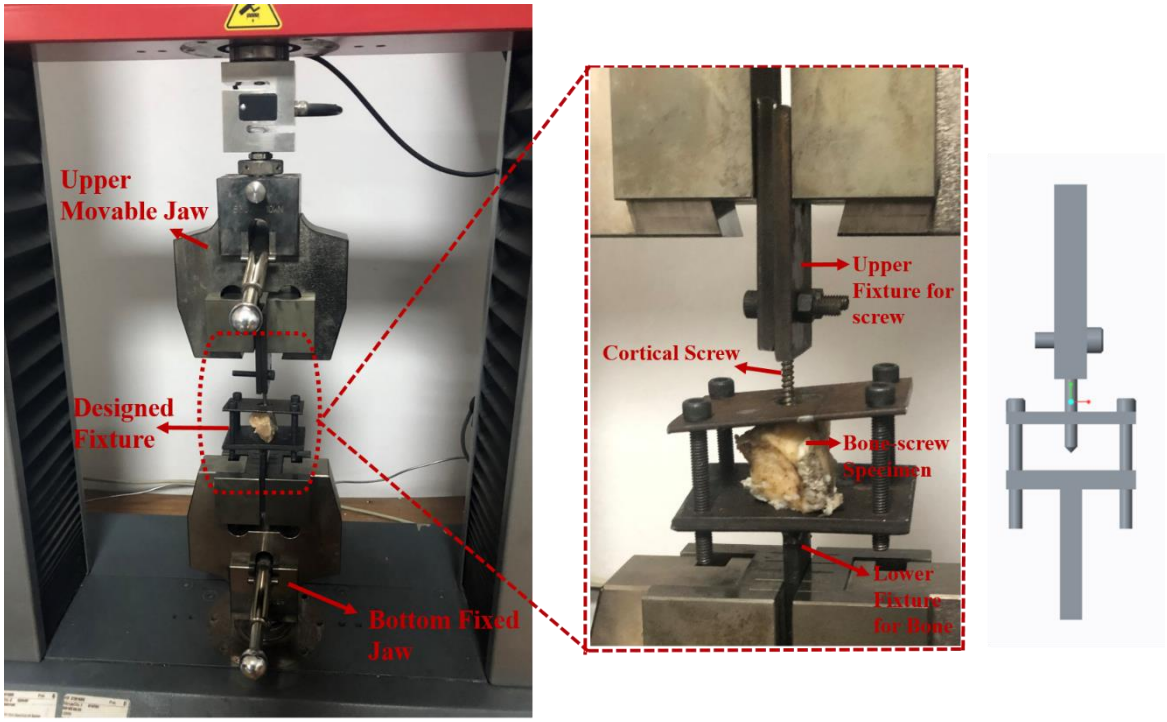

Figure 3.22 UTM machine with fixture and bone screw sample

CHAPER: 4 RESULT AND DISCUSSION

The surface roughness is the measurement of fine surface irregularities in surface texture of bone. Surface roughness (Ra) is the arithmetic average deviation of surface valleys and peaks expressed in micrometres (µm). The Ra of drilled bone specimen varies with different process parameters, the effect of these parameters on Ra can be observed as follows:

4.1 SURFACE ROUGHNESS (Ra) MEASURMENT

As the Ra of all nine samples was measured, four reading was measured for each one sample (2 readings on each cut sample). The data of four values measured roughness is given in table 4.1. These values is averaged for final roughness for each sample. The analysis of average final value of surface roughness (table 4.1), are used to observe optimized combination of parameters suggested by Taguchi method.

Table 4.1: Average of Surface Roughness based on four measured Ra (µm)

Serial No.	Orthogonal array (L_9)	Surface Roughness (µm)				Average Surface Roughness (Ra) (µm)
		Ra_1	Ra_2	Ra_3	Ra_4	
1	L_1	0.95	0.94	0.976	1.01	0.972
2	L_2	1.29	1.31	1.298	1.25	1.287
3	L_3	1.53	1.4	1.31	1.32	1.390
4	L_4	0.61	0.72	0.79	0.8	0.730
5	L_5	1.02	0.98	0.916	0.98	0.974
6	L_6	1.66	1.6	1.45	1.402	1.528
7	L_7	0.54	0.46	0.51	0.446	0.489
8	L_8	1.1	1.24	1.182	1.15	1.168
9	L_9	1.23	1.21	1.2	1.14	1.195

In this case larger, the better is taken, because it is expected that, higher surface texture provide higher stability and higher anchorage strength to cortical screw in implants. In order to find out parameters that are most significant in affecting surface roughness, an analysis of variance (ANOVA) has been performed. ANOVA is very helpful DOE tool, which is used as a computational technique that helps to estimate the relative contributions of each control factor.

4.1.1 Effect of major parameters on Ra

The effect of process parameters on surface roughness as shown in Figure 4.1. Here the effect of roughness on each process parameter can be understood at each level selected.

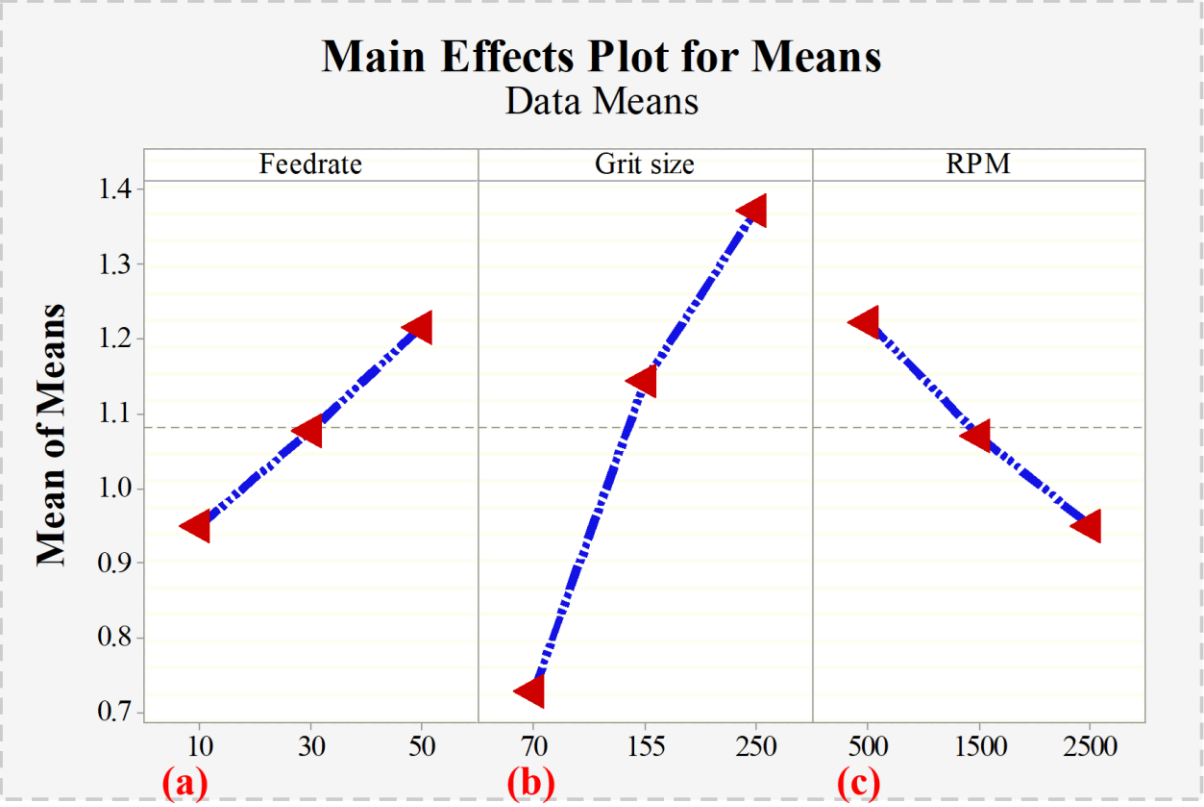

Figure 4.1 Surface Roughness results based on: A) Feedrate; B) Grit Size; C) RPM

4.1.1.1. Feedrate vs roughness

As an increase in feedrate resulted in a significant increase in Ra, which is also shown by the results in Figure 4.1(a). The reason behind this sudden increase is due to surface contact between the tool and bone specimen. As feedrate increases, the friction and centrifugal force increases also reported by the researchers [32][30]. Hence, the observed surface roughness is increased. Also at higher feedrate, the cutting time is reduced as the tool engagement with the bone decreased. While taking higher the better, we consider 50 mm/min as our optimized parameter of feedrate.

4.1.1.2. Grit size vs roughness

The effect of increase in gritsize (microns) of diamond abrasive particles results in significant increase in the surface roughness as mentioned in Figure 4.1(b). It means coarse type (grit size

of 250µm) diamond burr gives the maximum surface roughness. Since large gritsize gives more contact between the bone and tool, the material removal rate is higher which gives higher surface texture. Whereas the medium type (grit size=155µm) results central surface texture lower than coarse abrasive but higher than fine abrasive type. As the maximum surface roughness is observed at using coarse abrasive type tool (grit size of 250µm) which is our optimized parameter in view of maximum roughness.

4.1.1.3. Rotational speed (RPM) vs roughness

Effect of RPM on surface texture of bone samples is shown in Figure 4.1(c). It has observed that the roughness of bone is inversely proportional to rotational speed, as on increasing the rpm gradually the surface roughness decreases. Within increase in the RPM, the cutting forces are being reduced due to which surface roughness decreases. Since highest surface texture was obtained at rotational speed of 500rpm due to getting more size in chip formation. At lower rotational speed we are getting macro level chips whereas at higher rpm, micro type of chip formation is observed as shown in figure 4.2 [30]. Hence, 500 rpm is the optimized rotational speed parameter in view of maximizing the surface texture of bone.

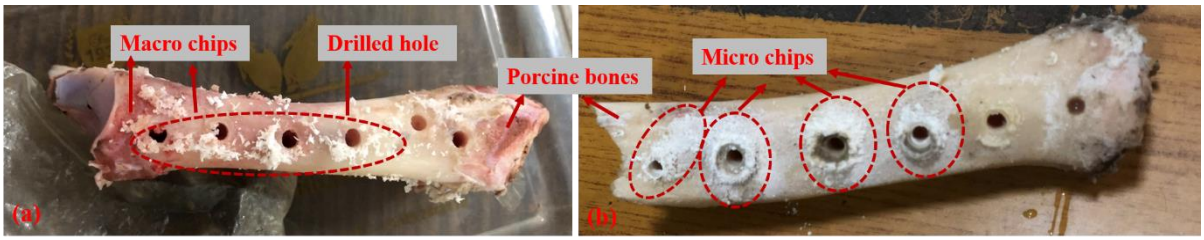

Figure 4.2 specimen drilled with (a) coarse diamond hollow bit, (b) fine diamonds hollow bit

4.1.2. Statistical analysis for surface roughness

The details of the data analysis of means for surface roughness have been presented in Table 4.2. The table shows tabulated F ratio values at this analysis is 19.37 and calculated F ratio of rotational speed is 20.67 (13% Contribution) and for feedrate is 19.69 (12.38% Contribution) during the experimentation. All these statistics were more than tabulated values of 19.37, so these factors are significant. However, the most significant parameter observed for surface roughness was the grit size of diamond tool. It shows the F ration value of 117.57 (73.97% contribution), which is very high contribution in this experiment. It confirm that the diamond grit size is the major important factor for controlling the surface texture of bone.

Table 4.2: ANOVA of means for Ra (μm)

Source	DOF	Seq. SS	Adj. MS	F	P	% Contribution
Feed rate	2	0.105944	0.052972	19.69	0.048	12.38%
Grit size	2	0.632732	0.316366	117.57	0.008	73.97%
RPM	2	0.111227	0.055613	20.67	0.046	13%
Residual Error	2	0.005382	0.002691			
Total	8	0.855284				

DOF - degrees of freedom, MS - mean squares (Variance), SS - sum of squares, F-ratio of variance of a source to variance of error. Tabulated F-ratio = 19.37

Response table of mean for (Ra) surface roughness is shown in table 4.3, which explains the ranking order of the process parameters. Moreover, according to response table, the grit size is marked as first rank for all three levels followed by the feedrate and rotational speed is response out. The maximum surface roughness was shown at level 3 in 1st rank (shown by table 4.3) which is coarse type diamond tool (grit size 250) (from table 3.1). According to second rank, RPM that is rotational speed of drilling tool, from table 4.3, maximum surface was observed at level 1 which is 500 rpm. Thus, optimal settings of these parameters for maximum surface roughness are at minimum rotational speed (500 rpm), at maximum feedrate of 50 mm/min and using coarse sized diamond tool. Hence, from the analysis of variance of mean and response table, it is very clear that grit size of abrasives be the primary variable effecting the surface roughness of bone during experiment.

4.1.2.1. Interaction graph for surface roughness

From the response table 4.3, it is very clear that main effect of surface roughness is due to rank 1 and 2 which is grit size of abrasives and rotational speed. Hence an interaction plot has been plotted using MINITAB 16 software between the gritsize and rotational speed with surface roughness as shown in Figure 4.3. According to interaction plot, gritsize and surface roughness was compared with respect of rotational speed (RPM) as shown in Figure 4.3 (a). In the Figure

4.3 (a) green colour, indicate the 250 coarse type abrasive tool, red line is medium type and blue line is fine type according to notations. According to Figure 4.3 (a), 500 RPM and coarse type tool (green line) shows maximum surface roughness at L6, which is (1.528 µm). Similar results was shown by interaction of RPM and gritsize (Figure 4.3 (b)). From Figure 4.3, it`s clear that, interaction at RPM and grit size shows variation in Ra for good response at 500 RPM and coarse type diamond tool produces maximum Ra.

Table 4.3: Response Table for Means for Ra (µm)

Level	Feed rate	Gritsize	RPM
1	0.9507	0.7303	1.2227
2	1.0773	1.1430	1.0707
3	1.2163	1.3710	0.9510
Delta	0.2657	0.6407	0.2717
Rank	3	1	2

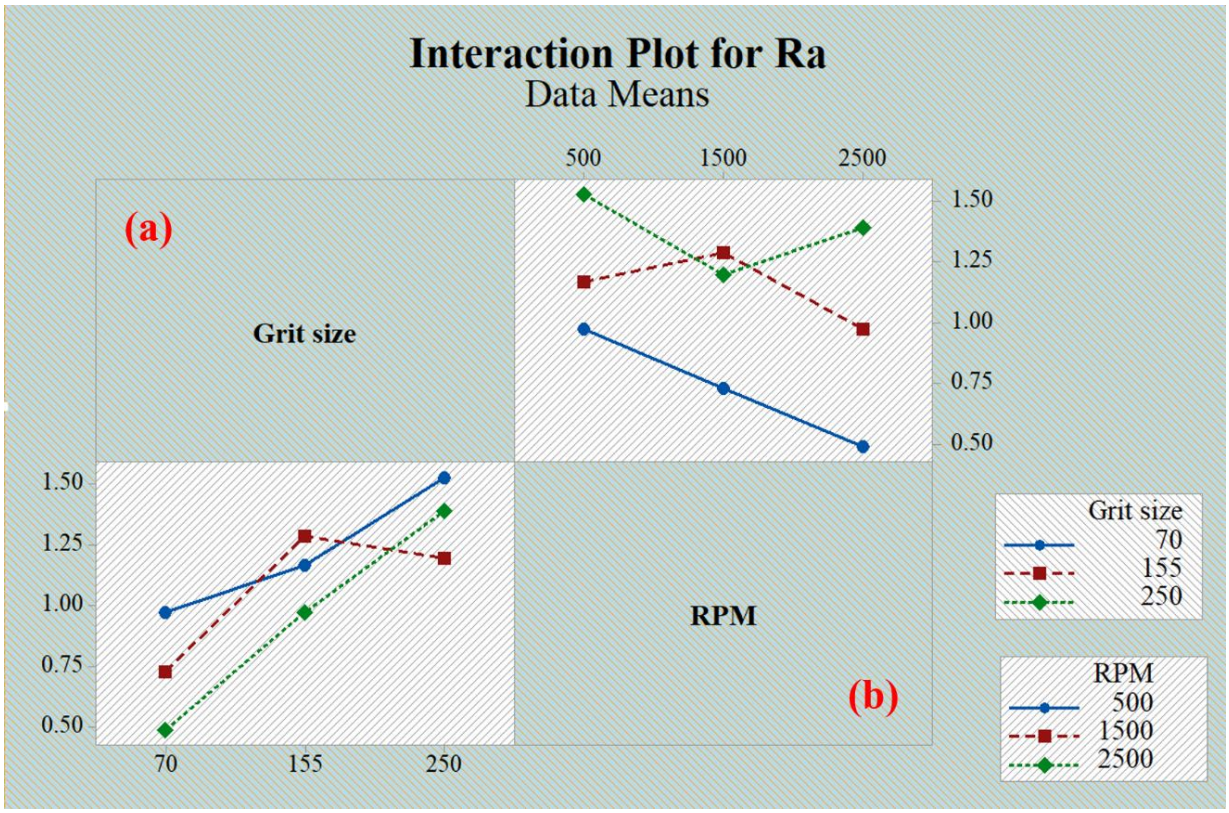

Figure 4.3 interaction graph between gritsize and RPM with surface roughness (Ra)

4.1.2.2. Residuals plot for Ra

For a great analysis, these three tests must be accounted which are normal distributed plot, constant variance test and residual versus fits. Figure 4.4 explains the residual plots for mean. In this normal probability plot shows the normal distribution of residuals i.e. the residual are fall on a straight line. Versus fits, shows the residuals are randomly distributed. These do not follow a pattern. The versus order is constant variance test. This three-test condition must be satisfied for a reliable study.

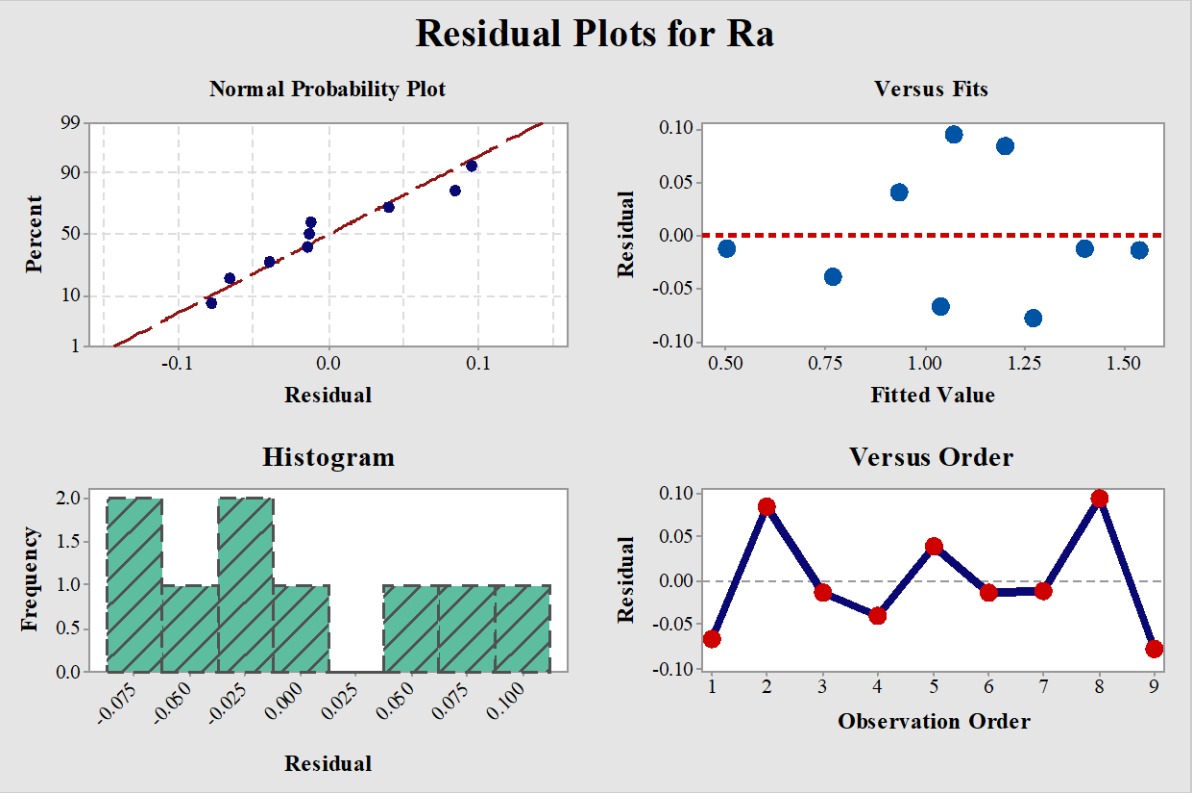

Figure 4.4 Residuals plot analysis for surface roughness (Ra)

4.1.2.3. Regression equation used for Ra calculation

The equation used for measure Ra of bone using these parameters was designed based on the regression method in the tool section of MINITAB 16 software used for creating distinct DOE equations. At the optimal settings of gritsize, RPM and feedrate, the surface roughness equation was as follows:

Ra = 0.5260 + 0.003537 gritsize - 0.000136 RPM + 0.00664 feedrate …… (1)

4.1.2.4. Confirmation Tests

At the optimal level of selected process parameters, the confirmation tests were performed to verify the surface roughness. From the response table and contribution percentage of each process parameters, we can conclude about the maximum and minimum surface roughness observed parameters. According to results maximum surface roughness (Ra_{max}) was observed feedrate of 50 mm/min (A3), using coarse abrasive tool which is 250 (B3) and at 500 rpm (C1) as mentioned in table 4.4. For all these parameters, the confirmation experiments are performed for response of surface roughness as shown in Table 4.4. In this table, predicted value of mean is the value that is calculated using the regression equation whereas the actual mean the value which is obtained at with the surface roughness tester.

Table 4.4: Confirmative experiments at optimal settings

S. No.	Response	Optimum setting	Predicted mean	Actual mean	% Error
1.	Ra_{max}	$A_3B_3C_1$	1 .67	1.75 (figure 4.5 a)	4.5%
2.	Prediction	$A_3B_2C_2$	1.20	1.17 (figure 4.5 b)	2.5%

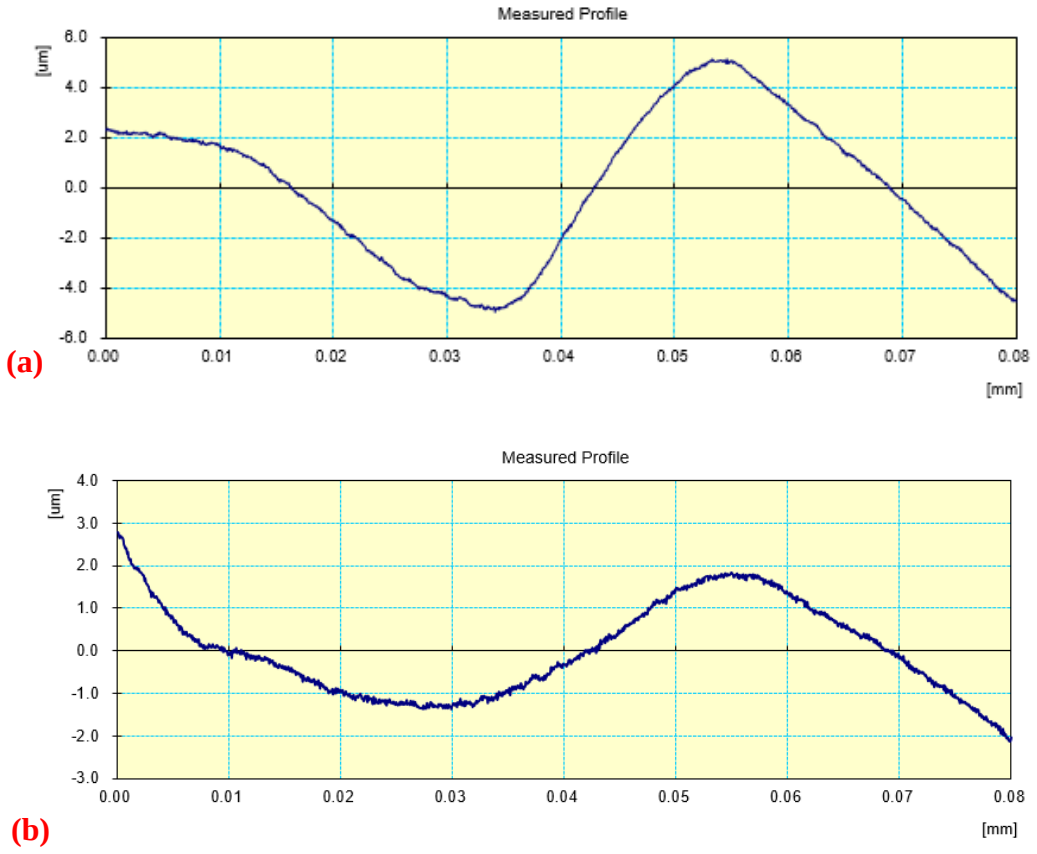

Figure 4.5 graphs of surface roughness for all conformation tests

From table 4.4, it can easily be explained that at optimum setting the variation in percentage error was from 4.5% to 2.5% that is under 5%. Hence, it shows a good reproducibility.

With the same optimized parameters, conventional drilling is also attempted and corresponding roughness in noted down as shown in table 4.5 and according to these optimized parameters, the pullout testing drilling parameters were chosen as shown in table 4.6.

Table 4.5: Surface roughness in conventional bone drilling

S. No.	Feed Rate (mm/min)	Abrasive Grit Size	Drilling tool	Average Surface Roughness (Ra) (in µm)
1	50	70	Twisted type	1.052
2	50	155	Twisted type	1.304
3	50	250	Twisted type	1.401
4	30	70	Twisted type	0.771
5	30	155	Twisted type	1.10
6	30	250	Twisted type	1.65
7	10	70	Twisted type	0.60
8	10	155	Twisted type	1.186
9	10	250	Twisted type	1.210

Table 4.6: Parameters for CBD and UBD based on maximum value of surface roughness for Pullout study

Based for	Tool Type	Rotational speed (rpm)	Federate (mm/min)	Grit size	Surface Roughness (R_a)
UBD	Hollow	500	50	Coarse (250)	$R_a$max
CBD	Twisted	500	50	NA	$R_a$max

4.2. MICROCRACKS ANALYSIS

The SEM images of conventionally drilled hole using twisted drill bit and ultrasonically drilled hole using fine, medium and coarse type diamond hollow tools are shown in figure 4.6, 4.7, 4.8 and 4.9 respectively.

According to SEM images of conventionally drilled hole, the images conclude for maximum surface roughness of bone as shown in magnified image at 2000X (figure 4.6(a)). At 1000X, the morphology of bone expresses more surface texture in bone throughout the curvature as shown in figure 4.6 (b). At 40X of magnification, the bone shows small pockets with less bone defects as shown in figure 4.6 (c).

The complete bone specimen for all three-diamond grit sizes can be observed at 40X in figure 4.7 (a), (b), (c) for fine, medium and coarse abrasives respectively. From figure 4.7 (c) it is clear that using coarse abrasive grit in the tool gives very small cracks to particular places in surrounding surface. In addition, figure 4.7 (a) shows using fine abrasive grit tool the surface of bone obtained is smooth as well as with large bone defects highlighted with the red mark, whereas using medium grit gives delamination from the edges and the bottom side of bone as shown in figure 4.7 (b). Whereas using coarse abrasive results no delamination but peaks and valleys for extremely recommended surface texture as shown in figure 4.7 (c) for better anchorage strength of bone screw joint. Figure 4.7 (a) and (b) shows larger bone defects of bone drilled using fine and medium abrasive hollow tool, which are highlighted with red colour. Whereas Figure 4.7 (c) shows a better-roughened surface texture of bone highlighted with yellow colour.

The completely drilled surface morphology of bone can be observed at Figure 4.8 (a), (b), (c) at 1000X for fine, medium and coarse abrasive grit sizes respectively. According to these zoomed out images, using medium-type diamond tool produces a little rough surface or peak as compared to fine-type diamond tool whereas using coarse-type diamond tool produces the complete rough surface as can observe in figure 4.8 (c). The reason behind it is due to coarse grit size removes more material because of the large size of diamond grit. Hence, it produces the complete rough area where diamond grits contacts with the bone specimen. From the microstructure, we can say that, using coarse diamond sized tool is optimized for producing high surface roughness of bone during ultrasonic bone drilling as shown in figure 4.8 (c) because of its irregular, rugged and uneven surface texture.

In Figure 4.9, the comparison was made at 2000X of focus for fine, medium and coarse type of abrasive grit sizes are shown respectively. At this magnification, it is observe that the microstructure of bone using coarse type diamond grit size (figure 4.9 (c)) gives the maximum pockets and porous structure to bone, which gives maximum surface morphology to bone surface due to which higher bone growth can be expected. However in figure 4.5 (a) the fine type abrasive grit size is image shows the better, uniform and less pockets surface. Figure 4.5 (b) image uses the medium abrasive grit size and shows shaggier surface then fine abrasive.

Hence, from analysing the images at 40X, 1000X and 2000X for fine, medium and coarse diamond grits tool for ultrasonic drilling and twisted drilling tool for conventional drilling, we can observe that the surface texture of bone produced by twisted drill bit during conventional drilling gives maximum surface roughness. Whereas during ultrasonic drilling, the coarse type diamond tool have the maximum peaks and pockets as compared to fine and medium type of hollow tool.

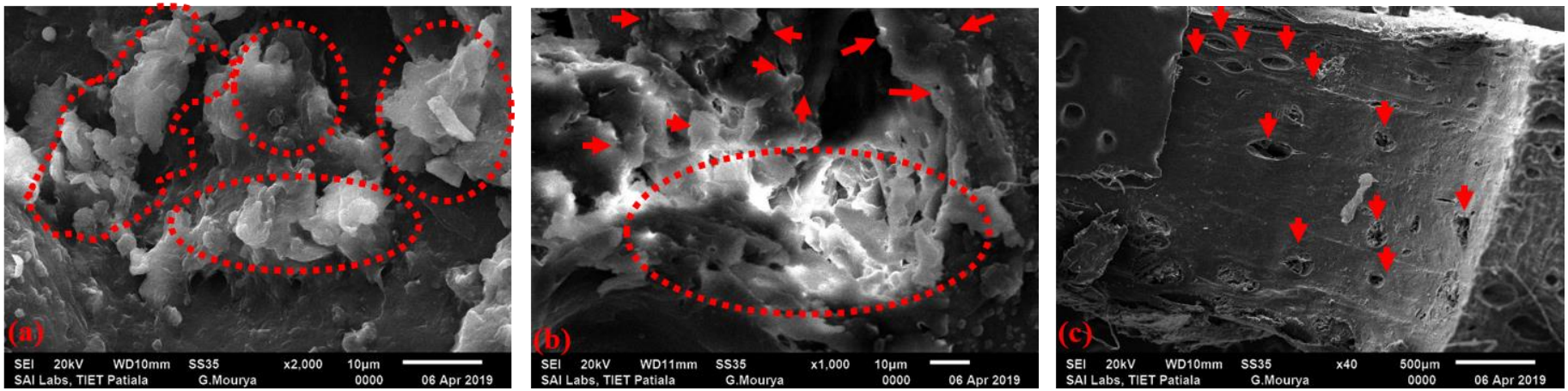

Figure 4.6 SEM image for comparison of surface texture of conventional drilled bone at (a) 2000X; (b) 1000X; (c) 40X

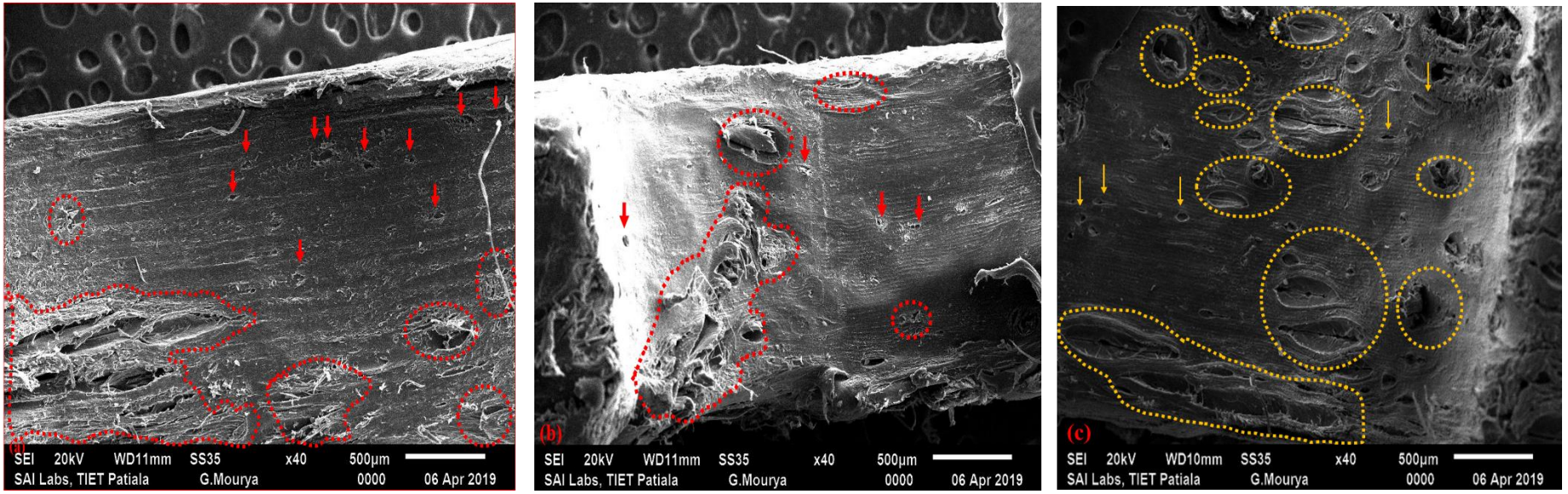

Figure 4.7 SEM image for comparison of surface texture of ultrasonic drilled bone (UDB) at 40X using: (a) fine; (b) medium; (c) coarse abrasive

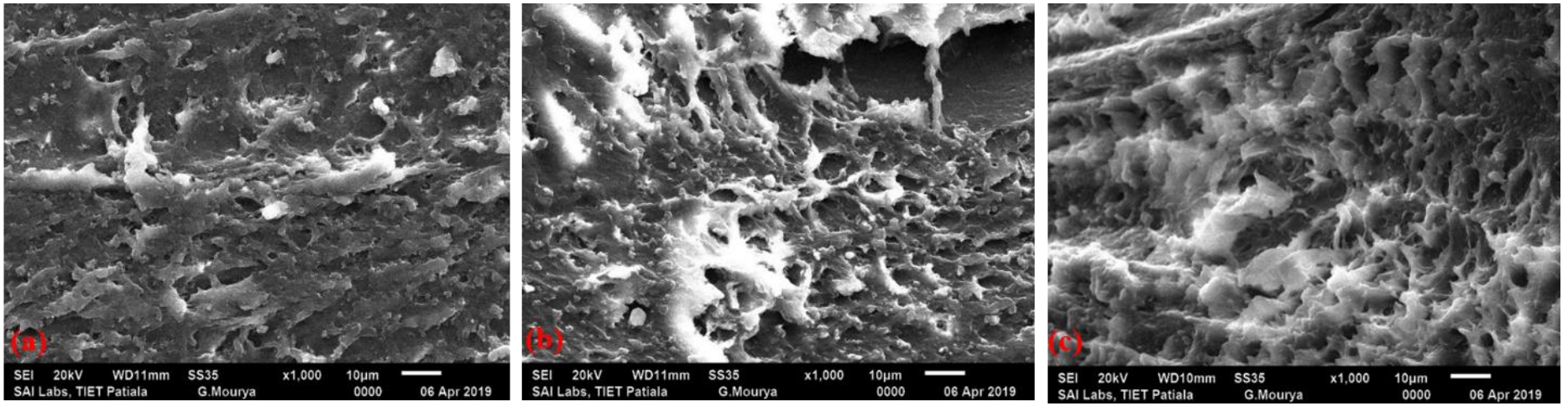

Figure 4.8 SEM image for comparison of surface texture of UDB at 1000X using: (a) fine; (b) medium; (c) coarse abrasive grit tools

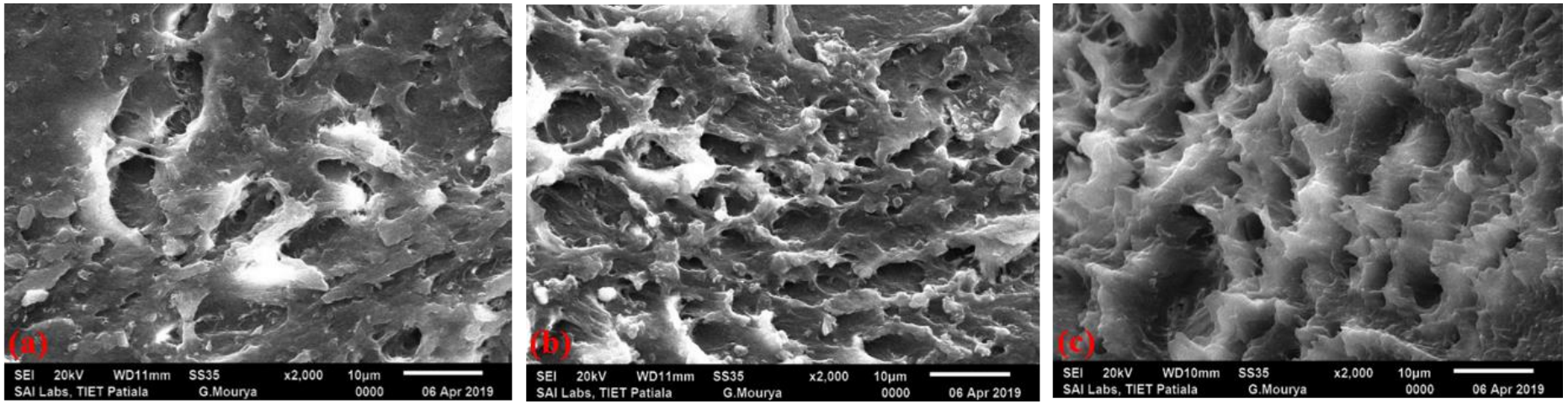

Figure 4.9 SEM image for comparison of surface texture of UDB at 2000X using: (a) fine; (b) medium; (c) coarse abrasive grit tool

4.3. BIOLOGICAL ASSESSMENT (APATITE GROWTH DURING DIFFERENT TIME SPANS)

The samples are merged in SBF solution without screw inserting in the hole. This is just to observe the growth of apatite or formation of calcium phosphate in the bone samples after different intervals of time. Separate samples are prepared with screw in the hole and immerged into the SBF solution for pullout testing.

For ultrasonic maximum roughness and conventional maximum roughness, the study of apatite formation is done for keeping the samples for 1 week of interval. The observation of micro growth of apatite in bone is observed with the help of Nikon Eclipse E100 microscope. For observing the proper growth of apatite, the area was calculated for every sample by using Digimizer image analysis software and the results of magnified images with calculated surface area are observed and shown in table 4.7.

As we have seen, the conventionally drilled hole shows rough and irregular surface finish as compared to the hole drilled with coarse sized diamonds hollow tool ultrasonically shows less rough surface texture. When both the samples were immersed in SBF solution calculated area was slightly different as shown in table 4.7 at (a), (b). Whereas the tool diameter for both the methods of tools were similar 3.5 mm. The difference in the area of both the methods is due to cutting techniques and intiror structure. Using coarse diamond hollow tool gives a precise and perfect cutting of bone whereas the conventional drilling gives overacting during drilling of bone. This can be proved from the difference observed from the actual area of drilled circle and the area calculated using digimizer for both methods.

Diameter of cutting tools (D) = 3.5 mm

Radius of cutting tools (r) = D/2 = 3.5/2 = 1.75 mm

Area of circle = πr^2

Area of circle = 3.14*1.75mm*1.75mm

Actual area of drilled circle = 9.616 mm^2

Area calcualted for conventionally drilled hole 9.836 mm^2 and for ultrasonically drilled hole 9.686 mm^2. The difference of area for both the methods was 0.15 mm^2 at the 0^{th} day, when the samples were as drilled hole.

After 7 days, when the microscopy done, the ultrasonically drilled hole shows surprisingly much better apatite growth as compared to conventionally drilled hole as shown in table 4.7 at (c), (d). This owes due to pockets and porous structure of surface of ultrasonically drilled bone, which provides peaks to grow the tissues faster. Pockets and porous morphology of bone surface helps to grow tissues faster when kept in SBF solution. The area calculated for ultrasonic drilled hole 6.047 mm^2 and for conventionally drilled hole 9.291 mm^2 as shown in table 4.7 (after 7 days row). The difference between the areas of growth rate to compare the ultrasonically drilled hole growth rate to the conventionally drilled hole was 3.244 mm^2. The ultrasonically drilled hole shows 31.91% of better bone growth as compared to conventionally drilled hole after 7 days of interval comparision.

After 14 days, when the specimens was observed, they show a massive growth rate as compared to the results observed at 7^{th} day. Specially in ultrasonic drilled hole maximum area of drilled hole is covered, which says the higher growth rate of bone healing as compared to conventionally drilled hole. The comparison of bone growth rate can be observed in table 4.7 at (e), (f). According to the area calculated for both the methods, the ultrasonically drilled hole shows 35.48% of better bone growth as compared to conventionally drilled hole after 14 days of interval comparision.

After 21 days, the observation shows a better bone healing of ultrasonically drilled hole as compared to conventionally drilled hole as shown in table 4.7 at (g), (h). Ultrasonic drilled hole shows a massive growth rate of apatite formation because of the higher apatite formation of preceding 7 days growth The area percentage of ultrasoniacally dilled hole was 48.21%, when they are kept in SBF solution for 21days. Whereas conventionally drilled hole shows 21.40% of infill percentage.

At 28^{th} day, the microstructure of ultrasonic and covnetionally drilled hole bone samples was observed and from the results, it can be concluded that ultrasonically drilled hole shows better biocompatible nature and apatite growth of bone as compared to conventionally drilled hole as shown in table 4.7 at (i), (j). The calculated areas of both methods are mentioned in the table. The growth rate is very massive and abount in the bone sample of ultrasonic method at 28^{th} day, the empty area calculated for ultrasonic method (53.11%), shows that more then half bone tissues has been healed and properly grown. Reason behind it, due to the core temperature of 37^0C provided by the incubator gives the same atomphere to bone as present in the human body and the precise cutting by the coarse diamond hollow tool.

This is quiet obvious that with increase in number of days, the apatite growth will also increase. From different interval of keeping the samples in SBF shows, that ultrasonic drilled bone shows better bone growth as compared to conventionally drilled hole due to precise cutting, rough surface, pockets and porous structure of bone.

This high growth rate of ultrasonic drilled bone may have higher pullout strength of cortical screw as compared to conventionally drilled hole, which may reduce the implant failure.

Table 4.7: Comparison of conventional Ra max and ultrasonic Ra max with distinct days preserved in SBF to observe area of empty void left after apatite formation

Days	Conventional Ra maximum	Ultrasonic Ra maximum
As drilled sample (0^{th} day)	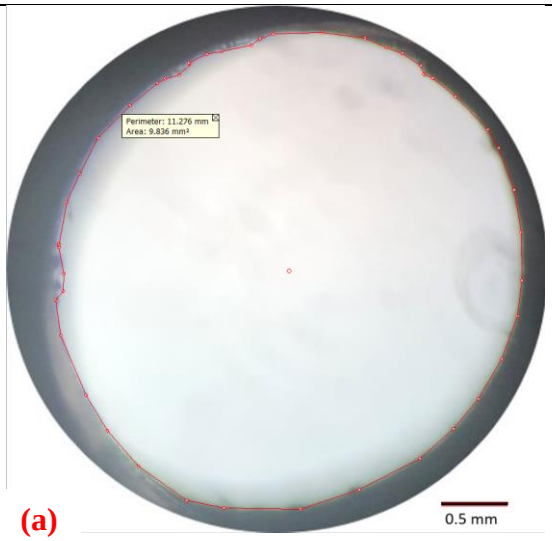	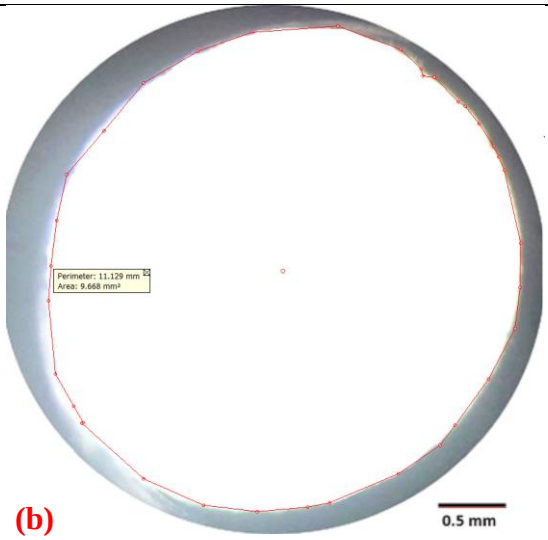
Area	9.836 mm^2	9.668 mm^2
After 7 days	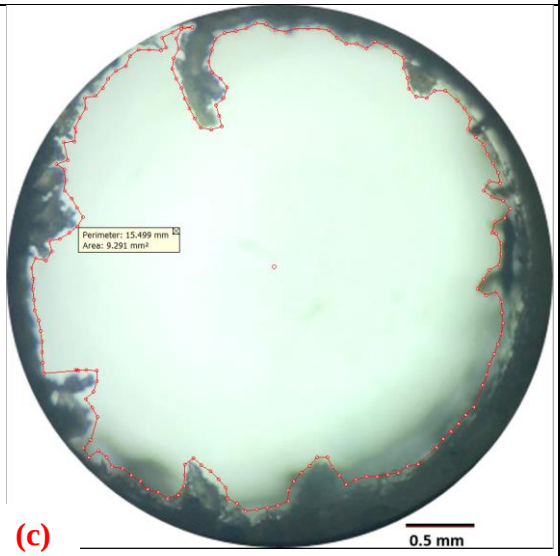	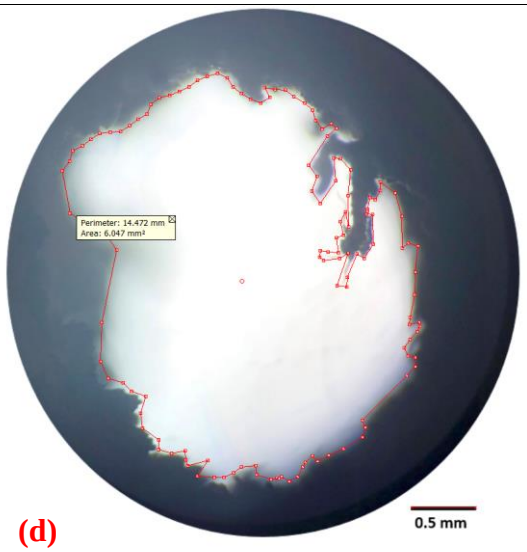
Area	9.291 mm^2	6.047 mm^2

After 14 days	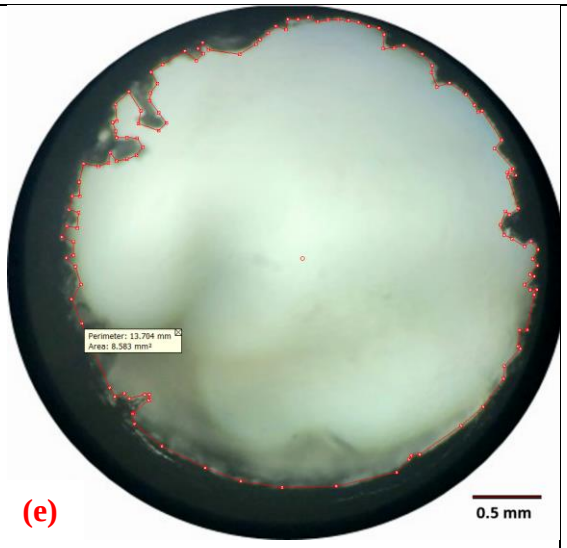	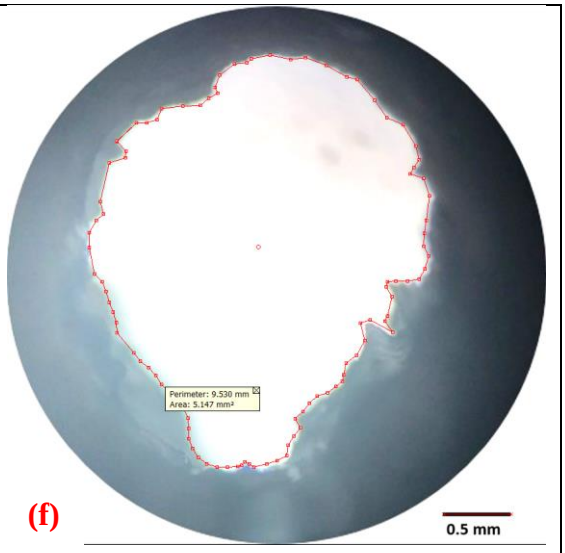
Area	8.583 mm^2	5.147 mm^2
After 21 days	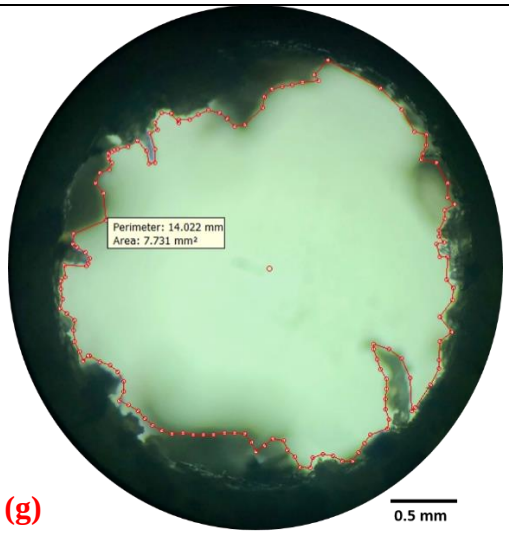	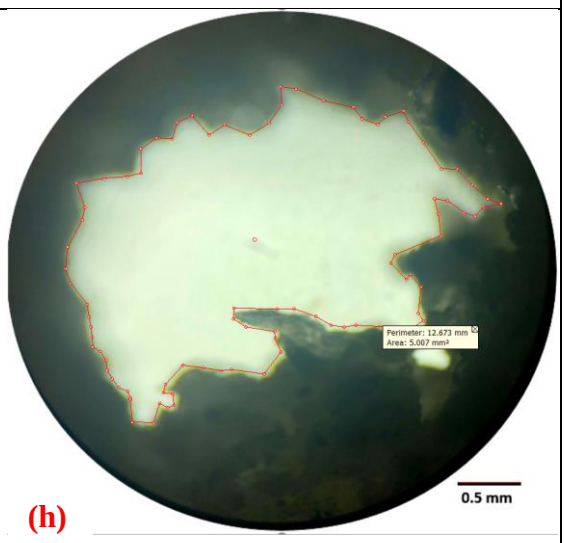
Area	7.731 mm^2	5.007 mm^2
After 28 days	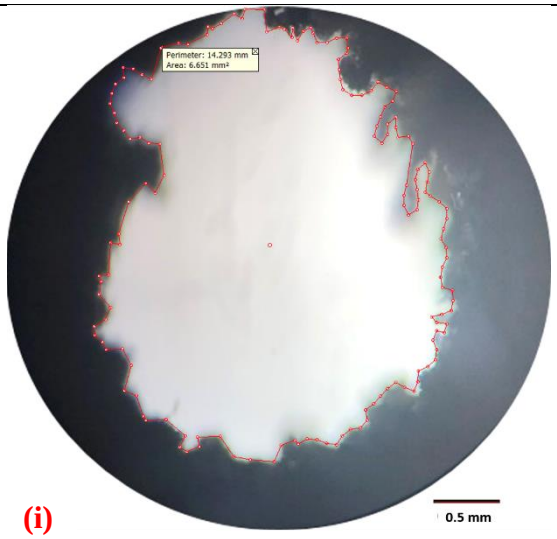	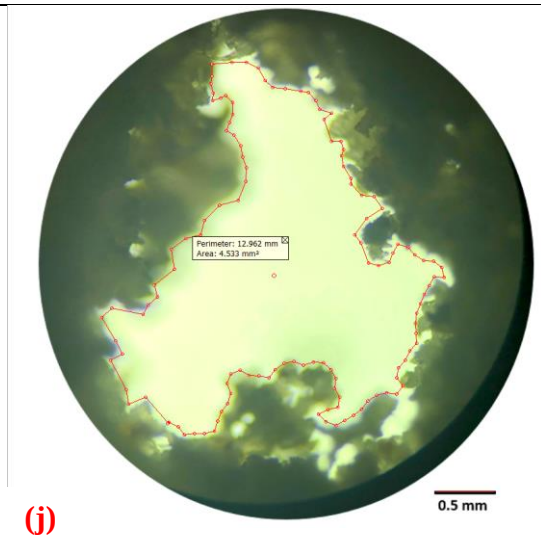
Area	6.651 mm^2	4.533 mm^2

Total area calculated for both conventional and ultrasonically drilled hole are 9.836 mm^2 and 9.686 mm^2. So the apatite growth can be calculated by total area of bone minus empty area calculated using Digimizer for each interval. Table 4.8 express the growth of bone according to several days interval for conventional and ultrasonically method of bone drilling.

Apatite growth rate = Total area of bone – Area calculated for empty space during bone growth

Table 4.8: Growth of bone area wise at 7 days of interval

Apatite growth rate	For conventional drilling	For ultrasonic drilling
At 0^{th} day (as drilled sample)	9.836-9.836=0 mm^2	9.836-9.668=0.168 mm^2
After 7 days	9.836-9.291=0.545 mm^2	9.668-6.047=3.621 mm^2
After 14 days	9.836-8.583=1.253 mm^2	9.668-5.147=4.521 mm^2
After 21 days	9.836-7.731=2.105 mm^2	9.668-5.007=4.661 mm^2
After 28 days	9.836-6.651=3.185 mm^2	9.668-4.533=5.135 mm^2

The area calculated using Digimizer image analysis software for ultrasonically and conventionally drilled bone growth rate is shown in Figure 4.10. The change in area in comparison of every 7 days interval is also compared. The calculated area express the growth of bone. The calculated area gives the percentage difference growth related to every 7 days interval gap. At the time when samples were not immersed in SBF solution, the area calculated can be considered as complete area (9.836 mm^2) for conventionally drilled hole and (9.668 mm^2) for ultrasonically drilled hole, which will be used during calculation of percentage infill. The future results areas can be considered as the growth rate (after 7, 14, 21 and 28 days). By calculating, the area from equation 2, the difference between the complete area and particular area the percentage infill is calculated as expressed in Table 4.9.

$$Bone\ Healing\ \% = \frac{complete\ area\ of\ 0^{th}\ day - Area\ of\ 7^{th} day}{complete\ area\ of\ 0^{th} day}\ X\ 100$$

…… (2)

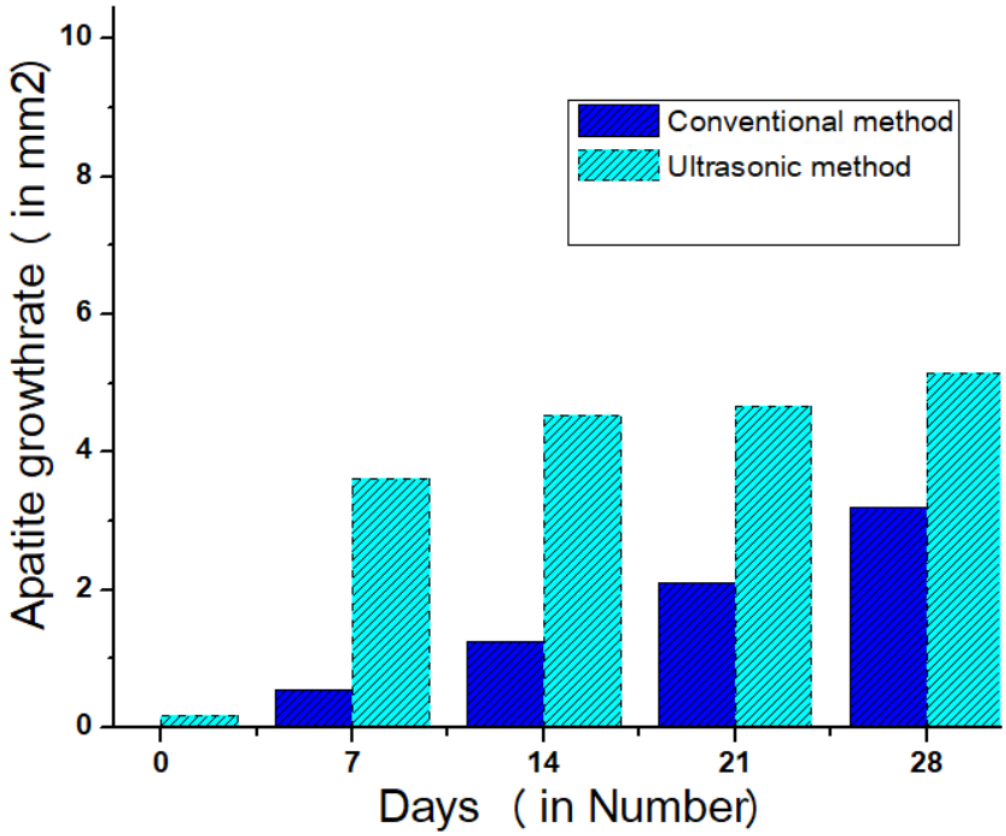

Figure 4.10 comparison of apatite growth for each 7 days interval during conventional and ultrasonic methods

Table 4.9: Comparison of growth rate of apatite in conventional and ultrasonic drilled hole after 1 week of interval

Days	Conventionally growth rate	Ultrasonically growth rate
After 7 days	5.54%	37.45%
After 14 days	12.73%	46.71%
After 21 days	21.40%	48.21%
After 28 days	32.38%	53.11%

Ultrasonic drilled bone growth have a massive impact of reagents of simulated body fluid from the first week results as compared to conventionally drilled bone growth rate.

Figure 4.11 expresses the growth rate of bone in terms of infill percentage to every week transition to compare the ultrasonic and conventional drilled bone growth rate.

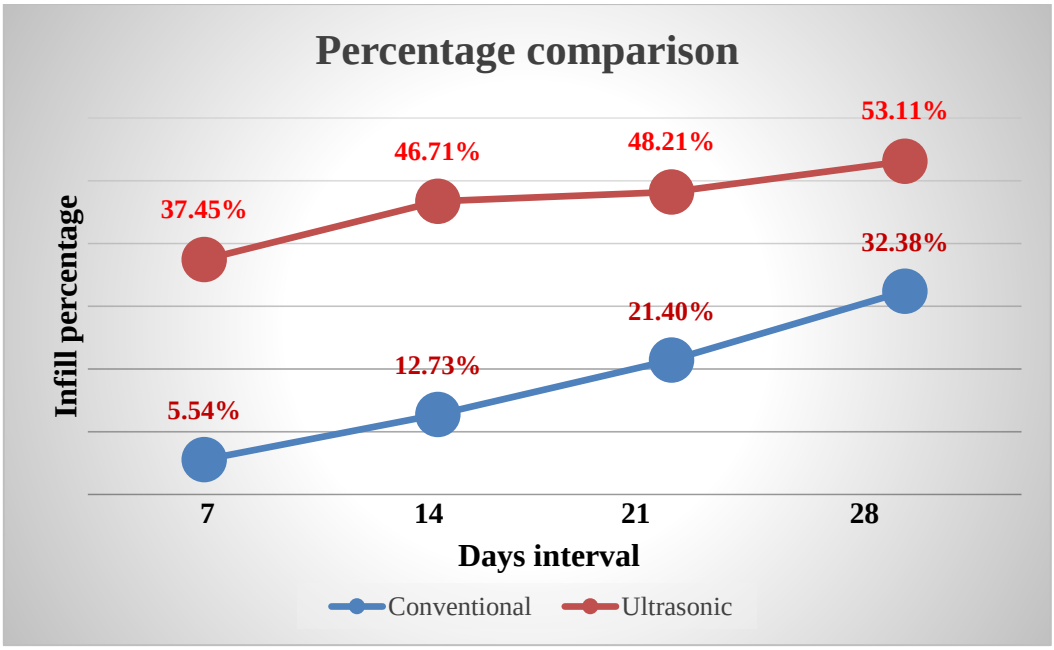

Figure 4.11 percentage comparison of conventional and ultrasonic bone growth rate

4.4. X-ray ANALYSIS

The bone screw samples for conventionally drilled hole and ultrasonically drilled hole were sent for X-ray imaging at Dhillon diagnostic centre, Patiala to observe the morphology of screw inside the bone. As shown by the results of X-ray images, the ultrasonically inserted screw gives better anchoring stability of cortical screw to the surrounding of bone, as the gap between the screw and drilled hole was 0.988 mm which is very close to 1 mm (ideal gap between the drilled hole and cortical screw) as shown in figure 4.12 (b). Whereas the conventionally inserted screw is forcibly inserted in the drilled hole and gives the interface of 0.896 mm which is not suggested by the orthopaedic surgeons as shown in figure 4.12 (a).

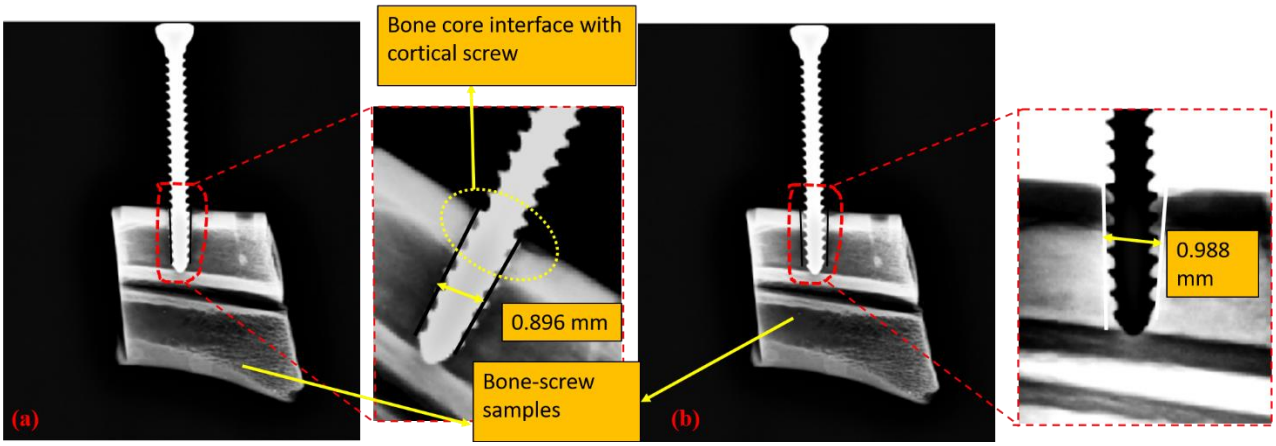

Figure 4.12 X-ray images of bone screw samples (a) using conventional drilling, (b) using rotary ultrasonic drilling

4.5. PULLOUT STRENGTH RESULTS

From the UTM machine, the pullout strength of cortical screw has been measured. Bone screw samples were attached in bone screw holding fixture. The first group of bone screw samples were tested (when samples were not kept in SBF); corresponding results are mentioned with the values obtained for it (in N) are shown in table 4.10. Similarly second group samples (after 7 days of interval in SBF), third group (after 14 days in SBF), fourth group (after 21 days in SBF) samples and fifth group (after 28 days in SBF) samples were tested. These entire groups shows maximum displacement of cortical screw with respect to travel time for ultrasonically maximum surface roughness drilled hole parameters. The growth of each sample for every group shows ultrasonically maximum parameter drilled hole have maximum pullout strength as compared to all other parameters methods.

Table 4.10: Values of result of pullout strength for both the methods (in N)

Method	**Days**				
	0	**7**	**14**	**21**	**28**
Con(N)	146 N	286 N	291 N	584 N	684 N
Con(X)	302 N	500 N	550 N	650 N	705 N
Ult(N)	560 N	938 N	963 N	1000 N	1300 N
Ult(X)	1100 N	1200 N	1390 N	1710 N	2090 N

The results showed by the fifth group (after 28 days of SBF) shows, there was not much difference between the pullout strength of bone screw joints at conventional minimum and maximum surface roughness parameters (figure 4.13). However, a massive increase in pullout strength of cortical screw can be observed at ultrasonically drilled hole with maximum surface roughness parameter as compared to ultrasonic minimum roughness parameter as shown in Figure 4.13.

The maximum value of pullout strength is obtained in final group which 2090 N for ultrasonic maximum roughness parameters and 1300 N for ultrasonic minimum roughness parameter which is the big difference from conventionally drilled hole results. For conventional minimum parameter 684 N and for ultrasonic maximum 705 N is the force, which was obtained from UTM results. From these values it is very clear that using ultrasonically maximum parameter (2090 N), the bone screw joint shows almost three time the strength of cortical screw as compared to using conventionally maximum parameter.

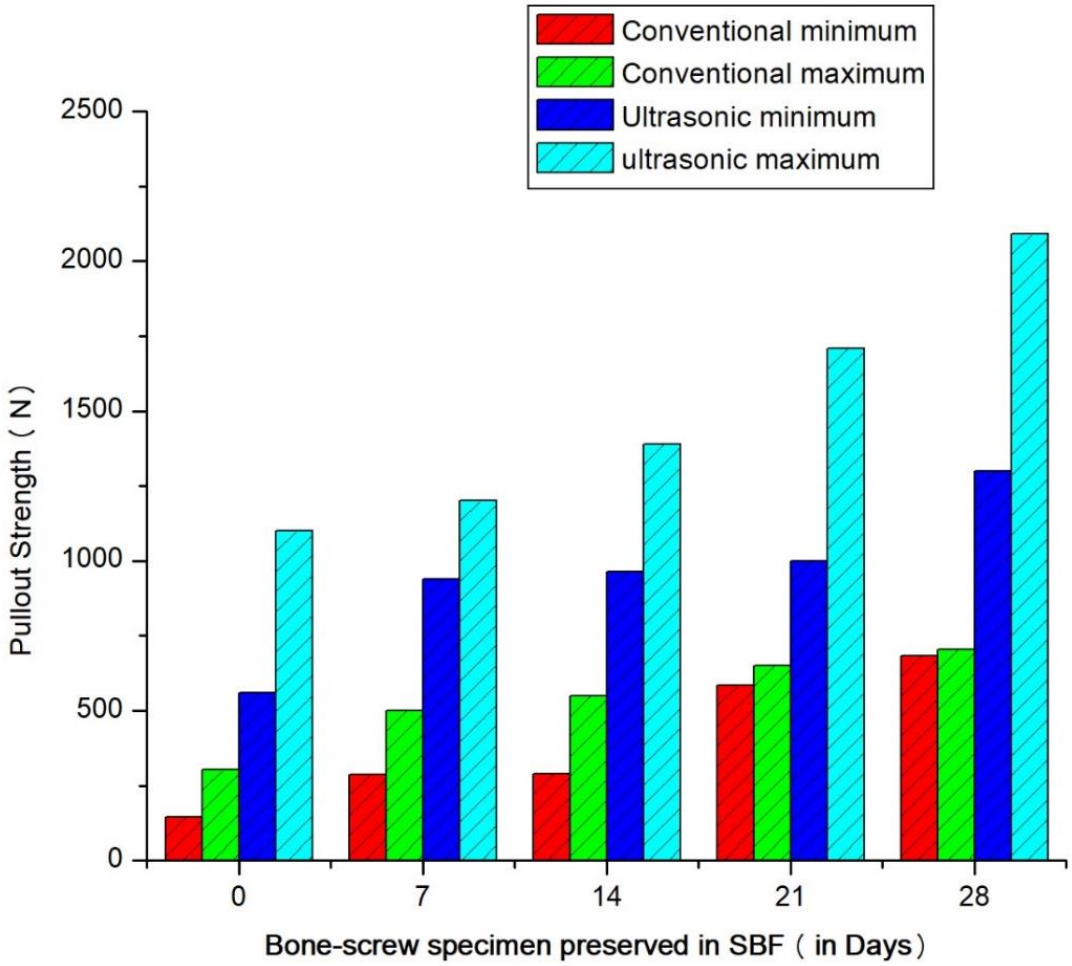

Figure 4.13 Pullout strength of cortical screw at each group (0, 7, 14, 21 and 28 days interval)

For comparing this final fifth group (after 28 days of keeping the samples in SBF), values of results of measured pullout values are presented in a resultant graph, plotted using Origin 6.1 software which is shown in figure 4.14. According to this graph, ultrasonic maximum roughness parameter shows very good results as compared to other parameters as the same time. The reason behind it is maybe due to the peaks of ultrasonically drilled hole and precise cutting of bone, which gives the bone fusion to grow bone very faster. In this main graph the values of pullout for each parameter with the extracted cortical screw images is shown figure 4.14. From these images it is very clear that at ultrasonically maximum roughness parameter, the bone was broken due to very high sustainability of bone with the cortical screw and high bone debris can be observed at ultrasonically minimum roughness parameter as compared to conventional method. According to these result and extracted screw images, it can be concluded that the apatite growth is actually very high in ultrasonically maximum roughness

drilled hole, which influence the maximum pullout strength of the cortical screw and hence the breakage of bone occurred. This may leads to decrease the failure of implant.

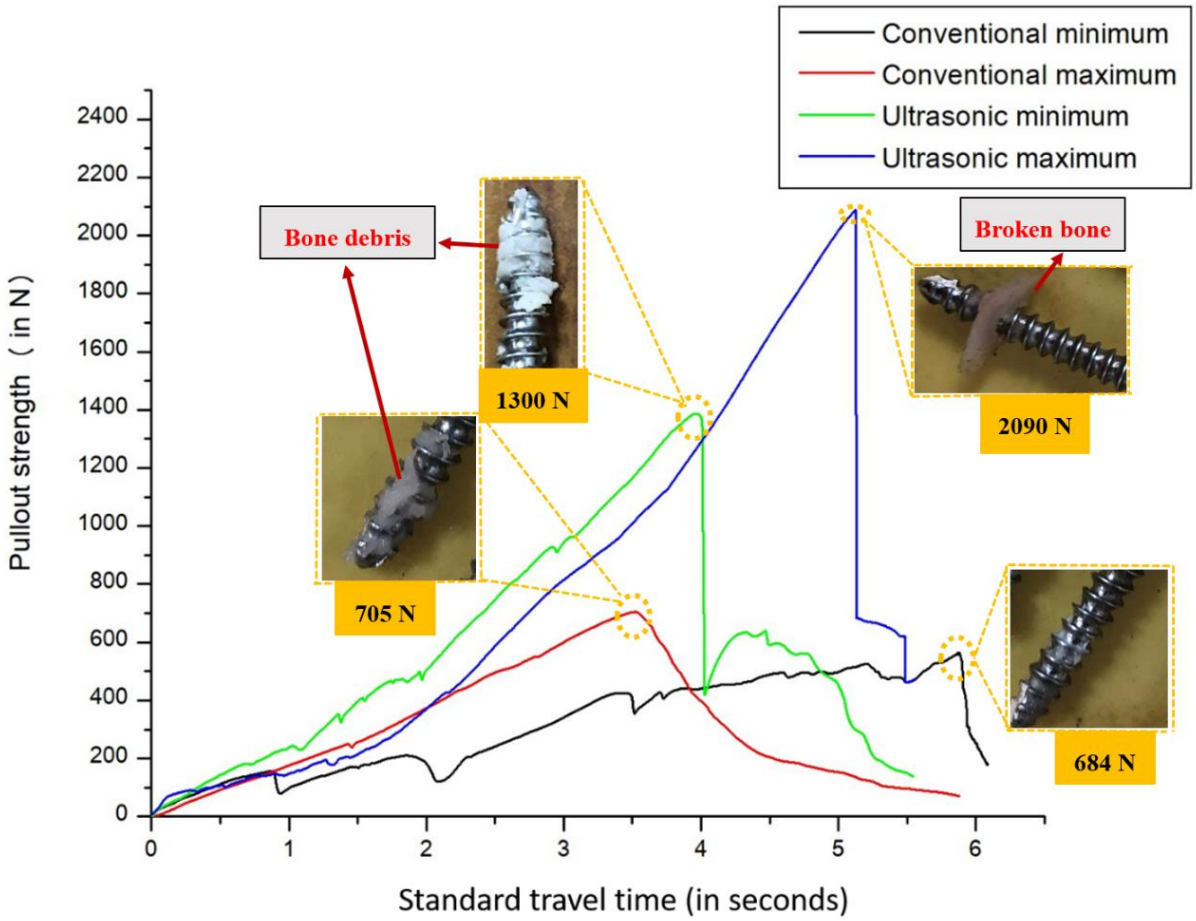

Figure 4.14 Comparison of result of all the processes with tool bone debris

An after result image of all four samples are shown in figure 4.15. According to these images, the figure (a) shows the conventional minimum roughness parameter, according to which normal force is observed which does not affect any of the surrounding area of bone.

Figure 4.15 (b) shows the conventional maximum roughness parameter which shows the broken of surrounding debris. From the figure 4.15 (c), it can observe that the strength of cortical screw in the ultrasonic minimum roughness parameter is so high that the bone is broken from the attached segment in the bone, same results were shown by ultrasonic maximum roughness parameter but with much higher pressure on cortical screw. Figure 4.15 (c) and (d) shows the ultrasonic minimum and maximum parameters respectively and for both the parameter of ultrasonic drilling shows the bone breakage, which means the maximum strength of cortical screw and better sustainability of cortical screw.

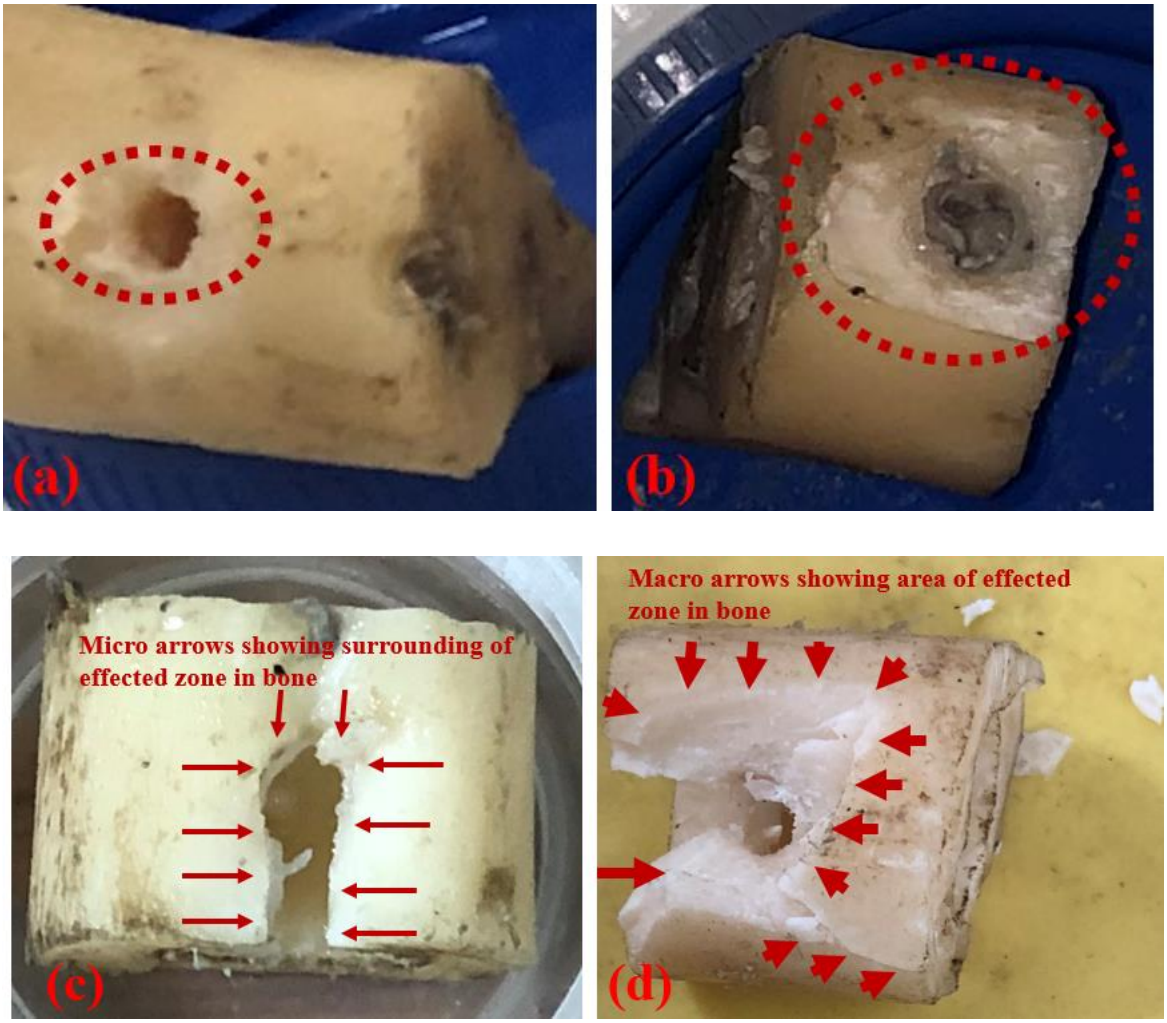

Figure 4.15 Bones after pullout testing of cortical screw extracted from bone screw samples (a) for conventional minimum, (b) for conventional maximum, (c) for ultrasonic minimum, (d) for ultrasonic maximum

5.1. GENERAL

The present study was to check the surface texture of bone in view to increase the pullout strength of cortical screw immersed in SBF solution in-vitro study. The three distinct major effecting parameters as rotational speed, feedrate and abrasive grit size changes upto 3 unlike dissimilar levels to examine the effects on surface roughness and pullout strength of cortical screw.

From the results of pullout and bone images of extracted cortical screws, it can be concluded that the ultrasonically maximum drilled parameter is the best-optimized parameter for maximizing the pullout strength. The reason behind is due to grooves of the cortical screw stabilize with the roughened surface of bone, which helps in increasing the anchoring strength of bone screw joint also using ultrasonic bone drilling we are getting very precise cutting of bone. The role of SBF solution can also observe at 28^{th} day, which shows the maximum growth of bone as according to other groups.

The ultrasonically maximum parameter was using grit size of 250 which is coarse diamond girts, rotational speed of 500 rpm and 50 mm/min of feedrate. Hence using these above parameters the maximum surface roughness, maximum pullout strength of cortical screw and minimum microcracks can be obtained. Maximum surface roughness of bone specimen results maximum pullout strength of cortical screw and can help in reducing the failure of bone screw and screw loosening.

5.2. CONCLUSION

1. Surface roughness is directly relative to abrasive grit size, as compared to significant effect of rotational speed and feedrate. The coarse diamond grits gives the larger effect on the surface of bone. As greater, the size of grit produces high area of bone removal rate, which produces highly rough surface texture of bone.
2. The calcium phosphate (apatite) formation on the deep-seated area of bone shows the biocompatible nature of the porcine bone. The results clearly show the high amount of development of apatite on surface of ultrasonic drilled bone (UDB) as compare to conventionally drilled bone (CDB) hole. Apatite growth rate of UDB shows linearly high massive bone growth rate at 28^{th} day as compared to CDB hole.

3. All four configurations of samples kept in simulated body fluid for ultrasonically drilled hole shows aftereffect in undisturbed bone healing as compared to conventionally drilled hole, also are considered safe for orthopaedic and biological application.
4. A new hollow diamond bits has been designed, also compared to conventional surgical bits. These hollow bits was much more efficient in drilling of bone and produces better surface texture with pockets and porous morphology. The new hollow bit penetrated at a faster rate and drilling is faster. We believe that use of these new hollow drill bits will make drilling of bone easier and maximize the possibility of precise cutting of bone. Moreover, the pullout strength is increased using new hollow diamond tool of coarse type because it produces the accurate cutting of bone as compared to conventional drill bit which gives overcutting of bone which takes more time during healing and growth.

5.3. FUTURE SCOPE

According to present in vitro investigation, there can have following future scope:

I. Currently the experimentation have performed on in-vitro study during this investigation; also in future in-vivo study for bone drilling can be implemented.
II. The chosen set of three distinct grit sizes; future study can explore for varying various grit sizes and abrasives.
III. During ultrasonic drilling of bone, the given constant vibrational frequency and constant amplitude of 20 kHz and 20μm respectively can be varied.
IV. While keeping the bone screw samples in SBF solution, the observation of apatite formation made for only 28 days, we can vary the study up to 80-90 days.

[1] M. S. Features, “Bone Structure and Biomechanics ☆,” vol. 4, pp. 392–400, 2018.

[2] J. D. Currey, “The structure and mechanics of bone,” *J. Mater. Sci.*, vol. 47, no. 1, pp. 41–54, 2012.

[3] J. W. Hole and N. A. Corbett, *Essentials of Human Anatomy & Physiology*. Wm. C. Brown Publishers, 1995.

[4] E. Salamanca *et al.*, “A novel porcine graft for regeneration of bone defects,” *Materials (Basel).*, vol. 8, no. 5, pp. 2523–2536, 2015.

[5] E. Salamanca *et al.*, “Bone regeneration using a porcine bone substitute collagen composite in vitro and in vivo,” *Sci. Rep.*, vol. 8, no. 1, pp. 1–8, 2018.

[6] G. Singh, R. Jindal, V. Jain, and D. Gupta, “Effect of tool and drilling parameters on surface topography of bone drilled holes: An in vitro study,” *2016 Int. Conf. Students Appl. Eng. ICSAE 2016*, pp. 196–200, 2017.

[7] M. Marco, M. Rodríguez-Millán, C. Santiuste, E. Giner, and M. H. Miguélez, “A review on recent advances in numerical modelling of bone cutting,” *J. Mech. Behav. Biomed. Mater.*, vol. 44, pp. 179–201, 2015.

[8] R. Orozco, J. M. Sales, and M. Videla, *Atlas of internal fixation: fractures of long bones*. Springer Science & Business Media, 2013.

[9] R. K. Pandey and S. S. Panda, “Drilling of bone: A comprehensive review,” *J. Clin. Orthop. Trauma*, vol. 4, no. 1, pp. 15–30, 2013.

[10] G. Singh, V. Jain, and D. Gupta, “Comparative study for surface topography of bone drilling using conventional drilling and loose abrasive machining,” vol. 229, no. 3, pp. 225–231, 2015.

[11] A. R. Eriksson and T. Albrektsson, “Temperature threshold levels for heat-induced bone tissue injury: A vital-microscopic study in the rabbit,” *J. Prosthet. Dent.*, vol. 50, no. 1, pp. 101–107, 1983.

[12] B. R. Chrcanovic, T. Albrektsson, and A. Wennerberg, “Reasons for failures of oral implants,” *J. Oral Rehabil.*, vol. 41, no. 6, pp. 443–476, 2014.

[13] X. Zhuang, B. Yu, Z. Zheng, J. Zhang, and W. W. Lu, “Effect of the Degree of Osteoporosis on the Biomechanical Anchoring Strength of the Sacral Pedicle Screws An In Vitro Comparison Between Unaugmented Bicortical Screws,” vol. 35, no. 19, pp. 925–931, 2010.

[14] C. T. Us and J. A. Miller, “(12) United States Patent (10) Patent No .: st Z :,” vol. 2, no. 12, 2011.

[15] G. Augustin, S. Davila, K. Mihoci, T. Udiljak, D. Stjepan, and V. Anko, “Thermal osteonecrosis and bone drilling parameters revisited,” pp. 71–77, 2008.

[16] M. T. Hillery and I. Shuaib, “Temperature effects in the drilling of human and bovine bone,” *J. Mater. Process. Technol.*, vol. 92–93, pp. 302–308, 1999.

[17] R. Kumar and S. S. Panda, “Optimization of Bone Drilling Process with Multiple Performance Characteristics Using Desirability Analysis,” *Procedia - Soc. Behav. Sci.*, vol. 9, no. Icbee 2013, pp. 48–53, 2014.

[18] X. Li, W. Zhu, J. Wang, and Y. Deng, “Optimization of bone drilling process based on finite element analysis,” *Appl. Therm. Eng.*, vol. 108, pp. 211–220, 2016.

[19] D. Ciglar, “INVESTIGATION INTO BONE DRILLING AND THERMAL BONE NECROSIS,” vol. 2, pp. 103–112, 2007.

[20] V. Gupta, P. M. Pandey, A. R. Mridha, and R. K. Gupta, “Effect of Various Parameters on the Temperature Distribution in Conventional and Diamond Coated Hollow Tool Bone Drilling : A Comparative Study,” *Procedia Eng.*, vol. 184, pp. 90–98, 2017.

[21] S. Saha and J. A. Albright, “Surgical Drilling : Design and Performance of an Improved Drill 1,” 2016.

[22] K. Alam, A. V Mitrofanov, and V. V Silberschmidt, “Medical Engineering & Physics Experimental investigations of forces and torque in conventional and ultrasonically-assisted drilling of cortical bone,” *Med. Eng. Phys.*, vol. 33, no. 2, pp. 234–239, 2011.

[23] E. Shakouri, M. H. Sadeghi, and M. R. Karafi, “An in vitro study of thermal necrosis in ultrasonic-assisted drilling of bone,” vol. 229, no. 2, pp. 137–149, 2015.

[24] J. Machining, “An investigation on thermal necrosis during bone drilling Gurmeet Singh *, Aman Gahi , Vivek Jain and Dheeraj Gupta,” vol. 18, no. 4, pp. 341–349, 2016.

[25] W. Wang, Y. Shi, N. Yang, and X. Yuan, “Experimental analysis of drilling process in cortical bone,” *Med. Eng. Phys.*, pp. 6–11, 2013.

[26] V. Gupta and P. M. Pandey, “Experimental investigation and statistical modeling of temperature rise in rotary ultrasonic bone drilling,” *Med. Eng. Phys.*, vol. 38, no. 11, pp. 1330–1338, 2016.

[27] G. Singh, V. Jain, D. Gupta, and A. Sharma, “Parametric effect of vibrational drilling on osteonecrosis and comparative histopathology study with conventional drilling of cortical bone,” 2018.

[28] V. Gupta, P. M. Pandey, and V. V Silberschmidt, “Rotary ultrasonic bone drilling : Improved pullout strength and re duce d damage,” vol. 41, pp. 1–8, 2017.

[29] Y. Wang *et al.*, “Medical Engineering & Physics Experimental investigations and finite element simulation of cutting heat in vibrational and conventional drilling of cortical bone,” *Med. Eng. Phys.*, vol. 36, no. 11, pp. 1408–1415, 2014.

[30] V. Gupta and P. M. Pandey, “An in-vitro study of cutting force and torque during rotary ultrasonic bone drilling,” 2016.

[31] K. Alam, A. V Mitrofanov, and V. V Silberschmidt, “Measurements of Surface Roughness in Conventional and Ultrasonically Assisted Bone Drilling,” pp. 312–320, 2009.

[32] G. Singh, V. Jain, and D. Gupta, “Multi-objective performance investigation of orthopaedic bone drilling using Taguchi membership function,” pp. 1–7, 2017.

[33] G. Singh, V. Jain, D. Gupta, and A. Ghai, “Optimization of process parameters for drilled hole quality characteristics during cortical bone drilling using Taguchi method,” *J. Mech. Behav. Biomed. Mater.*, vol. 62, pp. 355–365, 2016.

[34] K. Chao *et al.*, “Medical Engineering & Physics Biomechanical analysis of different types of pedicle screw augmentation : A cadaveric and synthetic bone sample study of instrumented vertebral specimens,” *Med. Eng. Phys.*, vol. 35, no. 10, pp. 1506–1512, 2013.

[35] Y. Kim, W. Choi, and K. Rhyu, “Assessment of pedicle screw pullout strength based on various screw designs and bone densities — an ex vivo biomechanical study,” *Spine J.*, vol. 12, no. 2, pp. 164–168, 2012.

[36] B. B. Abshire, R. F. Mclain, A. Valdevit, and H. E. Kambic, “Characteristics of pullout failure in conical and cylindrical pedicle screws after full insertion and back-out,” vol. 1, pp. 408–414, 2001.

[37] R. Zdero, “and Effective Shear Stress in Synthetic Third Generation,” vol. 129, no. April 2007, pp. 289–293, 2013.

[38] Q. H. Zhang, S. H. Tan, and S. M. Chou, “Effects of bone materials on the screw pull-out strength in human spine,” vol. 28, pp. 795–801, 2006.

[39] A. Gracco *et al.*, “Effects of thread shape on the pullout strength of miniscrews,” *Am. J. Orthod. Dentofac. Orthop.*, vol. 142, no. 2, pp. 186–190, 2012.

[40] J. Wu *et al.*, “Pullout strengths of orthodontic palatal mini-implants tested in vitro,” *J. Dent. Sci.*, vol. 6, no. 4, pp. 200–204, 2011.

[41] T. K. Ã and H. Takadama, “How useful is SBF in predicting in vivo bone bioactivity ? $,” vol. 27, pp. 2907–2915, 2006.

[42] D. Singh, A. Babbar, V. Jain, D. Gupta, S. Saxena, and V. Dwibedi, “Synthesis , characterization , and bioactivity investigation of biomimetic biodegradable PLA scaffold fabricated by fused filament fabrication process,” *J. Brazilian Soc. Mech. Sci. Eng.*, vol. 41, no. 3, pp. 1–13, 2019.

[43] F. A. N. Xin, C. Jian, and Z. O. U. Jian-peng, “Bone-like apatite formation on HA / 316L stainless steel composite surface in simulated body fluid,” *Trans. Nonferrous Met. Soc. China*, vol. 19, no. 2, pp. 347–352, 2008.

[44] M. Fini *et al.*, “Biological assessment of the bone – screw interface after insertion of uncoated and hydroxyapatite-coated pedicular screws in the osteopenic sheep,” 2002.

[45] C. Hsu, C. Chao, J. Wang, S. Hou, Y. Tsai, and J. Lin, “Resea r c h Increase of pullout strength of spinal pedicle screws with conical core : biomechanical tests and finite element analyses,” vol. 23, pp. 788–794, 2005.

[46] T. H. E. Pig, A. S. A. Model, and F. O. R. Human, “THE PIG AS A MODEL FOR HUMAN,” 1987.

[47] W. H. Yang and Y. S. Tarng, “Design optimization of cutting parameters for turning operations based on the Taguchi method,” vol. 84, pp. 122–129, 1998.

[48] R. J. P. S. K. Krishnaiah, “Quality management research by considering multi-response problems in the Taguchi method – a review,” pp. 1331–1337, 2005.

[49] H. Beyer and B. Sendhoff, “Robust optimization – A comprehensive survey,” vol. 196, pp. 3190–3218, 2007.

ANNEXURE A

The program of CNC machine used for drilling in porcine bone for L1.

O0003 G90 G21;

G00 X0 Y0 Z0;

G90 G54 M03 S500 F50;

G01 Z-1.5;

G01 Z1.5;

M05;

M30;

%

M.Tech Thesis

ORIGINALITY REPORT

12%	5%	11%	5%
SIMILARITY INDEX	INTERNET SOURCES	PUBLICATIONS	STUDENT PAPERS

PRIMARY SOURCES

1	Vishal Gupta, P.M. Pandey, Mohinder Pal Garg, Rajesh Khanna, N.K. Batra. "Minimization of Kerf Taper Angle and Kerf Width Using Taguchi's Method in Abrasive Water Jet Machining of Marble", Procedia Materials Science, 2014 Publication	1%
2	journals.sagepub.com Internet Source	1%
3	Vishal Gupta, Pulak M. Pandey, Vadim V. Silberschmidt. "Rotary ultrasonic bone drilling: Improved pullout strength and reduced damage", Medical Engineering & Physics, 2017 Publication	1%
4	www.researchgate.net Internet Source	1%
5	Gurmeet Singh, Vivek Jain, Dheeraj Gupta, Abhimanyu Sharma. "Parametric effect of vibrational drilling on osteonecrosis and comparative histopathology study with	1%